

RUSSIAN ACADEMY OF SCIENCE
RUSSIAN NATIONAL COMMISSION FOR UNESCO
COMMITTEE ON SCIENCE AND HIGHER EDUCATION OF THE GOVERNMENT OF SAINT-PETERSBURG
COUNCIL OF RECTORS OF SAINT-PETERSBURG HIGHER EDUCATION ESTABLISHMENTS
SAINT-PETERSBURG STATE UNIVERSITY OF AEROSPACE INSTRUMENTATION (SUAI)
UNESCO CHAIR "DISTANCE EDUCATION IN ENGINEERING" OF SUAI
RUSSIAN SECTION OF THE INTERNATIONAL SOCIETY OF AUTOMATION

**ИЗВЕСТИЯ КАФЕДРЫ UNESCO
«ДИСТАНЦИОННОЕ ИНЖЕНЕРНОЕ ОБРАЗОВАНИЕ» ГУАП**

Сборник статей
Выпуск 1

**BULLETIN OF THE UNESCO DEPARTMENT
"DISTANCE EDUCATION IN ENGINEERING" OF THE SUAI**

Collection of the papers
Issue 1

РОССИЯ, САНКТ-ПЕТЕРБУРГ 2016 SAINT-PETERSBURG, RUSSIA

ББК 74.58
УДК 378.1
И33

И33 Bulletin of the UNESCO department “Distance education in engineering” of the SUAI: Collection of the papers. St. Petersburg, Issue 1. – SPb.: SUAI, 2016. – 93 p.
ISBN 978-5-8088-1099-0

ISA District 12 (The International Society of Automation) and SUAI (Saint-Petersburg State University of Aerospace Instrumentation) have organized the Twelfth ISA European student paper competition (ESPC-2016). Papers of professors and the best students were included into this issue of the Bulletin of the UNESCO department “Distance education in engineering” of the SUAI. Papers can be interesting for students, post-graduate students, professors and specialists.

International editor’s committee:

Ovodenko Anatoly (Russia) – chairman,
Antokhina Yulia (Russia),
Bobovich Alexander (Russia) – secretary,
Cockrell Gerald (USA),
Collotta Mario (Italy),
Presti Giovambattista (Italy),
Krouk Evgueni (Russia),
Mirabella Orazio (Italy),
Zamarreno Zesus (Spain).





On behalf of the International Society of Automation, I extend congratulations to the ISA Russia Section, ISA District 12, and the St. Petersburg State University of Aerospace Instrumentation (SUAI) on successfully completing the 12th ISA European Student Paper Competition.

Students are the future for our Society. The potential of these talented students is enormous and I am confident they will “set the standard for automation” and influence the quality and security of our world in the years ahead. No matter which career path they choose, we hope ISA will have a place in their continuing education and professional development.

The papers published in this volume, selected by the advisory committee, represent the best contributions from among an excellent group of papers. I commend the students who committed their time to prepare a paper and on having their work selected for this publication.

Sincerely,

A handwritten signature in black ink that reads "James W. Keaveney". The signature is written in a cursive, flowing style.

James W. Keaveney
2016 ISA President

Standards
Certification
Education & Training
Publishing
Conferences & Exhibits

International Society of Automation
67 Alexander Drive
P.O. Box 12277
Research Triangle Park, NC27709
PHONE (919) 549-8411
FAX (919) 549-8288
E-MAIL info@isa.org
www.isa.org



I would like to extend congratulations to the ISA Russia Section, ISA District 12, Indiana State University (ISU), and the St. Petersburg State University of Aerospace Instrumentation (SUAI) for successfully organizing the 12th ISA European Student Paper Competition. This international forum has become one of the foremost conferences in the world.

As a longtime educator and member of ISA for almost 30 years, I continue to appreciate the sharing of technical information by students and faculty members. This global sharing will serve to help advance the technical knowledge base and help in the global collaboration of ideas. I always look forward to having the opportunity to share with students the amazing challenges and personal rewards that a life in automation can bring. ISA is honored to have the opportunity to nurture the next generation of automation professionals.

Indiana State University and the International Society of Automation look forward to our continued relationship between the Russia Section, District 12, and SUAI. Through distance learning classes on project management and ongoing international forums, we are developing new understandings in the technical, cultural, and personal arenas.

Congratulations to those who have developed papers for this volume and to the advisory committee who have the difficult task of making paper selections.

Sincerely,



Gerald W. Cockrell
ISA Former President (2009)
Professor Emeritus (ISU)
SUAI Honored Doctor

Standards
Certification
Education & Training
Publishing
Conferences & Exhibits

ISA
67 Alexander Drive
P.O. Box 12277
Research Triangle Park, NC 27709
PHONE (919) 549-8411
FAX (919) 549-8288
E-MAIL info@isa.org
www.isa.org

THE ESPECIALLY SCATTERING OF ULTRA-WIDEBAND PULSE WEDGE-SHAPED FIELD

A. F. Kryachko,

Dr. Sci., Professor

M. A. Kryachko,

postgraduate student

K. V. Antonov,

postgraduate student

Y. Y. Levin,

postgraduate student

V. K. Losev

postgraduate student

Saint-Petersburg State University of Aerospace Instrumentation
Saint-Petersburg, Russia

kartovan@gmail.com

Abstract

On the basis of diffraction problem known solutions on a wedge in the case of harmonic effects using frequency method was analyzed the UWB pulse scattering on the impedance wedge. The features of the diffraction different kinds of pulses were revealed. We were defined the influence of the wedge's electrical and geometrical parameters, sensing conditions and monitoring, as well as probing signal spectrum shape and the diffraction pulse energy. In study of the time dependence influence the type of probe pulse on the scattering field was tested a time-frequency method.

Keywords: impedance wedge, UWB impulse, diffraction, frequency method.

It is known that in ultra-wideband (UWB) radar [1] the scattering of the probe pulse at specific local centers largely determines the nature of the total field of diffraction. Under certain conditions the main contribution to the total effective scattering cross section (SCS) of the object with complex geometric shapes makes the scattering at its edges and kinks. Therefore, practically important task is the study of the diffraction of a UWB pulse for the impedance wedge, which in some cases can be used as an electrodynamic model in the study of scattering on the edges of the real object.

Currently well enough developed methods for solving diffraction problems for the electromagnetic field in the regime of steady harmonic oscillations. It is much harder to solve the diffraction problems in cases where the primary source varies in time non-sinusoidal. To solve this unsteady problem also different methods have been devel-

oped [2]. Most of them are based on the use of the superposition principle, which is used for the solution of any linear differential equations. In some cases, it seems appropriate to use frequency method [3], the main advantage of which is the ability to apply for known solutions found for the case of diffraction of the waves monochromatically, in the study of non-stationary scattering. The resulting field is defined as a superposition of responses to the elementary impact of the spectral components of UWB pulses.

Under the UWB signal we mean a signal with a large relative width of the spectrum [4]. The width of the spectrum $\Delta f = f_u - f_l$, where f_u, f_l are the upper and lower frequencies in the signal spectrum, and $f_0 = (f_u + f_l)/2$ – average frequency.

An indicator of the high bandwidth signal is defined by the expression:

$$\mu = \Delta f / f_0 \quad (1)$$

Signals, for which $\mu \geq 1/2$, are considered of UWB. The interest in nonstationary diffraction is caused by the scattering of pulses with the rate of the bandwidth $\mu \geq 1/2$ greatly differs from phenomena occurring during diffraction of the harmonic signal and requires separate consideration.

Let the impedance wedge with the opening angle F (fig. 1), formed by two semi-infinite edges, which in the case of H-polarization are characterized by the normalized impedances Z_{\pm} / Z_0 (Z_0 – the impedance of free space), diffracted ultra-wideband pulse at an angle φ_0 .

Under H-polarization is understood to be the case when the incident field vector H parallel to the edge of the wedge. The z axis of a cylindrical coordinate system aligned with the edge of the wedge.

To be determined the time dependence of the diffracted field in the observation point $M(r, \varphi)$. For this the frequency method is used [3]. The exact

solution for the case of harmonic vibrations has the form:

$$H = -\frac{A_{ot}}{4\Phi} \times \int_{\gamma} \exp[-ikr \cos \alpha] \frac{\psi(\alpha + \varphi) \cos(\pi\varphi_0 / 2\Phi) d\alpha}{\left(\frac{\psi(\varphi_0) [\sin(\pi(\alpha + \varphi) / 2\Phi) - \sin(\pi\varphi_0 / 2\Phi)]}{\sin(\pi\varphi_0 / 2\Phi)} \right)} \quad (2)$$

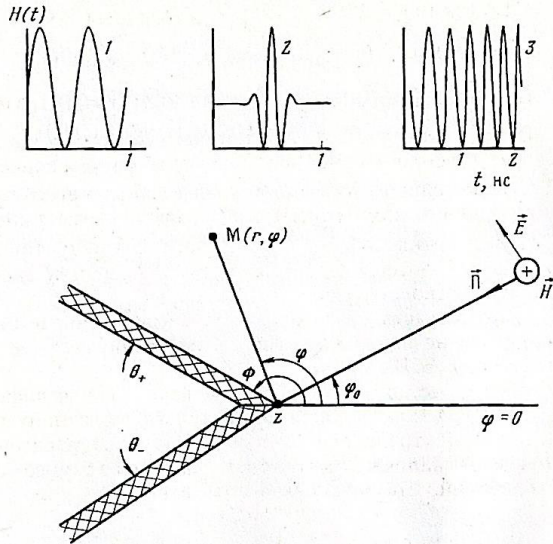


Fig. 1. Impedance wedge and the kinds of probing UWB pulses:
1 – rectangular pulse; 2 – perfect sounding pulse;
3 – linear frequency modulation pulse

Part of subintegral expression of the function $\psi(\delta)$ is expressed through the function of Maluzintz ψ_m [5]. In the case of diffraction of a plane IBM at impedance for the wedge equation (2) gives the value of the field in any point of space outside the wedge. However, its direct use in numerical simulations is difficult because the integral is not expressed through known functions. Away from the edges (i.e. when the condition $kr \gg 1$) it can be calculated by an approximate asymptotic method [5].

Full field in this case is represented as the following sum of asymptotic series:

$$H_z^{pl}(r, \varphi) \cong H_{scat}^{cil} + H_{inc}^{pl} + H_{refl+}^{pl} + H_{refl-}^{pl} + H_{zsur\pm} \quad (3)$$

where

$$H_{scat}^{cil} = A_0 \pi \cos[\pi\varphi_0 / 2\Phi] [\sqrt{2\pi kr} \times (2\Phi\psi(\varphi_0))]^{-1} \times \times [[\psi(\varphi - \pi) \sin[\pi(\varphi - \pi) / (2\Phi)] - \sin[\pi\varphi_0 / 2\Phi]]^{-1} - [[\psi(\varphi + \pi) \sin[\pi(\varphi + \pi) / (2\Phi)] - \sin[\pi\varphi_0 / 2\Phi]]^{-1} \times \times \exp[i(kr + \pi / 4)]$$

characterizes cylindrical IBM, scattered in space edge wedge; H_{inc}^{pl} and $H_{refl\pm}^{pl}$ respectively, and z-components of magnetic field intensity vector of incident and reflected from the faces of the wedge of electromagnetic waves. Component $H_{zsur\pm}$ determines the impedance at the excited faces of the wedge surface electromagnetic waves, which in the

case of inductive impedance faces, and in the absence of losses is sustained and propagated along the edges of the wedge to infinity.

In practice there is no need to compute all partial components. It is enough to analyze the behavior of those who make the main contribution to the Effective Surface Scattering (ESS).

According to the frequency method, the approximate solution for diffraction at the wedge impedance UWB can be found as a result of the inverse Fourier transform of the spectral density of the probing signal and function reflecting the dependence of field strength with frequency in the case of steady-state harmonic oscillations. It can be written as:

$$H(t) = \frac{1}{2\pi} \int_{-\infty}^{\infty} F(i\omega) \dot{H}_z(\omega, \varphi, r) \exp[i\omega t] d\omega, \quad (4)$$

where $F(i\omega) = \int_{-\infty}^{\infty} S(t) \exp[-i\omega t] dt$ – is the spectral density of the probing signal, and $\dot{H}_z(\omega, \varphi, r)$ – the solution to this problem for the case of harmonic oscillations (3).

Bulky the algorithm for computing special functions of Maluzintza $\psi_m(z)$ can be replaced by more simple approximation of its values [5]:

$$\psi_m(z) = \exp\left\{ \frac{1}{2}(U + iV) \right\}, \quad (5)$$

where

$$U = -0,3 \sum_{n=1}^5 \frac{\text{ch}[(0,3n-0,15)x] \cos[(0,3n-0,15)y] - 1}{\left((0,3n-0,15) \text{ch}[\pi(0,3n-0,15)/2] \times \times \text{sh}[2\Phi(0,3n-0,15)] \right)},$$

$$V = 0,3 \sum_{n=1}^5 \frac{\text{sh}[(0,3n-0,15)x] \sin[(0,3n-0,15)y]}{\left((0,3n-0,15) \text{ch}[\pi(0,3n-0,15)/2] \times \times \text{sh}[2\Phi(0,3n-0,15)] \right)}$$

In the study of the influence of the form of the time dependence of the incident field at the diffraction of a pulse with fixed terms of sensing and monitoring the electrical and geometrical characteristics of impedance wedge is advisable to use a time-frequency method.

First you need to define the functional dependence of field strength $\dot{H}_z(\omega, \varphi, r)$ on frequency in case of harmonic oscillations. Then the result is inverse Fourier transform of this function finds the spatial impulse response of the wedge:

$$h(t) = \frac{1}{2\pi} \int_{-\infty}^{\infty} \dot{H}_z(\omega, \varphi, r) \exp[i\omega t] d\omega. \quad (6)$$

The time dependence of the scattered field can now be defined as the result of the convolution of the spatial impulse response signal and the time dependence of the field strength of the probing signal:

$$H(\tau) = \int_{-\infty}^{\infty} \dot{H}_{pr}(\tau) h(t - \tau) d\tau. \quad (7)$$

While of numerical calculations, we have analyzed the diffraction of a UWB pulse of several

types (fig. 1). Survey have shown that the form of the time dependence of diffraction of the pulse (DP) at the point of observation, its magnitude, duration, and energy largely depend on the geometrical and electro-physical parameters of impedance wedge, and environment sensing and monitoring.

Fig. 2 shows the time dependence of diffracted pulses of different types: 1, 2 – rectangular; 3, 4 – perfect probe pulse (impulse type 2) (fig. 1); 5, 6 – signal with linear-frequency modulation (chirp signal).

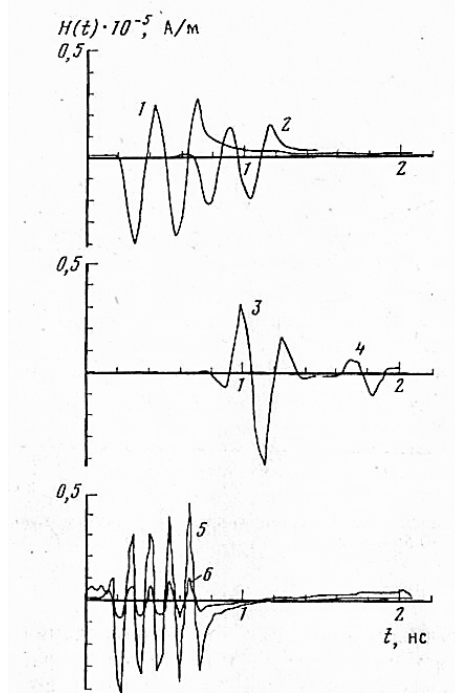


Fig. 2. Time dependence of the diffraction pulses: $\text{Im}(\theta_{\pm}) = 0,01$ (1); $0,5$ (2); $F = 100^\circ$ (3); 140° (4); $\varphi = 40^\circ$ (5, 6)

The increase in the reactive component of the impedance edges of the wedge (fig. 2, curves 1, 2) leads to a decrease of the amplitude of DI. This is due to the intensive excitation of surface waves on the edges of the wedge. Dependency analysis 3 and 4 in fig. 2 allows us to conclude that the decrease in the opening angle of the wedge (the increasing angle F) essentially changes the shape of the scattered pulse. The position of the point of observation (curves 5 and 6 in fig. 2) significantly affects the amplitude and duration of the scattered pulse. Type of the time dependence of the probe pulse and its spectrum under other equal conditions has a significant impact on the process of scattering at the wedge. One reason for this is the frequency dependence of the impedance faces of the wedge [5]. Compare for example a rectangular pulse and an ideal sounding pulse (fig. 1, curves 1, 2). The proportion of the shape of the spectrum of a rectangular pulse and spatial phase characteristics of the wedge is such that with the diffraction of this pulse on the wedge increases the level of low-frequency components compared with the components of the middle part of the spectrum. Strongly reduced level

of high-frequency spectrum components still makes a negligible contribution to the pulse energy. The above reason leads to a decrease in the energy of the signal delays of the rise and fall, increasing the pulse duration (fig. 2, curves 1 and 2).

The shape of the amplitude and phase spectrum of the ideal pulse is such that its spectrum undergoes even greater changes than in the case described above. There is a shift of average frequency and spectrum shift in the lower frequency area. Change energy and type of time dependence DI (fig. 2, curves 3, 4) are bigger than in the first case. The nature of the changes of the diffraction of the pulse depends on the bandwidth of the signal μ . With increasing μ to a value approximately equal to $0,5$, the shape of the pulse does not undergo significant changes. Therefore, for such signals it is possible to use the ratio found for the case of diffraction of harmonic waves (with certain amendments). With a further increase μ the nature of the time dependence of DI is changed substantially.

In fig. 3 is shown the dependence of diffraction of the pulse energy from the opening angle of the wedge for various angles of incidence Φ_0 . Moreover, the angle of observation Φ is chosen equally to the angle of incidence. Analysis of energy changes of DI showed that all the curves have a maximum corresponding to the case of mirror reflection from the faces of the wedge.

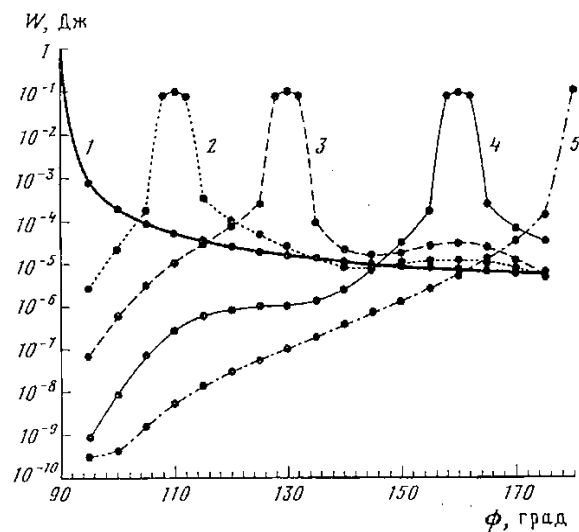


Fig.3. Dependence of the energy DI from the opening angle of the wedge: $\text{Im}(\theta_{\pm}) = -0,5$; $F = 0^\circ$ (1); 20° (2); 40° (3); 70° (4); 90° (5)

In case of equality to zero of the values of the angle of incidence and the angle of observation (curve 1), diffraction of the pulse energy takes the highest value of all studied cases (curves 2–5) when the opening angle of the wedge F , equal to the value $0,5\pi$, i.e. when the wedge degenerates into an infinite impedance plane. This is explained by the fact that in the impedance plane in the absence of inhomogeneities there are no excited surface waves.

Equality $\lim_{\theta_{\pm} \rightarrow 0} |H_{zsur\pm}| = 0$ can be considered

as a proof of asymptotic stability of solutions to change the opening angle of the wedge.

At other angles of incidence of the pulse, the position of the maximum is also determined by the ratio $F = \varphi_0 + 0,5\pi$ (to $\varphi_0 = \varphi = 20^\circ$, $\Phi_m = 110^\circ$, to $\varphi_0 = \varphi = 40^\circ$, $\Phi_m = 130^\circ$, etc.). The value of the opening angle of the wedge corresponding to the maximum shifts towards higher values. Such character of change of energy DI is determined by the dependence of the energy of surface waves from the opening angle of the wedge.

The scatter plots (fig. 4) have a clearly cut diffraction. In their structure two characteristic petals are distinguished, the position of which does not depend on the magnitude of the impedance and is determined only by the values of the angles φ_0 and F , i.e. the geometry of the problem. In case of equality of the impedance faces of the petals are arranged symmetrically relative to the axis of the wedge.

Therefore, fig. 4 shows only one petal. The direction of one of them coincides with a boundary region of a mirror reflection of the illuminated face $\varphi' = 2\Phi - \pi + \varphi_0$. The energy of surface waves in this case is minimal, and the main contribution to the scattered field introduces diffraction component. When you remove the angle from the maximum observation, energy of the diffraction field made by surface wave increases, and the energy of the diffraction component is reduced.

Reducing the opening angle of the wedge (fig. 4, curves 2, 3) change the conditions of excitation of surface waves on the sides and causes a shift in the position and magnitude of the maximum petal of the scattering diagram.

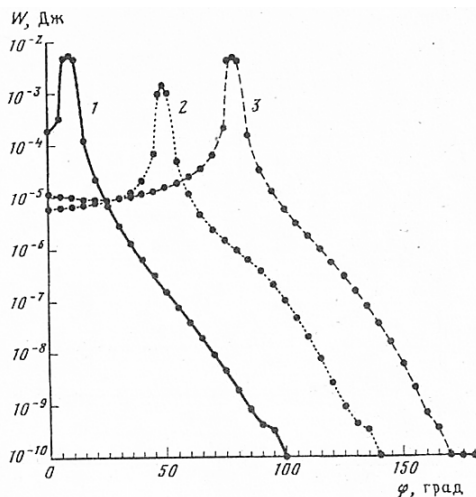


Fig. 4. Scatter plot of $\text{Im}(\theta_{\pm}) = -0.5$; $F = 100^\circ$ (1); 140° (2); 170° (3)

The position of the second petal depends on the condition $\varphi_0 < \pi - \Phi$. If this condition is fulfilled, then the corresponding equal angle $\varphi'' = -2\Phi + \pi - \varphi_0$. Otherwise this angle is

$\varphi = \varphi_0 - \pi$. When reducing the opening angle of F , petals will approach and in case of equality of angle of aperture value $0,5\pi$ will merge into one. This phenomenon can be given a physical explanation. Back scattering patterns also have two petals. However, the main petals correspond to the angles of mirror reflection from the faces ($\varphi' = \Phi - \pi$, $\varphi'' = -\Phi + \pi$).

The increase of the module $|\theta_{\pm}|$ results in the scattering of H -polarized wave to the fact that a significant part of the energy of the incident pulse is scattered along the edges of the wedge. Naturally, in this case decreases the value of the $|H_{zsur\pm}|$ sector $|\varphi| < 60^\circ$ (fig. 5, a).

The increase in the modulus of the impedance also leads to the change of DI type in the time domain (fig. 2).

In fig. 5 is presented the results of numerical calculations of energy values of the diffraction of a pulse the value of the imaginary part of impedance for different values of the parameter $\text{Re}|\theta_{\pm}|$ (curves 1, 2), which characterizes the heat losses at the wedge's edge. With increasing real part of θ_{\pm} , the energy of the surface waves decreases, and as faster as the more imaginary part θ_{\pm} is. The total field energy also decreases. Increase of the impedance value leads to an increase in the proportion of surface waves energy. The total field energy by increasing the reactive part of the impedance from 0 to 1 (curves 1, 2) decreases by 2 orders of magnitude. When reducing the opening angle of the wedge (curves 3, 4) the influence of impedance in comparison with the described case is not essential.

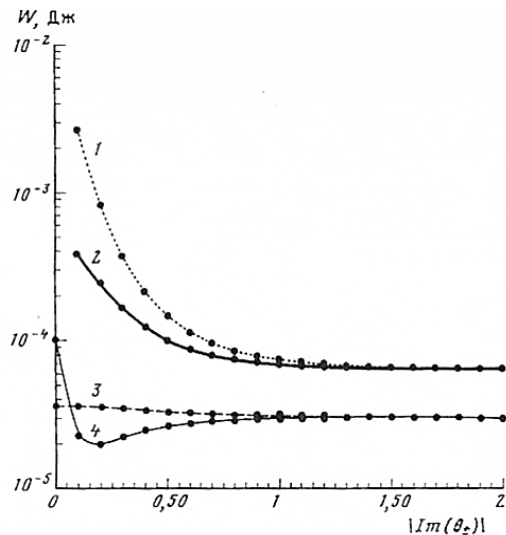


Fig. 5. DI Energy Dependence on the magnitude of the impedance: $\varphi = \varphi_0 = 40^\circ$; $\text{Re}(\theta_{\pm}) = 0.1$ (1); 0.5 (2, 4); 0 (3); $F = 100^\circ$ (1, 2); 120° (3, 4)

CONCLUSIONS

Summarizing the results of the work, it can be noted that the process of diffraction of UWB pulses at the impedance wedge is significantly

different from the case of diffraction of harmonic waves. Type of diffraction of the pulse, its energy depend on the angle of signal arrival, the position of the observation point, geometrical and electro-physical parameters of the wedge, the type of the probe pulse. These characteristics determine the conditions of excitation of surface waves, redistribution of energy between the partial components of the scattered field. The method of calculation of the diffraction field change in time during irradiation of impedance wedge ultra-wideband pulse has a simplicity and physical clarity, saves computational resources (since it contains only one operation of integration).

REFERENCES

- [1] *Астанин П.Ю., Костылев А.А.* Сверхширокополосные радиолокационные измерители. М.: Изд-во МО СССР. 1983.
- [2] *Анкудинов В.Е., Романов Е.А.* // Зарубежная радиоэлектроника. 1991. № 41. С. 6.
- [3] *Зернов Н.В.* // Доклады АН СССР. 1951. Т. 80. № 91. С. 33.
- [4] *Астанин Л.Ю., Костылев А.А.* Основы сверхширокополосных радиолокационных измерений. М.: Радио и связь. 1989.
- [5] *Крячко А.Ф., Лихачев В.М., Смирнов С.Н., Сташкевич А.И.* Теория рассеяния электромагнитных волн в угловых структурах. СПб.: Наука. 2009.
- [6] *Нертао J., Volakis I., Senior T. et al* // IEEE Trans. 1987. V. AP. № 9. P. 1083.
- [7] *Марков Г.Т., Чаплин А.Ф.* Возбуждение электромагнитных волн. М.: Радио и связь. 1983.

**ANALYSIS OF THE TECHNICAL STATE OF THE SYSTEM
BASED ON THE EXPERT EVALUATIONS*****Nikolai N. Maiorov***

PhD, associate professor

Vladimir A. Fetisov

Dr. Sci., Professor,

Vitali E. Taratun

assistant

Saint-Petersburg State University of Aerospace Instrumentation,
Department of System Analysis and Logistics
Saint-Petersburg, Russia*sciencesuai@yandex.ru***Abstract**

In the article revealed the approach to the study of the technical state of the system on the basis of the distribution desirability Harrington. It is possible to estimate the possibilities and ways of technical modernization using analyzing partial factors desirability of specific parameters.

Keywords: comparative analysis, the desirability of a generalized function Harrington, decision making under uncertainty.

I. INTRODUCTION

The methodology of the system analysis is universal instrument of research and design complex various technical systems of [1]. Modern processes are characterized by high variability and dynamics. Decision-making tasks under conditions of uncertainty, with regard to the different models of technical systems, may differ significantly from each other. In addressing management tasks have to deal with situations where finding the optimal solution is complicated by the need to simultaneously account for different groups of factors and relevant scenarios of accidental impact on the operation of the technical system. In this case the person making decision must have a full set of baseline data for the system view of the all situations. On the basis of this data set is necessary to form a decision on further optimization of the system. The approach statement of decision-making problems under uncertainty consists of the following steps [3]:

1) determine the set of all possible situations that affect the result of appropriate decisions within the framework of the analyzed technical system;

2) create a list of all alternative solutions that you want to analyze, and to which the result will depend on the marks of the "external" situation;

3) identify the expected results for the cases where a decision is taken (from the set of the above alternatives analyzed) and external, independent of the person making the decision, the situation was such, that corresponds to a given event (from the set of the complete group of events affecting the result);

4) decision-making under uncertainty require further consideration from a set of alternative solutions to choose one alternative (best alternative).

Mathematical models have certain variation for a variety of technical systems. They are implemented in specialized software. It is well known that the technical systems are compared by their own technical quantitative and qualitative characteristics. The comparison results are usually different depending on the criteria and parameters. The criteria set must use to evaluate the technical system.

II. METHODS SOLUTIONS

To solve multi-criteria problems (for example, optimization of the multidimensional object as automated control system) use different methods for constructing generalized index. The criteria of choice in conditions of uncertainty include the criterion of Savage, Hurwitz, and several others [1, 2, 4]. But at the same time for a comprehensive assessment of one of the most convenient ways is distribution desirability Harrington.

The proposed method of comparison of different technical systems on the basis of assessments of their performance on the desirability of a generalized function Harrington gives some ways to the

universalization of the overall approach to the problem of assessing the effectiveness of existing and newly developed systems for various purposes. Instead of simply comparing the system parameters, they are translated into numerical values, and then processed to provide a total system rate. These ratios compare different systems. This allows you to more objectively evaluate the possibility of different types of equipment, and also facilitates the comparison process.

Let $A = \{a_1, a_2, \dots, a_n\}$ – the set of initial parameters of the technical system; $K = \{k_1, k_2, \dots, k_m\}$ – set of criteria, which are assessed; $C = (c_{ij})_{j=1,n}^{i=1,m}$ – assessment of the proposal a_j by criteria k_i

Baseline data is converted to a matrix form (table 1.)

Table 1
Presentation of the original data

K	A					
	a1	a2	...	a _j	...	a _n
k ₁	C ₁₁	C ₁₂	...	C _{1j}	...	C _{1n}
k ₂	C ₂₁	C ₂₂	...	C _{2j}	...	C _{2n}
...
k _i	C _{i1}	C _{i2}	...	C _{ij}	...	C _{in}
...
κ	C _{m1}	C _{m2}	...	C _{mj}	...	C _{mn}

It is necessary to rank the options in order to select the optimal solution. Assessments can take a numeric value (some value or performance), and is an expert statements such as "good", "satisfactorily", etc. In addition, there may be linguistic experts fuzzy statements like "the criterion K_i the offer system a_j much better". So, for a decision on the selection of appropriate to apply the method of fuzzy preference relations.

One way to construct such a scale is a function of the preferences desirability Harrington [2–4] (fig. 1), which allows to simulate the process of coordinated behavior of individual subsystems of a whole, take account of links and impacts between them in solving the problem of the choice of a set of existing alternatives. The basis for the construction of priority and the possibility of a generalized function is the transformation of the natural values of particular parameters of various physical nature and dimension in a single dimensionless scale of desirability (preference).

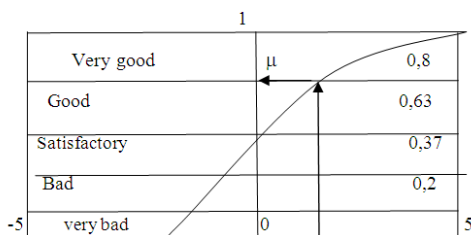


Fig. 1. Graphical representation of the function Harrington

Harrington function was derived empirically. Y-axis coordinate is called the scale of private indicators. The axis d – the scale of desirability. The spacing of the effective values on the scale of private indicators – [-5; 5]. Desirable range is divided into a range from 0 to 1 for five subbands: [0; 0.2] – "very bad", [0.2; 0.37] – "bad" [0.37; 0.63] – "satisfactory" [0.63; 0.8] – "good", [0.8; 1] – "very good". The specific parameters of the compared systems are distributed on a scale corresponding to the requirements imposed on them in the interval of the effective values of the scale of private indicators. Then, the corresponding figures are translated into marks on the desirability scale (table 2).

Table 2
Linguistic assessment and scale Harrington

Linguistic assessment	Value	Scale Harrington
Very good	5	0,8–1
Good	4	0,63–0,8
Satisfactory	3	0,37–0,63
Bad	2	0,2–0,37
Very bad	1	0–0,2

We use the function Harrington (for each criterion):

$$\mu(x) = \exp(-\exp(-x)); x \in [\underline{x}, \bar{x}]; \mu: [\underline{x}, \bar{x}] \rightarrow [0, 1],$$

$$\text{где } x = 10 \frac{c_{ij} - \underline{c}_i}{\bar{c}_i - \underline{c}_i} - 5; \quad (1)$$

$$\underline{c}_i = \min_j (c_{ij}, \underline{C}), \bar{c}_i = \max_j (c_{ij}, \bar{C}); \quad (2)$$

\underline{C}, \bar{C} – are the upper and lower limits, asked an expert (eg, regulatory or projected average value of the corresponding criterion); \underline{x}, \bar{x} – minimum and maximum value argument.

Harrington function is continuous, smooth and monotonic in the entire domain. Clearly, $x=0$ – inflection point function, $\mu(0)=e^{-1}=0,37$, $\mu(x)=1-e^{-1} \approx 0,63$ at $x = 0,78$. Sensitivity functions in areas that are close to zero and one, substantially lower than in the middle zone, which is consistent with the principles of peer reviews. The main advantage of the proposed scale (fig. 1) is that it allows you to move from the absolute values of the estimated parameter for the assessment of his linguistic and vice versa. Applying Harrington function to the raw data form (table 3).

Table 3
The data on the scale of Harrington

K	A					
	a1	a2	...	a _j	...	a _n
K ₁	μ ₁₁	μ ₁₂		μ _{1j}		μ _{1n}
K ₂	μ ₂₁	μ ₂₂		μ _{2j}		μ _{2n}
...						
K _i	μ _{i1}	μ _{i2}		μ _{ij}		μ _{in}
...						
K _m	μ _{m1}	μ _{m2}		μ _{mj}		μ _{mn}

Here $\mu_{ij} = \mu(k_i, a_j)$ – the level of compliance with the requirements of proposals a_j based at k_i .

Compose tables m (according to the number of criteria) of fuzzy preference relations. Table of contents 3 is determined by the formula

$$\mu_{ij}^i = \mu^{k_i}(a_i, a_j) = \left\{ \begin{array}{l} \mu_{il} - \mu_{ij}, \text{ если } \mu_{il} \geq \mu_{ij} \\ \mu_{ij} \end{array} \right. \left(\begin{array}{l} l = \overline{1, n} \\ l \neq j = \overline{1, n} \end{array} \right),$$

$$(i = \overline{1, m}) \quad (3)$$

Obviously, in the tables, similar to table 3, not less than $\frac{n(n-1)}{2}$ zero elements. These relationships preferences (for all criteria table 3) are collapsed into one by using the weight coefficients w_i

$$\sum_{i=1}^m w_i = 1; \mu_i = \mu(a_i, a_j) = \sum_{i=1}^m w_i \mu_{ij}^i \quad (i, j = \overline{1, n}). \quad (4)$$

Integral preference ratio shown in table 4.

Table 4

Integral preference relation

K	a_1	a_2	...	a_j	...	a_n
a_1	1	μ_{12}	...	μ_{1j}	...	μ_{1n}
a_2	μ_{21}	1	...	μ_{2j}	...	μ_{2n}
			
a_1	μ_{i1}	μ_{i2}	...	μ_{ij}	...	μ_{in}
			
a_n	μ_{n1}	μ_{n2}		μ_{nj}	...	1

Finally, proposals are ranked according to the formula

$$\mu(a_j) = \mu_j = 1 - \sup(\mu_{ij} - \mu_{ji}); (j = \overline{1, n});$$

$$j \neq i = \overline{1, n} \quad (5)$$

Obviously, selected with the highest value μ_j . Highest value μ_j represents the possibilities to modernization technical system.

III. CONCLUSION

Using real values of the parameters for calibration within the boundaries of the effective range allows more objectively evaluate the possibility of comparing the technical systems taking into account the achieved performance. Moreover, in case of lack of the required values of specific systems can be introduced into a hypothetical analysis of the system that they may possess. In this case, however, should take into account the mutual comparison parameters. Private coefficients converted into generalized systems of coefficients to allow almost "mathematical" precision judge their advantages and disadvantages. It is also possible to assess the prospects of modernization and further development of those or other technical systems.

For example, if the system is a factor in the desirability of the lower curved portion Harrington function, it is in principle not possible to upgrade. While the need to "tightening" of almost all parameters to an acceptable level (due to the high cost of time and effort that must be assessed correctly) in

order to achieve satisfactory results. Prospects for the long-term development of such systems is very doubtful. It makes sense to consider its replacement. When the system has consolidated the desirability factor of 0.8 ... 0.9, in addition to that it is very good, we can say that the system is close to the limit of its development. Thus, analyzing the desirability of partial factors specific parameters, we can evaluate the possibilities and ways of upgrading the technical system.

IV. REFERENCES

- [1] Майоров Н. Н. Практические задачи моделирования транспортных систем / Н. Н. Майоров, В. А. Фетисов. – СПб.: Изд-во ГУАП, 2012. – 185 с.
- [2] Охтилев М. Ю. Интеллектуальные технологии мониторинга и управления структурной динамикой сложных технических объектов / М. Ю. Охтилев, Б. В. Соколов, Р. М. Юсупов. М.: Наука, 2006. – 410 с.
- [3] Бродецкий Г. Л. Системный анализ в логистике. Выбор в условиях неопределенности. / Г.Л. Бродецкий. - М.: Academia, 2010. - 336 с.
- [4] Дубров А. М. Моделирование рискованных ситуаций в экономике и бизнесе / Лагоша Б.А., Хрусталёв Е.Ю. и др.: Учеб. пособие / Под ред. Б.А. Лагоши. – М.: Финансы и статистика, 1999. – 176 с.

AN INNOVATIVE DESIGN IN ORDER TO REDUCE THE WORKLOAD OF A PILOT DURING THE FLIGHT

*Adriana Aiello, Antonio Alesci, Giovanni Manconi, Alessia Mantellina,
Marilena Tinervia, Luigi Villari, Walter Zapparrata*
students

“Kore” University of Enna
Enna, Italy

name.surname@unikorestudent.it

Abstract

We have tried to idealize a system to simplify the procedure to apply in the case of a failure. The pilot, how we know, has a higher workload during a failure procedure and he wastes a lot of time to consult the checklist to resolve the problem. With our idea, the pilot has the possibility to choose the correct checklist (for the moment we have studied it with just four different damages) on the cockpit, through a new display. Once the pilot has recognized the type of damage, a sequence of backlight will start to guide him in solving the problem in question. In this way we found a reduction of the time spent to restore the initial conditions.

Before our final solution, we tried to guide the pilot in a different way: using vocal commands. The result was unsuccessful because this new vocal commands were confused with the voice of the tower controller. After this results and some researches in literature, we come to the conclusion that the best solutions could be the backlight of the buttons/commands.

I. INTRODUCTION

This project foresees a method to simplify some procedures with a device during a failure. How we know there is a high number of accidents associated to the interaction human machine, for example we can mention the disaster of the Helios Airways 522, where a generic alarm started to play and the pilot didn't recognize it. When it started the pilots ignored it because they were in panic. In a few minutes the passengers and pilots passed out, the oxygen was low. The alarm which sounded was of the pressurization system, the consequence was a disaster.

All of that could be avoided with a device which helps the pilot during the use of the check list.

For our project we started to think that the biggest problem in aeronautical world is the human's mind and not the machine. Our mind is able to perceive all things thanks to sensory organs but this is subjective. There are many factors which could influence our perception: the wait, the routine and the anticipation.

In all flight there are events intersected between them, all these events are contributions which are useful for a successful flight.

Human behavior is based on very complex mental processes which are divided into several stages: perception, which makes use of the sense organs; recognition, which consists in recognizing the information once received, but this occurs only if the situation has already been lived at least once; the evaluation, which has the function to determine whether the sequence in place is taking place according to the plans; the representation, which is the way the mind devises an intervention to achieve this goal and the decision.

According to the aviation psychology studies the drivers take a decision following the Aeronautical Decision Making, this systematic approach is used by pilot to determine the best course of action in response to specific circumstances. To help you remember the elements of the process in the formation of the decision, the model "DECIDED" is defined: D (detect, discover a change); E (estimate, evaluating what we need for action); C (choose, choose a result); I (identify, identify the actions to be put into practice); D (do, do the necessary action); E (evaluate, assess the effect of the action).

Obviously there are factors that influence the formation of the decision: the pilot self-assessment, stress management, use of resources, situational awareness.

To fulfil our goal we have implemented a software that back-illuminate the switch to press in case of emergency, then such software is able to distinguish between various types of board failures and suggest the correct resolution of the problem without waste of time.

II. THE CHOICE OF THE CHECK LIST

The display allow us to choose the procedure to follow, to resolve the failure, and the system shows the buttons to press through the red backlight. For that we took some ideas from the studies of Richard Kelly (1910–1977). He was a pioneer of qualitative lighting design, which summed up in a single concept the stimuli taken from perception psychology and theatrical lighting. Kelly broke away from the principle of a uniform illumination as the central criterion for lighting design, replacing the problem of the amount of light with that of the individual quality of the light itself, according to a series of lighting functions oriented to the observer who perceives them. Kelly drew a distinction between three basic functions: ambient luminescence (light to see), focal glow (light to watch) and play of brilliants (light to observe).

What interests us is the "focal glow", translated as "the light to look at." With this form was assigned for the first time to light the explicit task of actively contributing to the transmission of information. He was taken into account so the illuminated areas instinctively attract the attention of people.

III. SOFTWARE FOR BACKLIGHTING COMMAND

The software developed to support the driver in case of breakdowns or malfunctions, provides a graphical interface where we have implemented the check list of the commands related to the 4 most common failures: engine failure, damage to cart, depressurization and de-icing malfunction (fig. 1).

The application has been designed entirely in Java with the material founded in network support.

The design of graphical interface provides for the addition of one screen inside the cockpit of the aircraft chosen. You can choose which of the most appropriate check list you need according to your problem. In the same monitor is also shown a proper success message, if the problem is resolved.

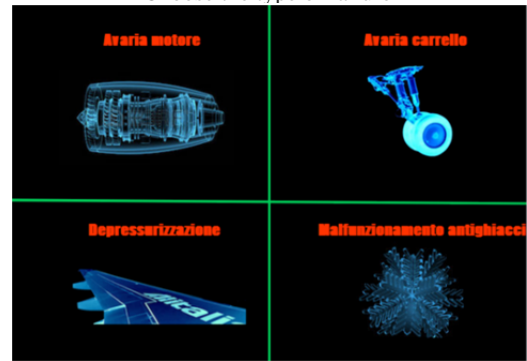
Choosing the failure, the command sequence is started. Each of them will flash until it is not executed, immediately after the next action will be lit until the end of the check list.

IV. TEST RESULTS

In the graphic (fig. 2) we show the results of some tests. In the "Scenario 1" the pilots used the manual checklist to solve the problem, in the "Scenario 2" the pilots followed the vocal commands and at the end in the "Scenario 3" we tested our solution (backlight buttons).

The graphic is an average of the results from 3 different pilots. It is clear that the final solution is the best approach to complete the task.

Simulation of a damage Choose the type of failure



To follow the backlight sequence



Positive feedback once you have completed



Fig. 1. Graphical interface

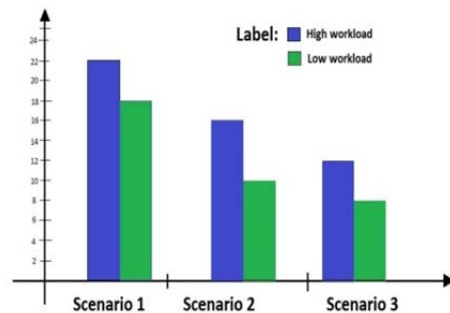


Fig. 2. The results of tests

V. ANALYSIS OF STRESS PILOT

Low workload has been linked to high error rates, in fact due to this there are: frustration, fatigue and poor situational awareness. From what we have learned, it seems that humans do their best when their skills are exercised and their abilities challenged, are neither bored nor overburdened, and when periods of work and rest are equitably mixed together. There are two problems to measure workload:

1) we would like to measure the workload, and due to this we need a measuring device. These measures would allow us to determine when the

person A is working harder than the person B or when the task A seems to require more work from a human than the task B. But this device doesn't exist yet;

2) we need to define practical and sensible limits for workload.

The measurement and evaluation of workload is far from the exact science, in fact there aren't workload measurement scales or techniques that offer the same reliability as the scales used to measure height, weight etc.

The advantage of physiological measures is that they are unobtrusive and objective, and may provide continuous information about mental effort. These physiological measures related to each other, can detect a level of stress that is not suitable to flight activity, precisely because during the flight the pilot must maintain a peaceful state of mind in order to avoid possible situations that could be fatal for all people that are into the aircraft. Stress can be also a positive stimulus to increase the level of attention, but within limits, and this is defined as eustress, or positive stress. After a certain limit of these values, which is very subjective, it becomes distress, or negative stress, where it has the decay of the performance, which can lead to procedures performed in the wrong way, and then to accidents. How can we determinate the difference between eustress and distress? But in literature this isn't studied yet. Through different biometrical sensors we could measure the physiological parameters of the subject, which are connected between them, and that may bring to a numerical measure of stress to the phase of negative stress. Four types of physiological sensors will be used during the experiment: electrocardiogram (EKG) or heart rate (HR), skin conductivity (also known as EDA, electro-dermal activation and GSR galvanic skin response), respiration (through the chest cavity expansion) and blood pressure. The sensors used will be highly ergonomic in such a way as not to results. The data recorded by this sensors, will be related to each other, so we can plot graphs in relation to time, and then to the asset or the task that had at that precise moment, and then determine through a scale, the level of the pilot stress. There are tools that in addition to record data in memory, that can send it in real time to a fixed computer station, where we can monitor the physiological state of the pilot. These data can be transferred to the station through Bluetooth, Wi-Fi and USB. The physiological parameters are then put in relation with the flight parameters such as altitude, climb speed VS, descent speed, ground speed, heading and other. In this way, if we recognize that there is some flight's parameter that does not match with the standard, we can control the physiological parameters, so we can see if the pilot was in a state of stress that could affect the flight's activity.

Through the biometrical signals and the flight parameters, the trainer could check constantly the pilot. When him is in a state where the parameters are different from the standards, this means that his workload will be bigger than before, if we consider the case in which failure happens an accident may occurs.

VI. REFERENCES

- [1] *Richard Kelly*. Progettazione illuminotecnica finalizzata alla percezione .Ercò guida, edizione 01.01.2013
- [2] *Atkinson – Hilgard*. Introduzione alla psicologia. PICCIN Padova, 2011
- [3] [*Dennis A. Vincenzi, John A. Wise, Mustapha Mouloua, Peter A. Hancock* – Human Factors in Simulation and Training – CRC Press]
- [4] [*Eduardo Salas, Dan Maurino* – *Human factor in Aviation* – AP]
- [5] [*Claudio De Sio Cesari* – Manuale di Java 8, programmazione orientate agli oggetti con java standard edition – Hoepli]
- [6] [*C. Thomas Wu* – a comprehensive introducing to object-oriented programming with Java – Higher Education]
- [7] *Maja Meško, Damir Karpljuk Zlatka Meško Štok, Mateja Videmšek, Tine Bertoncej, Andrej Bertoncej, and Iztok Podbregar*. Motor Abilities and Psychological Characteristics of Slovene Military Pilots. THE INTERNATIONAL JOURNAL OF AVIATION PSYCHOLOGY, 23(4), 306–318
- [8] *Mickaël Causse, Frédéric Dehais, and Josette Pastor*. Executive Functions and Pilot Characteristics Predict Flight Simulator Performance in General Aviation Pilots. THE INTERNATIONAL JOURNAL OF AVIATION PSYCHOLOGY, 21(3), 217–234
- [9] *Marie-Pierre Fornette, Marie-Héloïse Bardel, Camille Lefrançois, Jacques Fradin, Farid El Massioui, and René Amalberti*. Cognitive-Adaptation Training for Improving Performance and Stress Management of Air Force Pilots. THE INTERNATIONAL JOURNAL OF AVIATION PSYCHOLOGY, 22(3), 203–223
- [10] *Mickae l Causse, Bruno Baracat, Josette Pastor, Frederic Dehais*. Reward and Uncertainty Favor Risky Decision-Making in Pilots: Evidence from Cardiovascular and Oculometric Measurements. Appl Psychophysiol Biofeedback (2011) 36:231–242.
- [11] *Stephen M. Casner*, Ph.D NASA Ames Research Center, Moffett Field, CA *Brian F. Gore*, Ph.D. San Jose State University Research Foundation, San Jose, CA. Measuring and Evaluating Workload: A Primer. NASA/TM—2010-216395
- [12] *Y. I. Noy*. (2001) International harmonized research activities report of working group on intelligent transportation systems (ITS). Proceedings of the 17th International Technical Conference on the Enhanced Safety of Vehicles. [Online]. Available: <http://www-nrd.nhtsa.dot.gov/pdf/nrd-01/esv/esv17/proceed/00134.pdf>
- [13] *P. Burns and T. C. Lansdown*. (2000) E-distraction: The challenges for safe and usable internet services in vehicles. NHTSA Driver Distraction Internet Forum. [Online]. Available: <http://www-nrd.nhtsa.dot.gov/departments/nrd-13/driver-distraction/Papers.htm>
- [14] National Highway Traffic Safety Administration (NHTSA). Proposed driver workload metrics and methods project. [Online]. Available: <http://www.nrd.nhtsa.dot.gov/departments/nrd-13/driver-distraction/PDF/32.PDF>
- [15] *M. J. Skinner and P. A. Simpson*, “Workload issues in military tactical aircraft,” *Int. J. of Aviat. Psych.*, vol. 12, no. 1, pp. 79–93, 2002.
- [16] *G. F. Wilson, J. D. Lambert, and C. A. Russell*, “Performance enhancement with realtime physiologically controlled adaptive aiding,” *Proceedings of the Human Factors and Ergonomics Society 46th Annual Meeting*, vol. 3, pp. 61–64, 1999.
- [17] *H. Selye*, *Selye’s Guide to Stress Research*. Van Nostrand Reinhold Company, 1980.
- [18] *I. J. K. G. Eisenhofer and D. Goldstien*, “Sympathoadrenal medullary system and stress,” in *Mechanisms of Physical and Emotional Stress*. Plenum Press, 1988.
- [19] *A. Baddeley*, “Selective attention and performance in dangerous environments,” *British Journal of Psychology*, vol. 63, pp. 537–546, 1972.

PSICOTERAPY ACT ON SMARTPHONE

Martina Alé, Anna Dimino, Giulia Serra
students

“Kore” University of Enna
Enna, Italy

martina.ale@unikorestudent.it,
anna.dimino@unikorestudent.it,
giulia.srra@gmail.com

Abstract

Chronic pain is a problem that afflicts most of the population and involves different age groups. The therapy chosen by the customer, in order to create an app that can replace a manual self-help, is the ACT (*Acceptance and Commitment Therapy*). The customer's requirements were: suitable for all ages, easy access to users with reduced mobility of the limbs, easily understandable instructions and the user must be motivated in using the app. We tested what we considered being the final result of the app to and, after having analyzed the answers given, we made further changes using the opinions and advices given.

I. INTRODUCTION

As starting point we have revised a web app already implemented called “ActOnPain”, from the different requests we asked ourselves if and how we could make the app easier, considering the chronic pain a problem for children, adults and old people. Indeed, smartphones are own by everyone, also for people over 60, we thought about an app close to people, to use everywhere to update their profiles everywhere.

The app will allow the user to have a manual of self-help always with him, it will be based on “*Acceptance and Commitment Therapy*”, a form of psychotherapy Cognitive Behavioral Therapy, with a solid scientific basis (Hayes, 2004). The ACT is based on Relational Frame Theory (RFT): a research program on the operation of the human mind (Hayes, Barnes-Holmes, and Roche, 2001). It is an innovative therapeutic approach with strong science base, based on mindfulness, directed to develop “psychological flexibility” that allows you to overcome the critical moments and to fully live the present, moving in the direction outlined by their values.

So we immediately decided to add a *voice command*, operable either by a button located inside each page or using a key word, and a *remote control* that could be associated with the latter. The remote control that we thought it does not exist yet, but it should have a very simple structure (consisting of a switch, 4 arrows that allow to navigate throughout the app and internal sections and a button to enter the areas or to activate the voice command, if held longer).

We have made the interface *extremely simple* by introducing home screens that explain the relative app functions. After leading the user to register and access the application proposes a screen that will guide him to start his path with a few simple questions. Once the brief questionnaire is done the user will be directed to the main screen consisted of four main areas: “Diary”, “Exercises”, “My progress”, “Send information to the therapist”.

At this point the user can complete a daily diary, specify whether the pain limits their lives and if and when the drugs are taken; It will also have the opportunity to carry out some exercises based on ACT therapy in order to learn to not deprive yourself, because of the pain, to perform the most simple daily activities or guided exercises for relaxation.

These factors will be constantly monitored through sections of the constantly updated statistics, so you can choose whether or not to share with his therapist that may indicate by himself or locate via geolocalization. In addition, every week the patient will be asked to answer a questionnaire, the application will notify him via a notification.

The result of our prototype was also the result of a qualitative test that we submitted to *80 people between 9 and 74 years* and which has allowed us to make further changes to those as above, based on the results of questionnaires and the bugs in footnote page.

II. DEVELOPING A PROTOTYPE

Our starting point consisted in examining similar apps already developed and released, in

doing so we noticed that signing up and logging in are not straight forward enough, sections are not well defined, it can be difficult to navigate the web site and find what we are looking for, font used is quite small; furthermore, our app will have an option to send data to a therapist chosen by the user. At this stage, having a clear idea about both customers' feedback and the problems encountered when examining "ActOnPain", we started to think about a prototype for our app. As for our first step, we worked on paper prototyping during which we identified the main points that we thought the app should have, after which we can move to a *Java* version.

In our opinion, it is crucial *to motivate* the user in using the app and reduce the likelihood of taking medications meant to alleviate and/or prevent the pain; for this reason, we added a section where the user can keep track of which medication and when it was taken, all of this info can be monitored via some statistics that will be constantly updated.

One of the requests from our customers concerned the possibility to use this app for users with limited limb mobility, in order to address this issue we decided, in agreement with literature, to resort to a selection of IT tools. For this type of mobility difficulties, usually the following devices are used: eye tracker, sensors, input devices and speech recognition [4].

This prompted us to add a voice command, which will be triggered by a toggle button present on every page or by a keyword, furthermore a remote control could be paired with said voice command. The above mentioned remote control has not been developed yet, however it should have an extremely simple design (consisting of a power button, 4 directional arrows to navigate the app and its sections, and a key to access areas or activate a voice command, when being pressed down, fig. 1).

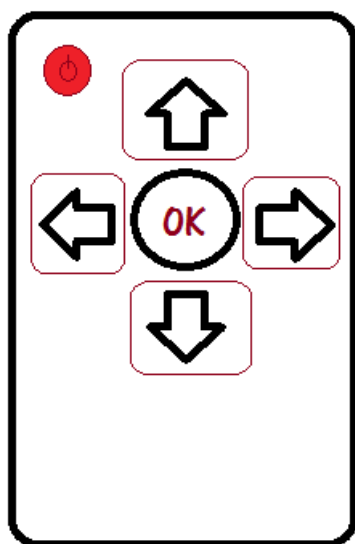


Fig. 1. Remote control design

We designed the user interface to be extremely simple with the introduction of landing pages aimed to explain how the app works. After guiding the user through signing up and log in, our user will be displayed a page that will direct him to his path after few simple questions. After a short questionnaire (fig. 2), our user will be directed to a home page consisting of four macro-areas: "Journal", "Exercises", "My Progress" and "SendData to Therapist" (fig. 3).



Fig. 2. Screenshot of the login page, where the user can put his data or register



Fig. 3. Screenshot of the home page, where the four sections are displayed

At this stage, our user will be able to keep a *daily journal*, noting down if pain hinders his life and, if and when he took any medications; he will also be able to carry out some *exercises based on ACTtherapy* aimed for him to learn how not to deprive himself from carrying out the most basic everyday activities because of pain or exercises for relaxing (fig. 4–8).



Fig. 4. Screenshot of the exercises that can be done by the user. Page is divided in three parts: diary, pain evaluation and medicine



Fig. 5. Screenshot of the personal diary page,



Fig. 6. Screenshot of the weekly test: the user estimates the answer in a scale from 0 to 10 where the minimum is “nothing”

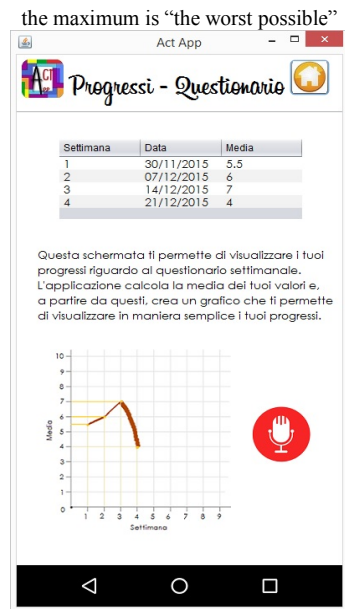


Fig. 7. Screenshot of the progresses of the tests. The app controls the progresses of all the tests done calculating the average of the and values given and providing the possibility to check the user improving condition



Fig. 8. Screenshot of the page that allows the user to contact the therapist. The user can add all the information about his therapist at his first login and then he can chose the information to send.

All of the above will be accessible for constant monitoring for the user via a section showing constantly updated, after which he can choose whether or not to share them with a therapist which he can choose directly or be suggested via geolocation. Furthermore, our user will be presented a questionnaire on a weekly basis, our app will display a notification in such case.

The outcome of our prototype was also influenced by a qualitative test which we submitted to 80 subjects with age ranging from 9 to 74, which allowed us to work on further changes, drawing on results from the surveys and bugs reported to us in the footnotes.

III. CONCLUSION

Starting from the work mentioned above, we reached a final prototype which we think addresses all of our customers' requests. We also recorded positive feedback from the research carried out on a large sample: our app is simple to use for both elderly people and those with poor technological knowledge. As previously mentioned, we think that it would prove useful to pair it with a remote control allowing navigation, however this should be postponed to a future implementation as such a device has not been designed yet. Furthermore, it will be possible to add more exercises and organize them in some levels that can be unlocked through perseverance and continuous use of the app.

VI. REFERENCES

- [1] http://www.salute.gov.it/imgs/C_17_pubblicazioni_2076_allegato.pdf
- [2] Tratto dal Journal of Contextual Behavioral Science - "Acceptance and Commitment Therapy for chronic pain: A diary study of treatment process in relation to reliable change in disability" - Kevin E. Vowles, Brandi C. Fink, Lindse L. Cohen
- [3] "NEUROBIOLOGICAL AND CLINICAL RELATIONSHIP BETWEEN PSYCHIATRIC DISORDERS AND CHRONIC PAIN" (Marijana Braš1, Veljko Đorđević1, Rudolf Gregurek1 & Maša Bulajić2 1Department of Psychological Medicine, University Hospital Centre Zagreb, Croatia School of Medicine University of Zagreb, Croatia 2Croatian Institute of Emergency Medicine, Croatia)
- [4] <http://elite.polito.it/files/courses/01OQM/slide2014/ausili-informativi-motori.pdf>
- [5] *Atkinson* – Hilgard. Introduzione alla psicologia. PICCIN Padova, 2011
- [6] *Baldi P. L.* (2007). Elementi introduttivi al testing psicologico (con esercizi svolti). Milano: Franco Angel
- [7] Pain Acceptance, Psychological Functioning, and Self-Regulatory Fatigue in Temporomandibular Disorder Tory A. Eisenlohr-Moul, Jessica L. Burris, and Daniel R. Evans
- [8] General psychological acceptance and chronic pain: There is more to accept than the pain itself Lance M. McCracken*, Jane Zhao-O'Brien
- [9] "ACTonPAIN" <http://www.oid.ibisinfo.net/Public/index.php#ind>

WEB SERVICE IRONBRAIN FOR IMPROVE REMEMBERING AS AN ALTERNATIVE TO ANKI

Yaroslav Baranow
student

Saint-Petersburg State University of Aerospace Instrumentation
Saint-Petersburg, Russia

kciray8@gmail.com

Abstract

This article mainly reviews learning techniques and web-service IronBrain (IB) [1]. First part of this survey describes spaced repetition algorithm and its implementation in Anki [2] and SuperMemo [5]. Second part is dedicated to overview IronBrain, its advantages and goals.

Keywords: learning techniques, IronBrain, Anki, SuperMemo.

I. INTRODUCTION

Our brains are efficient machines, and they rapidly discard information that doesn't seem useful. Chances are that you don't remember what you had for dinner on Monday two weeks ago, because this information is not usually useful.

The brain's "use it or lose it" policy applies to everything we learn. If you spend an afternoon memorizing some science terms, and then don't think about that material for two weeks, you'll probably have forgotten most of it. In fact, studies show we forget about 75% of material learnt within a 48 hour period [3]. This can seem pretty depressing when you need to learn a lot of information.

The solution is simple, however: review. By reviewing newly-learned information, we can greatly reduce forgetting.

The only problem is that traditionally review was not very practical. If you are using paper flashcards, it's easy to flick through all of them if you only have 30 of them to review, but as the number grows to 300 or 3000, it quickly becomes unwieldy.

There are special techniques and special software for easy remembering a large amount of information.

II. SPACED REPETITION

The *spacing effect* was reported by a German psychologist in 1885 [4]. He observed that we tend to remember things more effectively if we spread reviews out over time, instead of studying multiple times in one session. Since the 1930s there have

been a number of proposals for utilizing the spacing effect to improve learning, in what has come to be called *spaced repetition*.

One example is in 1972, when a German scientist called Sebastian Leitner popularized a method of spaced repetition with paper flashcards. By separating the paper cards up into a series of boxes, and moving the cards to a different box on each successful or unsuccessful review, it was possible to see at a glance a rough estimate of how well a card was known and when it should be reviewed again. This was a great improvement over a single box of cards, and it has been widely adopted by computerized flashcard software. It is a rather rough approach however, as it can't give you an exact date on which you should review something again, and it doesn't cope very well with material of varying difficulty.

The biggest developments in the last 30 years have come from the authors of SuperMemo [5], a commercial flashcard program that implements spaced repetition. SuperMemo pioneered the concept of a system that keeps track of the ideal time to review material and optimizes itself based on the performance of the user.

In SuperMemo's spaced repetition system, every time you answer a question, you tell the program how well you were able to remember it – whether you forgot completely, made a small mistake, remembered with trouble, remembered easily, etc. The program uses this feedback to decide the optimal time to show you the question again. Since a memory gets stronger each time you successfully recall it, the time between reviews gets bigger and bigger – so you may see a question for the first time, then 3 days later, 15 days later, 45 days later, and so on.

While there is no denying the huge impact SuperMemo has had on the field, it is not without its problems. The program is often criticized for being buggy and difficult to navigate. It only runs on Windows computers. It's proprietary software, meaning end-users can't extend it or access the raw data. And while very old versions are made available for free, they are quite limited for modern use.

Anki addresses these issues. There are free clients for Anki available on many platforms, so struggling students and teachers with budgetary constraints

are not left out. It's open source, with an already flourishing library of add-ons contributed by end-users. It's multi-platform, running on Windows, Mac OSX, Linux/FreeBSD, and some mobile devices. And it's considerably easier to use than SuperMemo.

Internally, Anki's spaced repetition system is based on an older version of the SuperMemo algorithm called SM2. Subsequent versions have managed to squeeze out a little more learning efficiency, but they come at the cost of greatly increased complexity, and they are more susceptible to scheduling errors in real-world use.

III. SUPERMEMO2 ALGORITHM

1. Split the knowledge into smallest possible items.
2. Repeat items using the following intervals:

$$I(1):=1$$

$$I(2):=6$$

$$\text{for } n>2: I(n):=I(n-1)*EF$$

where $I(n)$ – inter-repetition interval after the n -th repetition (in days), EF – E-Factor of a given item.

If interval is a fraction, round it up to the nearest integer.

3. After each repetition assess the quality of repetition response in 0–5 grade scale, where 5 – perfect response; 4 – correct response after a hesitation; 3 – correct response recalled with serious difficulty; 2 – incorrect response; where the correct one seemed easy to recall; 1 – incorrect response; the correct one remembered; 0 – complete blackout.

4. After each repetition modify the E-Factor of the recently repeated item according to the formula:

$$EF' := EF + (0.1 - (5 - q) * (0.08 + (5 - q) * 0.02))$$

where EF' – new value of the E-Factor, EF – old value of the E-Factor, q – quality of the response in the 0–5 grade scale.

If EF is less than 1.3 then let EF be 1.3.

5. If the quality response was lower than 3 then start repetitions for the item from the beginning without changing the E-Factor (i.e. use intervals $I(1)$, $I(2)$ etc. as if the item was memorized anew).

6. After each repetition session of a given day repeat again all items that scored below four in the quality assessment. Continue the repetitions until all of these items score at least four.

IV. IRONBRAIN ADVANTAGES

Web-service IronBrain based on SM2 algorithm and offer some valuable features.

1. Unlike Anki, IronBrain is full web-based. You can use it from any operation system without installing. In some cases, this is a useful feature. As example, you can use IronBrain on work even if you don't have a permission to install desktop applications.

2. Anki is oriented on enhance vocabulary and language studying. IronBrain is oriented on study sciences and remembering connected facts.

3. Flashcards in Anki is independent from each other [6]. This approach is good for memorizing words, but isn't very effective for scientific knowledge. IronBrain let you create any level hierarchical structure (fig. 1) and store flashcards in it. It's very convenient to create folders based on text-book structure.

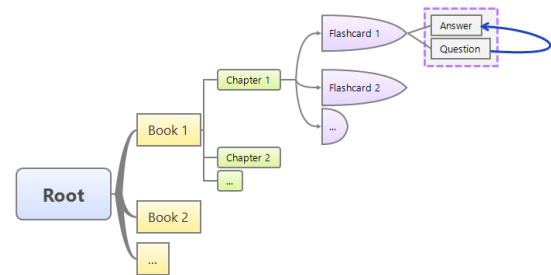


Fig. 1. Hierarchical structure

V. TARGETS

You can effectively use IronBrain for targets listed below.

1. Deep study of any programming language, like Java, C++, C# etc.
2. Deep study of graphics software, like Blender, 3Ds max, Photoshop etc.
3. Preparing to exams in university.
4. Preparing to job interview.

VI. CONCLUSION

The best way to remember is to make repetitions of the learned material. There are many programs that can make repetition easier and faster. They all have their own advantages and limitations. I believe that suggested system and its conceptions will take place in real education. IronBrain has some disadvantages, such as lack of support LaTeX and social functions, but I'm going to add them in the future.

VII. REFERENCES

- [1] Web service IronBrain. <http://www.ironbrain.org/main> (retrieved on 3 March 2016).
- [2] Friendly, intelligent flash cards. Remembering things just became much easier. <http://ankisrs.net/> (retrieved on 3 March 2016).
- [3] Human Memory: Theory and Practice", Alan D. Baddeley, 1997.
- [4] *Ebbinghaus, Hermann* (1885). Über das Gedächtnis. Untersuchungen zur experimentellen Psychologie [Memory: A Contribution to Experimental Psychology] (in German). Trans. Henry A. Ruger & Clara E. Bussenius. Leipzig, Germany: Duncker & Humblot.
- [5] SuperMemo - Learn fast and forget about forgetting. <https://www.supermemo.com/> (retrieved on 3 March 2016)
- [6] Anki manual - can I link cards together. <http://ankisrs.net/docs/manual.html> (retrieved on 3 March 2016).
- [7] Web service IronBrain for education. <https://habrahabr.ru/post/249187/> (retrieved on 3 March 2016).

ANALYSIS AND SYNTHESIS OF ORGANIZATIONAL AND TECHNICAL SOLUTIONS IN THE ORGANIZATION OF THE HIGH-TECH PRODUCTION

Alexander Chabanenko
Postgraduate

Saint-Petersburg State University of Aerospace Instrumentation,
Saint-Petersburg, Russia

Chabalexandr@gmail.com

Abstract

Development of scientific and technological progress is a driver of development of the high-tech production, the cost of which laid a large proportion R&D. For the sustainable development of scientific and technical potential of Russia requires analysis and synthesis of organizational and technical solutions Organization of production of high technology products. The priorities of the industrial policy of Russia at this stage are to increase competitiveness of production and effective promotion of high-tech products on the domestic and foreign markets. In policy documents of the Government aim is to modernize the economy, high-tech development, increasing the share of high-tech products exports. The solution to these problems is not possible with traditional approaches to knowledge production.

Keywords: Innovation, neural networks, high-tech industry, production organization.

Characteristic features of knowledge-based enterprises make the specifics of organization of production processes. Distinctive features of the organization of production processes, knowledge-based enterprises: high organizational flexibility and adaptability of production processes, the organization works for quick change over of equipment provisioning of the production process personnel of high qualification, coordination of all kinds of works, accelerated training of production and development of competitive high-tech products, ensuring the quality of production processes and products.

Particular organization of production processes of high-tech enterprises are subject to a certain logic, which is implemented through a system of principles. Synthesis of theoretical and practical provisions made it possible to form the basic principles of organization of production processes, knowledge-based enterprises and to clarify the content of tasks aimed at their implementation (table 1).

Table 1

Principles of organization of production processes of a knowledge-based enterprise

The name of the principle	The content of the principle	The contents of tasks aimed at the implementation of the principle
Parallelism	Reduction of production cycle	The simultaneous execution of operations and stages of the production process, both in the context of a knowledge-based businesses and stakeholders in the design and development of high-tech products
Flexibility	Rapid reconfiguration of production processes in the production of new products with a minimal loss of time and money	Rapid response in the restructuring and retooling of the production process in connection with the transition to the new knowledge-based products
Integration	Ensuring the association between the processes of design, development and production of high-technology products	Information Association of participants of the process of production of high-tech products, the formation of integrated organizational and production structure
Completeness	Minimum but enough participants to carry out the full complex of works on the design, development and production of high-technology products	Cost minimization in the design and manufacture of competitive products of high-technology products
Adaptability	Quick change over of equipment	Rapid adaptation of production processes to design and technological changes

The problem of the development and dissemination of science-intensive technologies are relevant because of their special importance for sustained development of economy and society, as they contribute to and ensure the improvement of living standards through intensive factors: productivity growth, lower relative consumption level and increase the efficiency of use of irreplaceable natural resources.

Belonging to the category of knowledge-intensive sectors of the economy is characterized by the indicator of knowledge-intensity of production, defined by the ratio of expenditure on research and development (VR&D) to the amount of the gross product of this industry (Vvp): $(VR\&D/V_{vp}) * 100\%$.

It is believed that for knowledge-based industries this indicators should be 1.2–1.5 and more time succeed average on heavy industry.

In world statistics, industry and enterprises are classified at high, medium and low technology based on the values of the data the coefficients research intensity.

In this classification, there are two basic approaches:

- classification of sectors of high-technology. The main criterion is the intensity of the use of innovation in the production process;
- classification in terms of product. The main criterion is raising the final product.

The main distinctive feature of high-tech industries considered mass production of science intensive technologies. Such technologies are created and implemented at all economic levels. Classification of industries represented in research intensity factor (table 2).

Table 2

Distribution technologies according to the ratio of research intensity

Technology	Research intensity ratio, %
High	More than 17
Medium-highlevel	5–17
Average lowlevel	2.3–5.5
Low	0.5–2.3

Criteria distribution technologies on groups are conditional in nature, so as the high-tech industries referred to only those for which the ratio of expenditure on R&D and volume of output products (research intensity) exceeds a certain value. However, to assess the performance of the industry or company you want to deal with and other factors: relevance of the number of employees engaged in scientific developments in industry to the over all number of employees, the cost for R&D in the calculation for one employee and so on [1].

Modern standards BS 7000 2013 production control systems. Establish a close relationship of production and R&D (research and development). On (fig. 1) you can see the role of R&D at the modern innovation production.

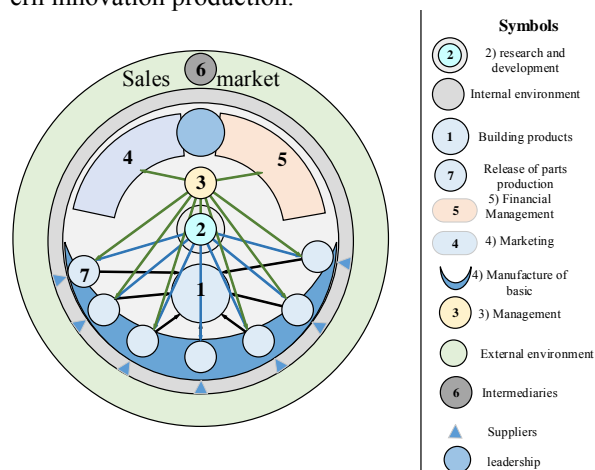


Fig. 1. Role of research and development in the work of the enterprise in BS7000

In Russia for the basis adopted classification of industries and enterprises on the degree of effectiveness based on the coefficients of the research intensity. By the West economists is traditionally high-tech considered those industries in which share costs on scientific development in manufactured products is more than 17%. On the extent of development of science and technology changes and list of high-tech industries. At the present day in Russia to high-technologies, include:

- manufacture of pharmaceutical products;
- production office equipment and computer technology;
- production of components, equipment for radio, television and communications;
- production of medical products, means of measurement, monitoring, control and testing; optical devices, photo and film equipment;
- production of flying machines, including the space.

You should have in mind that in present times occurs industrial mastering VI technological lifestyle, which includes in itself high-tech, genetic engineering of animals, multimedia interactive informational system, high-temperature superconductivity etc.

Many high-tech industries will form a high-tech complex, which plays a special role in the economic development of the country.

Firstly, the high-tech enterprises are developed and introduced the latest innovative technology, which then can be used in other less technologically advanced industries.

Secondly, the competitiveness of products, manufactured in high-tech industries, much higher on the world market and this requires the full sup-

port of the organization of the production of high technology products [2].

However, in view of the complexity of the proceeding processes in production research intensity gained popularity algorithms for solving problems of system analysis with application of neural network model.

Neural network used for solving control tasks, classification, forecasting. Such success is determined by the following factors:

Neural networks – is a powerful method for simulation of phenomena and processes, which allows you to display the most complicated dependencies. Neural networks are nonlinear in nature, at the same time, as for several years to create models applied linear approach. As well as, in many cases, neural networks have helped to overcome the so-called "curse of dimensionality", because the establishment of the model of nonlinear phenomena requires a lot of computing resources (in case of a large number of variables).

Next feature of neural networks is that learning mechanism is used. The user selects the representative system of neural data and starts the algorithm, which configures network settings without user intervention. From the user only requires a set of heuristic knowledge

How to prepare and select data, choose the necessary neural network architecture and to interpret the results. However, it should be noted that the level of knowledge required from the user, which is essential for the successful implementation of the neural system, much smaller than, for example, when using traditional methods.

For convenience, create a neural network Matlab software package was used.

Artificial neural network in Matlab represent a new trend in the practice of technical systems. Ability of neural networks to perform a compare operation on the model and classification of objects, inaccessible to traditional mathematics, allow you to create artificial systems for solving the problems of

pattern recognition, diagnosis, automatic analysis of documents and many other innovative applications.

Neural network constitute a system of interconnected and interacting of simple processors (neurons).

The network consists of neurons interconnected by synapses adders as follows (fig. 2). Signals arising during operation of the network are divided into direct (used in the delivery of results by the network) and dual (used in teaching). (Black-input layer neurons, Grey-hidden layer neurons (interim), White-output layer neurons).

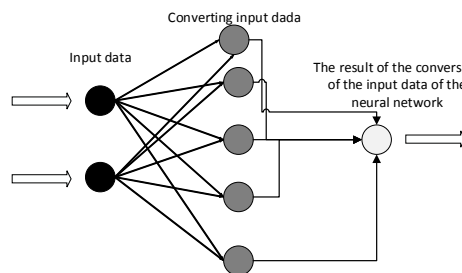


Fig. 2. Example of a neuron in a neural network

The neuron is the basic element of a neural network, a single simple computing processor able to perceive, transform and distribute signals in turn merging a large number of neurons into a network allows us to solve complicated tasks.

Neural network approach is model restrictions; it is equally suitable for linear and complex nonlinear problems, as well as classification tasks. Neural network training first is to change "power connections between neurons. Neural networks are scalable; they are able to solve problems, both within a single equipment, and the scale of plants in general.

Apply this neural network, it was decided to predict the number of patents, which is an integral part of the high technology industry in the country.

Data taken based on IPC with State Agency Rospatent (table3) [3].

Table 3

Number of invention patents of the Russian Federation [3]

IPC Section	2004	2005	2006	2007	2008	2009	2010	2011	2012	2013	2014
Human necessities	123	2054	200	1508	5252	6514	8468	8907	9506	8042	9890
Performing operations; transportation	220	556	25	1055	3454	3456	4711	4412	4969	4965	5331
Chemistry; metallurgy	202	3025	100	556	3499	3588	5167	5512	5524	5779	5154
Textiles; paper	355	956	50	229	202	390	320	301	274	271	305
Construction; mining	357	457	12	596	955	1402	1977	1603	1898	1807	2033
Mechanical engineering; lighting; heating; motors and pumps; arms and ammunition; blasting work	259	2257	123	914	988	2237	3062	2761	3246	3453	3459
Physics	300	4522	221	601	1720	2463	3734	3881	4381	4285	4484
Electricity	188	541	62	569	1087	3147	2883	2622	3082	3036	3294
Subtotal:	2004	14368	793	6028	17157	23197	30322	29999	32880	31638	33950

In the selection box of the input strings: [12345678; 910111213141516171819] where number 1–8 are the code of each indicator, and 9–19 coding for a year from 2004 to 2014, respectively.

Fig. 3 show the setting parameters of the neural network.

On fig. 4, a graph of the network learning where to find extrema using gradient functionality

on a configurable parameter error, *mu* shows reduction factor network errors, *val fail* displays the control vectors used to stop training early if the network performance on the validation vectors fails to improve or will remain at the same level for consecutive periods max fail, and on fig. 5 represented by the construction of the basic structure of the neural network forecasting in Matlab.

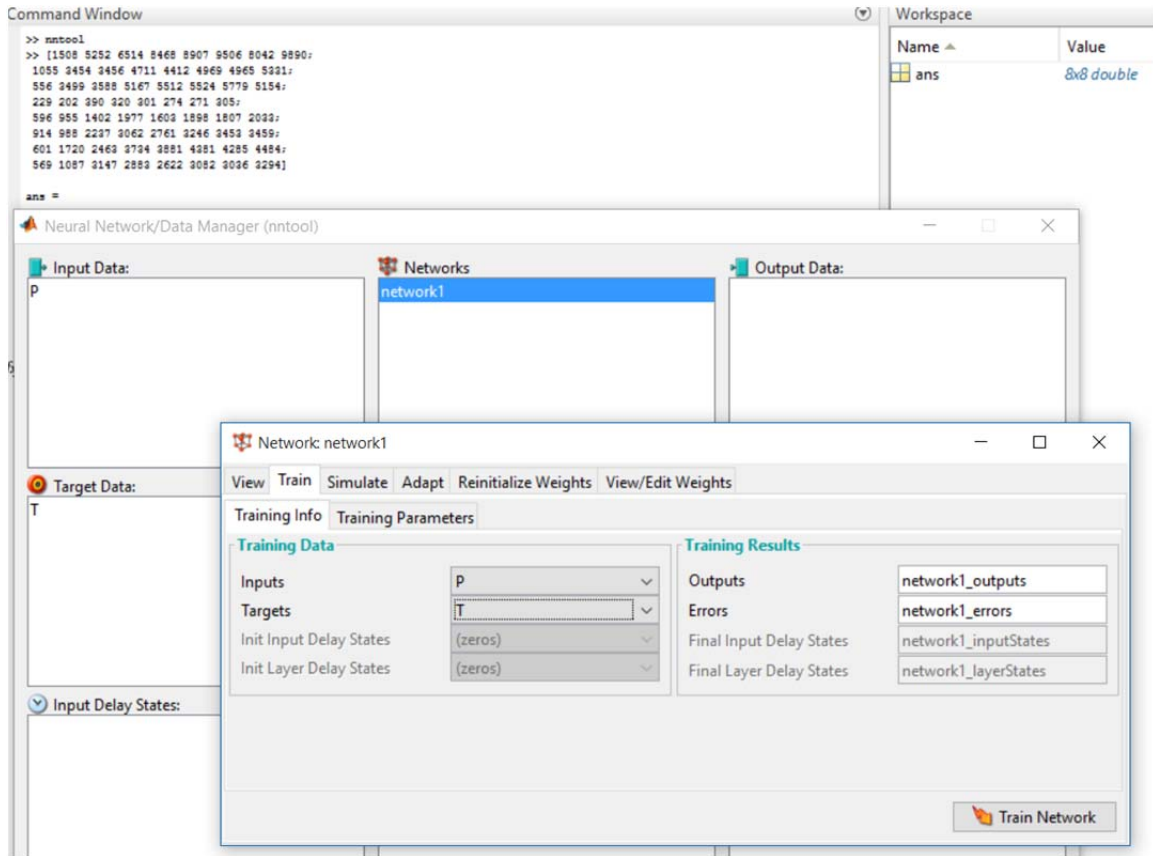


Fig. 3. Neural Network Settings

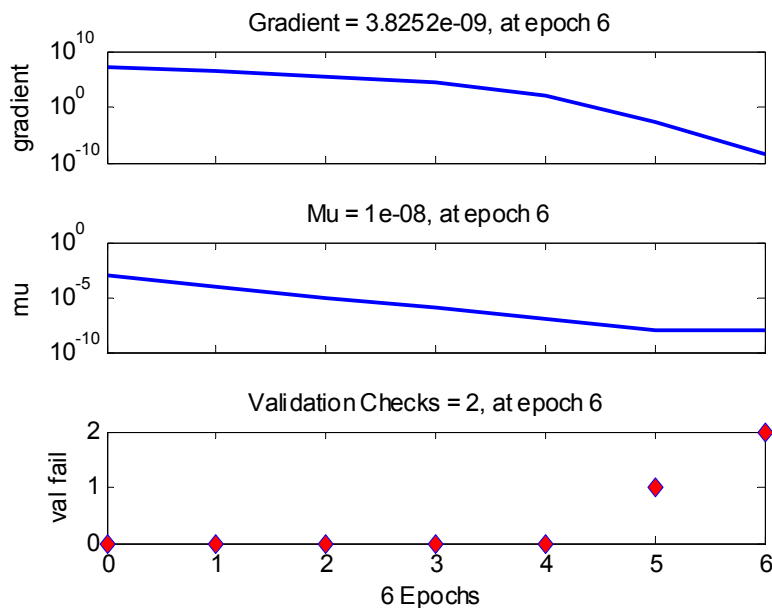


Fig. 4. Training neural network

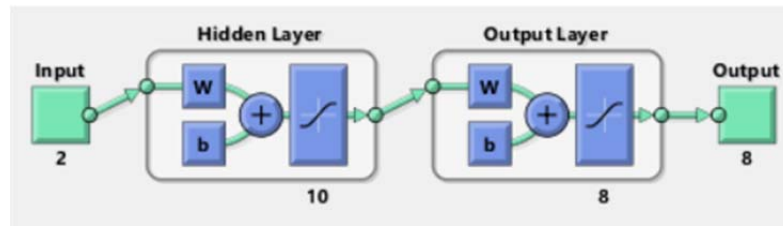


Fig. 5. A neural network structure

To evaluate the accuracy, an average absolute error in percentage, was a network error 7.95%, suggesting a productive system.

Comparing the data issued by the system, and the actual data, you can ensure that the neural network really makes forecasts closer to reality (table 4).

Table 4

These neural network forecasting and actual data from sources

The data obtained in the course of neural network 2015y.	Data from the source 2015y.
9790	9820
5055	4948
5437	5428
226	311
1906	1925
3477	3598
4297	4358
3182	3471

Technology of artificial neural networks a one of the most important of modern science. They are widely used in various fields of science and production.

CONCLUSION

Using organization-technical solutions in the organization of the high-tech production will not only improve the quality of targeted products and improve technical and economic indices, but also greatly reduce the time and cost of R&D while creating high technology products, as well as the use of innovative methods of analysis of the production efficiency to cope with related tasks.

Industrial and scientific centers were given the opportunity to exploit the full potential of scientific-technical complex for the successful introduction of new technologies, the solution of technolog-

ical problems in the process of production, as well as increasing and maintaining competitiveness.

REFERENCES

- [1] Чабаненко А. В. Стандартизация наукоемкой продукции // РИА Стандарты и качество. – М., 2015. – № 1. – С. 42 – 47.
- [2] Гулевитский А. Ю., Чабаненко А. В. Разработка и внедрение системы управления производством инновационной продукции // избранные научные труды: Материалы IVX междунар. конф. – М., 2015. – С. 159 – 164.
- [3] Federal service for intellectual property (Rospatent), the annual report on activity of Rospatent for year 2014. (Rospatent) [Electronic resource] // A report on the activities of the organization. URL: <http://www.rupto.ru/> (reference date: 02.10.2016).

ABOUT VERSION CONTROL SYSTEMS

Efim Golovin

postgraduate student

Saint-Petersburg State University of Aerospace Instrumentation
Saint-Petersburg, Russia

feanoref@gmail.com

Abstract

This article is a brief comparative review of the most popular version control systems. It provides a definition of version control system describes the main stages of its development and contains an example of its possible classification.

I. INTRODUCTION

Today's software development process includes quite a number of aspects and nuances and each of them demand comprehensive analysis. In order to win the race (given conditions of the modern economics) IT-companies spend time and resources to find the best solutions and ideas (so called 'best practices') for the fastest and qualitative implementation and delivering of their products. One of the key issues in this process is minimization of the impact of the human factor, in other words, automation.

There are a large number of various tools and instruments helping somewhat to automate some of the parts of the software development and delivering process. Thus, we have such kind of auxiliary software as integrated development environment (IDE), continuous integration and delivery systems (CI&CD) etc. They can simplify many of our daily tasks such as code analysis and refactoring, dependency analysis, compiling and testing process, application deployment and so on and so forth. Given that most of the software is being developed by several persons (teams) the importance of software development and delivering management is practically obvious. One of the most popular tools to somewhat solve this task is so called version control system (VCS). This article is a brief comparative review of the most popular VCSs.

II. THE DEFINITION OF VCS

First of all, what does "VCS" mean? A version control system or VCS is a software which is used to manage multiple versions of computer files

and programs [1]. It allows users to lock files so that only one person can edit them at a time, and to track changes to files. It also provides the ability to track who made the changes and when it happened and to get the previous versions of the files and programs.

III. MAIN STAGES OF VCSs DEVELOPMENT

The very first VCSs like, for instance, CSSC [2] and its successor, RCS [3] (which is being installed on some of the UNIX-compatible systems to this day [4]), had been working only on local machines. It was acceptable until team development approach had become more widespread. The logical continuation of those tools were centralized VCS (CVCS). CVCS had been allowing organizing collaboration between developers by means of computer networks with a dedicated server, which had been performing the functions of project versions storage. Two good examples of CVCS are Concurrent Versions System (CVS) [5] and its successor – Apache Subversion (SVN) [6]. CVCS had been providing several very useful features (especially, in comparison with local VCS (LVCS)). Thus, they provided [7]:

- an ability of centralized storing of the most relevant versions of the project;
- more reasonable way to organize storing of versions of the project (instead of many copies of database with versions of the project there had been only one database which was located on a dedicated server);
- a simplified approach of monitoring and distributing tasks between developers.

This model had been the standard of version control for many years (furthermore, some old projects, especially the large ones, use LVCS to this day). Nevertheless, it has its disadvantages. In this case, the most obvious one is server. If it is broken developers will spend a huge amount of time trying to gather all the pieces of the project and risks are that the whole history of the project will be lost. A good solution of this problem would be back-up but even if the history and source codes of the project is saved developers will not be able to collabo-

rate anyway due to server not working. This was the reason for the next step of VCS evolution, which is decentralized VCS (DVCS).

This kind of VCS also provides an ability of team collaboration yet it does not have those disadvantages that LVCSs do. In DVCSs each of the team members has its own full replica of the project and each of them can work as server and client. Thus, two developers can exchange their versions without any dedicated server at all. This approach is more complicated yet it solves those problems presented in LVCSs. Good examples of DVCSs are Git [8], Mercurial [9] and Bazaar [10].

All the previous VCSs are free. However, there are also a big number of proprietary VCSs exist. For LVCSs, good examples are Polytron Ver-

sion Control System (PVCS) [11] and Quoma Version Control System (QVCS) [12]. Panvalet [13] and Team Foundation Server [14] are good examples of proprietary CVCSs. Finally, Bit Keeper [15], Team Ware [16] and Plastic SCM [17] are proprietary DVCSs.

IV. A POSSIBLE VCS CLASSIFICATION

There are quite a big number of various VCSs and each of them differs one from another. It is possible, however, to derive specific characteristics, which can be used in order to classify all VCSs. Fig. 1 represents a possible example of that classification.

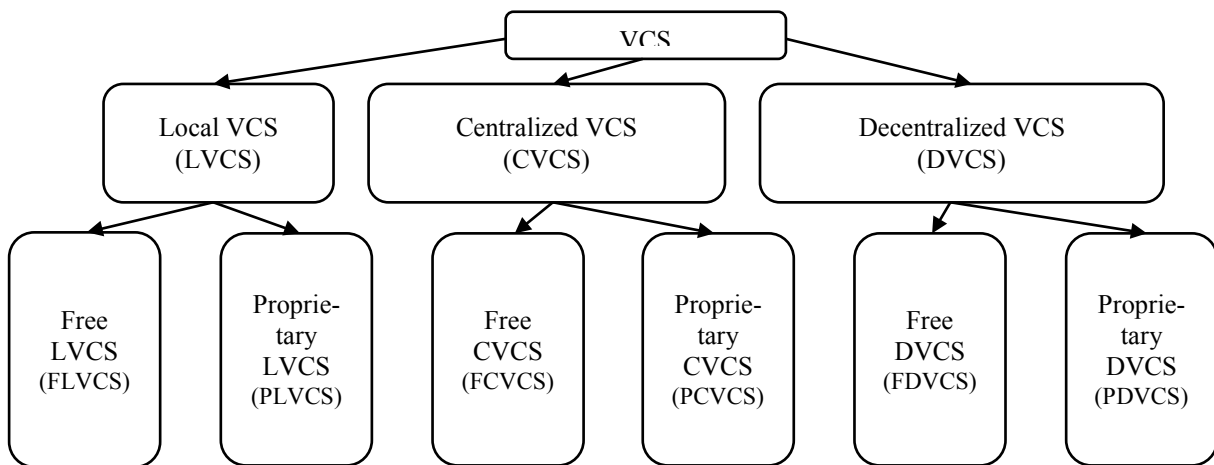


Fig. 1. A possible example of VCS classification

Apparently, exist other ways to classify VCS sand this classification provided here is only a rough approximation. Yet we already can name some of the characteristic of VCS having only an abbreviation. For example if we know about some VCS that it is FDVCS we already can say that it can be used in a network without having a dedicated server and we can use it for free. Thus, Git is FDVCS, which means that it has characteristics mentioned above while RCS is FLVCS and differs from the first one.

V. CONCLUSION

So, in this article VCS, LVCS, CVCS and DNCS were briefly discussed, some of the advantages and disadvantages were presented, for each kind of VCS several examples were given and an example of possible classification was introduced. Obviously, to consider this topic in more details an additional material is needed. However, in author's opinion the goal of this article, which is a brief review of the most popular VCSs is more or less accomplished.

VI. REFERENCES

- [1] http://techterms.com/definition/version_control – The Tech Terms Computer Dictionary.
- [2] <http://www.gnu.org/software/cssc/manual/Overview.html#Overview> – official site of CSSC (Compatibly Stupid Source Control).
- [3] <https://www.gnu.org/software/rcs/> – official site of RCS (Revision Control System).
- [4] Scott Chacon, Ben Straub – Pro Git, vol. 2, p. 27 – 28.
- [5] <http://savannah.nongnu.org/projects/cvs> – official site of CVS.
- [6] <http://subversion.apache.org> – official site of SVN.
- [7] Ben Collins-Sussman, Brian W. Fitzpatrick, C. Michael Pilato – Version Control with Subversion, book compiled from revision 1337, p. 8 - 19.
- [8] <https://git-scm.com> – official site of Git.
- [9] <https://www.mercurial-scm.org> – official site of Mercurial.
- [10] <http://bazaar.canonical.com/en/> – official site of Bazaar.
- [11] <http://www.serena.com/index.php/en/products/quality-release-management/pvcs-vm/> – official site of PVCS.
- [12] <https://github.com/jimmy39/qvcsos> – official site of QVCS.
- [13] <http://www.ca.com/us/products/ca-panvalet.html> – official site of Palvalet.
- [14] <https://www.visualstudio.com/products/tfs-overview-vs> – official site of Team Foundation Server.
- [15] <http://www.bitkeeper.com> – official site of BitKeeper.
- [16] <http://docs.oracle.com/cd/E19957-01/806-3573/TeamWareTOC.html> – official site of TeamWare.
- [17] <https://www.plasticscm.com> – official site of Plastic SCM.

“DISLHELP”: A VALUABLE AID FOR CONDUCTING EXERCISES TO DYSLEXIC

Marco Gravagno, Giuseppina Ferracane, Stefania Roncade, Gaia Burgio, Biagio Salamone
students

“Kore” University of Enna
Enna, Italy

marco.gravagno@unikorestudent.it; giuseppina.ferracane@unikorestudent.it;
stefania.roncade@unikorestudent.it; gaia.burgio@unikorestudent.it; biagio.salamone@unikorestudent.it

Abstract

Raising a child with dyslexia can stir up a lot of emotions. You may look ahead and wonder if this learning issue will affect your child’s future. But dyslexia is not a prediction of failure. Dyslexia is quite common, and many successful individuals have dyslexia.

A good way to understand dyslexia is to establish what it is not. It’s not a sign of low intelligence or laziness. It’s also not due to poor vision. It’s a common condition that affects the way the brain processes written and spoken language.

Our software application, “Dislhelp”, wants to facilitate the "information decoding process" which is missing with the dyslexic subjects. It is based on an hardcopy exercise already in use with psychologists. "Dislhelp" helps dyslexic childrens to study in a funny and quickly way. Nowaday it is a grafic interface only, but we plan to make it real.

Why do we have to make dyslexic childrens life harder?

I. INTRODUCTION TO DYSLEXIA

SLD (Specific Learning Disabilities) The term means a disorder in 1 or more of the basic psychological processes involved in understanding or in using language, spoken or written, which disorder may manifest itself in the imperfect ability to listen, speak, read, write, spell, or do mathematical calculations."They start manifesting with children from 6 to 10 years ages.

Specific learning disabilities may occur in the following areas of academic skill.

Reading

A specific learning disability in reading is commonly called dyslexia. This specific learning disability is “characterized by difficulties with accurate and /or fluent word recognition and by poor spelling and decoding abilities. Individuals with dyslexia experience difficulties with reading accu-

racy, rate and comprehension. They are also likely to struggle with phonological coding, or the ability to readily and easily associate speech sounds with individual letters and/or groups of letters, which is a central part of the reading process.

Written Expression

Also called dysgraphia and/or dysortography, this specific learning disability is focused on the production of written language. Motor dysgraphia relates to persistent handwriting difficulties associated with an impairment in motor coordination. Language-based dysgraphia is associated with difficulties in constructing meaningful and effectively structured written expression. These are students who have extreme difficulty getting their thoughts both in order and then down on paper. Many students with dysgraphia also have dyslexia.

Mathematics

Also called dyscalculia this specific learning disability presents as a severe difficulty with number faculty and mathematical ability.

Other factors influencing SLD may be characterized by behavioural attitudes like Hyperactivity, attentional deficits (ADHD), Emotional lability, Impulsivity, Distractibility, Perseveration.

Relying on the above, the related treatment should be based not only on the specific learning aspect, but also to the school and family environment and the socio-cultural and relational context.

A fairly explanatory model concerning human behavior and his learning history is being offered by the Relational Frame Theory, a post-Skinner's theory of language and human cognition.

Steven Heyes, founder of the theory (Hayes, Barnes-Holmes, Roche, 2001), proceeding beyond the concept of operant Skinneriana, it has extended the empirical Sidman studies basis of equivalence classes (Sidman 1994). Latter and in general the research on relational elicited responses, have helped to develop effective pathways in clinical and educational field. (Barnes-Holmes, Barnes-Holmes, Cullinan 2000)

For the learning of reading and writing, in our case, we experience two new and peculiar features of the training of equivalence classes: working directly on decoding and comprehension; secondly, education is reduced to only two reports from which are then deriving the other. And in virtue of this, researches set out to explore the effects of training and mainly on issues related to children with specific learning disabilities (such as dyslexia). For these reasons, we have tried to develop an application that allows a child with dyslexia to learn in an easy, quick and funny way. The description of the method will be outlined in the following chapter.

II. EQUIVALENCE CLASSES AND TRAINING

Both reading and writing are the topics affecting language development of children, when they have to take their schooling. The training sessions are based on reinforcing choosing a comparison stimulus (comparison) when a sample stimulus is showed (sample), and to reinforce, in a second phase, the choice of an alternative stimulus when a second sample stimulus is showed.

The execution of this technique takes place through the training phases and then with tests, which use the principles of equality, symmetry and transitivity

The first training will reinforce the first relation, $A=B$, by means of positive reinforcement which will be released as soon as the child's information respond correctly (fig. 1). From that, it follows a first test that will be referred to the principle of equality that if $A=B$, then $B=A$ (fig. 2). After learning this first relation, a second stimulus is given: the stimulus C from which begins the second learning training, $B=C$; following a subsequent test to obtain the confirmation of this new learning, $C=B$.

HOME



Fig. 1. Training $A=B$



SNOW

SAUCE

HOME

Fig. 2. Test $B=A$ (the triplet refers to Italian language exercises)

At the end of the first two trainings the child, through the principle of transitivity, will have learned that if $A=B$ and $B=C$, it follows that $A=C$. In order to ensure that this method is effective, positive reinforcements are introduced: rewards granted right after an action you want to repeat. The choice of an enhancer must be effective, so as to be easily available, given after a desired behavior, it can be used multiple times without causing a saturation and does not take too long in its consumption.

III. DESIGN AND DEVELOPMENT

The structure of this program is based on a technique that foresees the use of 5x5 sized cards where images are depicted, the words written in capital letters and words written in lower case with Arial font, size 36.

Research

Before proceeding with designing our program, we documented some of scientific papers which have pointed out that the child with dyslexia, besides having a learning disability, is unable to keep the attention for a long time.

Later we moved to the analysis of some already existing programs that are designed just as compensatory instruments. It appeared that some of them show a interface with its visual images and colors that could easily distract the child, intent in performing the exercises, unlike the results of research previously effected. Even voice synthesis appears unsuitable for training, not only because it devolved the child, but also because it would provoke a decline in motivation and attention.

Our software tries to overcome the shortcomings of other software, proving that it is possible to learn reading and writing skills also forgoing a vocal stimulus and administering only positive reinforcers, using a teaching technique without error.

Product development

In the initial stage of the program the child will be encouraged to proceed with the execution of the task and the first phase of the training will start to be followed by a test phase. This sequence is carried out twice for each triplet, followed by a final sequence of tests which will demonstrate the comprehension of the previously performed training. If the child, during the test phase, achieves an excessive errors percentage (roughly 80% of all responses), the exercise will automatically return to the training phase. Vice versa, if the test will succeed the child receive a reinforcement.

The training phase is characterized by the provision of a reinforcement, equal to one point, whenever the child gives the right answer (fig. 3).

Due to the anxiety component of the child in the event that he makes a mistake it will be corrected highlighting the right answer. In the testing phases, in

CLEVER!
You win a banana



Fig. 3. Reinforcement to training phase

case of error, the screen will clear and will continue with the next item (fig. 4). At the end of the task, he will receive a score equal to the number of correct answer. Afterwards the child can decide whether to leave the program or engage in game that will be a further test that does not provide penalizations in case of errors.



Fig. 4. Error to training phase

IV. CONCLUSION

Before being released will be necessary to perform tests concerning the level of learning. This test are:

- MT evidence of Cornoldi, Colpo and Tressoldi, which relies on using tasks with multiple choice answers, focused on reading a passage from and subsequently answer questions choosing between the different options;
- the DDE-2 of Giuseppe Sartori, Remo Job and Patrick E. Tressoldi, which allows us to evaluate the level of competence acquired in both reading and writing by administering 5 trials for analysis of the reading process, and 2 trials for the analysis of the writing process.

After collecting test results we proceed by administering the application for an estimated period of around two months, subsequently will be re-administered the test battery. The results of the first study will be compared to the results of the second study and placed in chart in order to make easier the reading of the learning curve.

To complete software's development we carried out additional research that led to the light of improvements, such as:

- easy reading Font: font only subjected to scientific studies, approved by AID (Italian Dyslexia Association), since the characteristics which make it unique are the presence of an essential design, in order to avoid the perceptual crowding and special factors, in order to prevent the exchange between similar letters;
- creating a mini world: a virtual environment that can be customized by the child by purchasing decorative elements through use of points accumulated during the course of the task. It has been thought that this could be an additional factor of investigation, for the psychologist, regarding the life of the child;
- "The Psychologist": the psychologist will access a program, linked to the exercise, which will enable him to monitor the developments in the child's learning step and Record any changes everyday, linked through a "Server-Client" service.

V. REFERENCES

- [1] (s.d.). Taken from EasyReading: <http://www.easyreading.it/home-page/>
- [2] A., N. D. (2014). *La caffettiera del masochista. Il design degli oggetti quotidiani.* (N. G., Trad.) Prato: Giunti .
- [3] ACT Italia - the Italian Chapter of the Association for Contextual Behavioral Science. (s.d.). Taken from da ACT Italia: <http://www.act-italia.org>
- [4] airipa. (s.d.). Taken from Airipa ITALIA: <http://www.airipa.it/materiali>
- [5] *Ana Leda de Faria Brino*, R. d. (2012). Restricted stimulus control in stimulus control shaping with a capuchin monkey. *Psychology & Neuroscience*, 5,1, 83-89.
- [6] *Arntzen, H. S.* (2014, May 26). Discrimination Learning in adults with neurocognitive disorders. (L. John Wiley & Sons, A cura di) *Behavioral Interventions*, 241-252. doi:10.1002/bin.1389
- [7] *Beatrice Bertelli, G. B.* (2007, Dicembre). *Giornale Italiano di Psicologia*, XXXIV(4), p. 941-963.
- [8] *Catelli, C. Z.* (2006, gennaio-aprile). *Psicologia Sociale*(1), p. 65-94.
- [9] *Claudia Pizzoli, L. L.* (Aprile 2008). *Psicologia clinica dello sviluppo / a. XII, n. 1*, 25-40.
- [10] *Cristina Burani, L. B.* (2001, Novembre). *Giornali italiano di psicologia*, XXVIII(4), p. 839-963.
- [11] *Elena Florit, M. C.* (2008, Settembre). *Verba Volant, Scripta Manent. Giornale italiano di psicologia*, XXXV(3), p. 641-662.
- [12] *Erickson.* (s.d.). *Dislessia e trattamento sublessicale.*
- [13] *Erickson.* (s.d.). *Dislessia Evolutiva.*
- [14] *Francesco Mannella, G. B.* (aprile 2006). *Sistemi intelligenti / a. XVIII, n. 1*, 75-84.
- [15] *Garry Martin, J. P.* (2000). *Strategie e tecniche per il comportamento - La via comportamentale* (Vol. Sesta edizione). (F. R. Paolo Moderato, A cura di) Milano: McGraw-Hill.
- [16] *Giovambattista Presti, M. S.* (2013). *Applicazioni in campo educativo della Relational Frame Theory.* ResearchGate, 298-319.
- [17] *Giunto O. S.* *Organizzazioni Speciali.* (s.d.). Taken from da <http://www.giuntios.it/catalogo/test/dde-2>.
- [18] *Greco, B.* (2000, Agosto). *Risultati di un training per il recupero delle difficoltà di comprensione sintattica.* *Psicologia clinica dello sviluppo / a. IV, n. 2*, 339-349.
- [19] *Greg Morro, H. A.* (2014, July 24). *Rapid Teaching of Arbitrary Matching in Individuals with Intellectual*

- Disabilities. (A. o. 2014, A cura di) Psychol Rec, 64, 731-742.
- [20] *Guidetti, V.* (2005). Fondamenti di neuropsichiatria dell'infanzia e dell'adolescenza. Bologna: Mulino.
- [21] *Harrie Boelens, M. V.* (2000). Symmetric Matching to Simple in 2-years-old children. The Psychological Record, 50, 293-304.
- [22] *Jennifer Preece, Y. R.* (2004). Interaction Design, beyond human-computer interaction. (F. Rizzo, A cura di) Milano: Apogeo.
- [23] *John T. Blackledge, U. o.* (volume 3, Issue 4, 2003). An Introduction to Relational Frame Theory: Basic and Applications. The Behavior Analyst today, 421-433.
- [24] *la-dislessia.* (s.d.). Taken from da <http://www.aiditalia.org>: <http://www.aiditalia.org/it/la-dislessia>
- [25] *Lucia Carriero, C. V.* (Agosto 2001). COST: a European project for the study of dyslexia and evaluation of the early stages of reading skills. Psicologia clinica dello sviluppo / a. V, n. 2, 261-271.
- [26] *Luigia Camaioni, A. P.* (2001, Aprile). Typical and atypical profiles of referential communication skills: comparison between normal subjects and subjects with specific learning disorder. Psicologia clinica dello sviluppo, V(1), 77-94.
- [27] *Militerni, R.* (2004). Neuropsichiatria Infantile, III edizione. Sorbona: Idelson-Gnocchi.
- [28] *Moderato, P.* (2010). Interazioni umane. Manuale introduttivo alla psicologia. Milano: Franco Angeli.
- [29] *Neuropsy.* (s.d.). Taken from da Neuropsy: <http://www.neuropsy.it/test/dislessia/01.html>
- [30] *Padovani, R.* (Dicembre 2006). Understanding of the written text at school age. A review on the normal and atypical development. Psicologia clinica dello sviluppo / a. X, n. 3, 369-398.
- [31] *Patrizio E. Tressoldi, C. V.* (Agosto 2008). Clinical significance in efficacy studies of treatments for learning disabilities: a proposal. Psicologia clinica dello sviluppo / a. XII, n. 2, 291-302.
- [32] *Patrizio E. Trissoldi, R. I.* (2007, Aprile). Further evidence on the effectiveness of automation sublexical recognition for the treatment of dyslexia. Psicologia clinica dello sviluppo / a. XI, n. 1, 27-37.
- [33] *Reed, L. M.* (2008). Using Relational Frame Theory to build grammar in children with Autistic Spectrum Conditions. (A. P. Association, A cura di) Special Complied Issue 2.4 - 3.1, 60-77.
- [34] *Simona Grazioli, M. G.* (2010, aprile). Learning risk presence in association with risk of attention disorders with / without hyperactivity: a survey of third-graders. Psicologia clinica dello sviluppo, XIV(1), 79-99.
- [35] *Simone Mazzotta, L. B.* (2005, Agosto). Frequency, imaginability and age of acquisition of words: to what extent affect the reading of Italian children? Psicologia clinica dello sviluppo, IX(2), 249-268.
- [36] *Stefania Marcolini, T. D.* (2006, Settembre). Length and morphology of the word: how they interact in the children's reading. Giornale Italiano di Psicologia, p. 649-659.
- [37] *Studio di Psicologia e Logopedia.* (s.d.). Taken from da psicologopedia: <http://www.psicologopedia.it/2012/03/05/caratteri-ad-alta-leggibilita-per-la-dislessia/>
- [38] *Timothy C. Bates, M. L.* (2011). Genetic Variance in a Component of the Language Acquisition Device: ROBO1 Polymorphisms Associated with Phonological Buffer Deficits. Behav Genet, 41, 50-57. doi:10.1007/s10519-010-9402-9
- [39] *Ughetta Moscardino, G. A.* (Aprile 2006). The measurement of temperament in the first three years of life through Infant Behavior Questionnaire and Toddler Behavior Assessment Questionnaire-Supplemented di Rothbart. Psicologia clinica dello sviluppo / a. X, n. 1, 67-92.
- [40] *University, H. B.-L.* (2000). Influencing children's symmetric responding in Matching-to-Sample Tasks. The Psychological Record, 50, 655-669.
- [41] *Vitale, V. C.* (2009). The contribution of Relational Frame Theory to the development of interventions for impairments of language and cognition. Best of JSLP-ABA, Consolidate Volume(4), 132-145.

METHOD OF DETERMINING THE SIZE OF THE SEARCH AREA A MOVING OBJECT ON APRIORI INFORMATION TO MEET THE CHALLENGES OF MODERN SEARCH MINISTRY FOR EMERGENCY SITUATIONS DISASTER ZONES STRUCTURE

Evgeniy Grigoriev, Artemij Zhuravlev, Ivan Yudin
students

Saint-Petersburg State University of Aerospace Instrumentation
Saint-Petersburg, Russia

Ivan-yudin@mail.ru

Abstract

This article discusses the optimal algorithm for searching the size of a moving object in a given area using radar on board the aircraft. The method is based on calculating the probability for coating, calculated according to the two-dimensional distribution law in the polar coordinate system. Special attention is paid to the dependence of the relationship between the parameters of the detection zone and the parameters of a moving object (further – MO).

Keywords: search area, coverage probability, distribution law.

I. INTRODUCTION

Subject is devoted to determining the minimum size zone of the search of a moving object for a given probability of detection in front of the aircraft viewing area. As the object may be a disaster area, the movement of a sinking ship, moving boats, the boat people. The method has wide application in the real terms for many applications. The method is based on the idea of narrowing the search area for a moving object, which is a vital factor to ensure safety in the event of natural disasters and catastrophes can be used to solve problems in the interests of the Russian Emergencies Ministry.

II. FORMULATION OF THE OBJECTIVE

The aircraft moves to the object, wherein the distance to the object is calculated relative to the MO. After the time t , when the calculated point, at a distance L , radar charts included a zone in which there is a search object. Search's center coordinates of the object on the plane of the coordinate system XOY , related to the aircraft, set equal to $(X=L, Y=0)$, and the size of range and azimuth area is de-

noted by $(\Delta L, \Delta\alpha)$, respectively (fig. 1). Next step is finding the size of the search area "covering" the object with a given probability P_{cov} , to do this, a mathematical model to describe the process of finding the object aircraft based on a priori information.

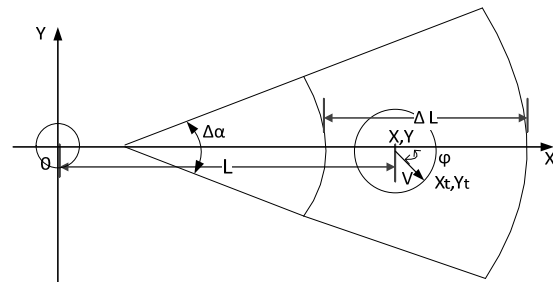


Fig. 1. The model of the moving object and the search area

III. MATHEMATICAL MODEL OF A MOVING OBJECT

During the time t the object is moving in an unknown direction ϕ with the velocity V .

The initial object coordinates (X, Y) are determined by a random error in calculating the coordinates of the object during the time of flight t is also accumulating an error, reason of them – peculiarities of the aircraft navigation system. Therefore, at the beginning of the search object's coordinates on the plane XOY relatively aircraft, are random variables. We accept that at the beginning of the search object's initial position (X_0, Y_0) on the plane XOY determined two-dimensional normal law of distribution [1].

$$f_0(X_0, Y_0) = \frac{1}{2 \cdot \pi \cdot \sigma_x \cdot \sigma_y} \cdot \exp\left(-\frac{(X_0 - L)^2}{\sigma_x^2} - \frac{Y_0^2}{\sigma_y^2}\right), \quad (1)$$

where σ_x^2 and σ_y^2 – object coordinate error variance in the search area. The errors are caused by errors of the initial positioning of the object, errors initial positioning itself aircraft, input data about object coordinates errors in navigation system and actual mistakes in navigation systems of aircraft [2], and errors in the system determines the

coordinates of the object during the flight time to the set point of inclusion of the active search for the object in the zone $(\Delta L, \Delta\alpha)$.

Dimensions of the search area will be maximized, if we take V_{\max} (maximum speed) as speed V , and φ will be a random variable uniformly spaced in the interval $(-\pi, \pi)$.

$$f_i(X_t, Y_t) = \frac{1}{4 \times \pi^2 \times \sigma_x \times \sigma_y} \times \int_{-\pi}^{\pi} \exp\left(-\frac{(X_0 - L - V_{\max} \times t \times \cos(\varphi))^2}{\sigma_x^2} - \frac{(Y_0 - V_{\max} \times t \times \sin(\varphi))^2}{\sigma_y^2}\right) d\varphi$$

where L – distance to object.

Lets analyze the particular case of the expression (2), put $\sigma_x = \sigma_y = \sigma$.

Object search area, when we use radiolocation system is define in polar coordinates (ρ_t, α_t) , where ρ_t – distance to the object, α_t – azimuth, $\alpha_t = 0$ along the axis $(0X)$. Lets change polar coordinates to [2],

$$\begin{cases} \rho_t = \sqrt{X_t^2 + Y_t^2}, \\ \alpha_t = \arctg \frac{Y_t}{X_t}, \end{cases} \quad \begin{cases} X_t = \rho_t \cos \alpha_t, \\ Y_t = \rho_t \sin \alpha_t, \end{cases} \quad (3)$$

as a consequence

$$f_i(\rho_t, \alpha_t) = f_i(X_t, Y_t) \times \begin{vmatrix} \frac{dX_t}{d\rho_t} & \frac{dY_t}{d\rho_t} \\ \frac{dX_t}{d\alpha_t} & \frac{dY_t}{d\alpha_t} \end{vmatrix} \quad (4)$$

when we put (3) at (4) we receive the expression:

$$f_i(\rho_t, \alpha_t) = \frac{\rho_t}{2\pi\sigma^2} \times \exp\left(-\frac{\rho_t^2 - 2\rho_t L \cos \alpha_t + L^2 + (V_{\max} t)^2}{2\sigma^2}\right) \cdot I_0\left(\frac{V_{\max} t \sqrt{\rho_t^2 - 2\rho_t L \cos \alpha_t + L^2}}{\sigma^2}\right), \quad (5)$$

Original expression for calculate search zone «covering» object with specified probability P_{cov} , and ΔL and $\Delta\alpha$ must satisfy the relation

$$P_{cov} = 2 \int_{L - \frac{\Delta L}{2}}^{L + \frac{\Delta L}{2}} \int_0^{\Delta\alpha} f_i(\rho_t, \alpha_t) \cdot d\rho_t \cdot d\alpha_t. \quad (6)$$

where I_0 – Bessel function of zero order of imaginary argument. For the particular case under consideration $\sigma_x = \sigma_y = \sigma$ [3].

Expression (6) defines the dimensions of the search area is ambiguously, namely, there are a plurality of pairs $(\Delta L, \Delta\alpha)$ which satisfy (6). Therefore, on the size of the zone in polar coordinates we can impose additional conditions. For example, the fixing number of the searching channels range by limiting the range ΔL , and fixing the time of the search (when scanning the search area by radar beam) limits $\Delta\alpha$.

So, the expression (6) becomes extremely small value close to zero.

Expressions obtained under the condition that the search $(\Delta L, \Delta\alpha)$ zone has a maximum size that is equivalent to giving the density distribution of random values (V, φ) in the form as the product of a uniformly distributed

$$f(V, \varphi) = \frac{1}{2\pi} \cdot \delta(V - V_{\max}), \quad (7)$$

on the interval $(-\pi, \pi)$ φ values and the determined value of V , the density distribution which is considered a delta function.

IV. CONCLUSIONS

The proposed method can be applied in real-world conditions for timely search and rescue people in the area aircraft circling, sinking ship, fires or other emergencies. An important aspect of this method is the fact that when you perform a search in front of the field of view, the aircraft movement may be adjusted before the disaster zone will be reached or identified as an emergency zone. This fact allows us to save time, the approach to the disaster area, compared with other methods of determining the size of the search area, for example, in the side-scan mode, in which you need to perform a U-turn. In addition, by adjusting the movement of the approach to the object in disaster area, distance to the object is reduced, thereby increasing the signal noise ratio that allows you to identify the disaster area with less probability of error.

V. REFERENCES

- [1] Быков В. В. «Цифровое моделирование в статистической радиотехнике». Изд-во «Советское радио», 1971, 328 стр.
- [2] О. И. Шелухин, А. М. Тенякиев, А. В. Осин «Моделирование информационных систем» Изд-во «Радиотехника», 2005, 368 стр
- [3] Шенета А. П. «Определение зоны поиска надводного объекта по данным предварительного целеуказания» Информационные–управляющие системы 4(59)/2012.

REMOTE ENERGY SUPPLY EFFICIENCY ESTIMATION FOR FAR-FIELD E/M

Ilya Ivanov, Maria Shelest
students

Saint-Peterburg State University of Aerospace Instrumentation
Saint-Peterburg, Russia

ilusha.51@yandex.ru, mshshelest@mail.ru

The reported study was partially supported by RFBR, research project No16-37-00197 mol_a

Abstract

The overview of remote energy sources transmitting their energy by means of far-field electromagnetic radiation and their possible use cases are subjects of this article. The main result covers investigation of dependency between distance from radiating point and remote charging efficiency. Numerical analysis shows that sources with radiation capabilities similar to modern high-end WiFi access points are the most promising among considered solutions.

I. INTRODUCTION

Conventional wireless system for remote energy supply is shown in fig. 1. It consists of the following three main elements [1]: set of low-power nodes, source of e/m energy, base station (BS) for data exchange with the nodes.

There are two types of sources mentioned in modern papers: dedicated and ambient. For dedicated sources their only purpose is radiation of a narrow-band signal for power supply of the nodes (e.g. Powercaster TX91501 [2]). Some considerations about standardization of DS are given in [3].

Ambient sources transmit their power for nodes supply as an indirect task. For example nodes, closely situated to such ambient sources as TV, 3G/4G, and WiFi reuse energy, radiated by them "for free".

In the next sections we will investigate efficiency and usability bounds of three mentioned types of ambient energy sources. The primary target is evaluation of utmost distance from the source for which harvesting process is possible.

A -20dBm level of RX power as an energy harvesting threshold was chosen.

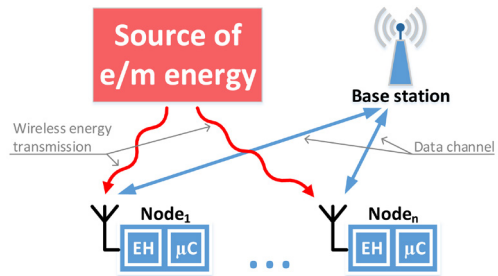


Fig. 1. Typical network with remote energy supply, where EH – energy harvester, µC – microcontroller

II. TV BROADCASTING

Television signals station is a widely investigated ambient energy source due to a high transmission power [4, 5]. The amount of TX power is regulated by FCC and commonly lays in a range 100W – 100kW for the middle-size towns [4].

For two scenarios (large city with 1 MW transmitter and medium city with 100 kW transmitter) and two carrier frequencies (500MHz and 900MHz) RX power vs. distance dependencies were calculated. Fig. 2 shows calculations results.

The calculation was made via conventional Okumura-Hata model:

$$L_U = 69,55 + 26,16 \log_{10} f - 13,82 \log_{10} h_B - C_H + [44,9 - 6,55 \log_{10} h_B] \log_{10} d.$$

For small or medium-sized city antenna height correction factor is:

$$C_H = 0,8 + (1,1 \log_{10} f - 0,7) h_M - 1,56 \log_{10} f.$$

For a large cities height correction factor is:

$$C_H = 3,2 (\log_{10} (11,75 h_M))^2 - 4,97$$

where L_U – path loss in urban areas, decibel (dB); h_B – height of base station antenna, meter (m); h_M – height of mobile station antenna, meter (m); f – frequency of transmission, megahertz (MHz); d – distance between the base and mobile stations, kilometer (km).

The given chart shows, that in non line-of-sight (NLOS) case harvester would operate just in a TV tower proximity (about 600 meters). This result agrees well with real experiments, described in [5].

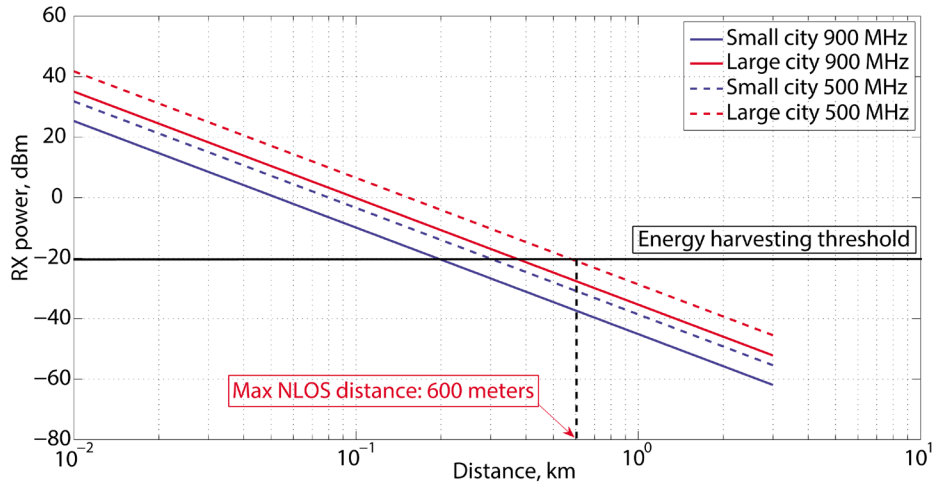


Fig. 2. Distance prediction for TV

III. CELLULAR NETWORKS

Also distance estimation was applied for energy harvesting of GSM900/1800 base stations

signals. GSM BS transmission power is typically 100W-1kW. In fig. 3 a prediction for maximum coverage radius can be found.

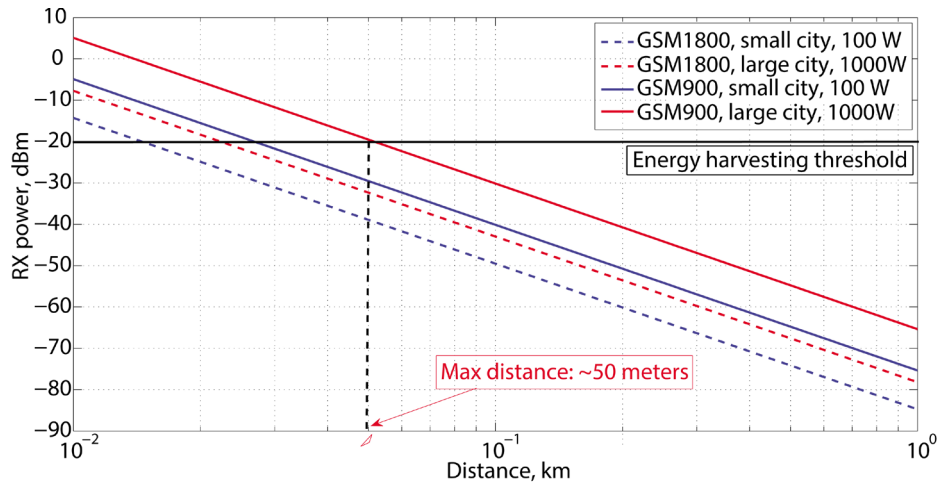


Fig. 3. Distance prediction for cellular base station

A curve for 900 MHz was calculated via Okumura-Hata model. A curve for 1800 MHz - via COST231 model:

$$L = 46,3 + 33,9 \log_{10} f - 13,82 \log_{10} h_B - a(h_R) + [44,9 - 6,55 \log_{10} h_B] \log_{10} d + C$$

For suburban or rural environments mobile station antenna height correction factor is

$$a(h_R) = (1,1 \log_{10} f - 0,7) h_R - (1,56 \log_{10} f - 0,8)$$

Here L - median path loss, decibel (dB); f - frequency of transmission, megahertz (MHz); h_B - base station antenna effective height, meter (m); d - link distance, kilometer (km); h_R - mobile station antenna effective height, meter (m).

The given figures agree with experiments, carried out in [6–8], which show that a harvesting process is possible in 10–50 meters distance from BS.

IV. WIFI ACCESS POINTS

Usage of WiFi access point seems to be very attractive due to cost/flexibility issues and relatively small distance between energy source (sources) and a harvester. From the other hand signals radiation process is interruptive in case of low-intensity traffic. So, almost in all of the papers the researchers had to force the APs transmission by means of artificial downloading of long files with closely situated smartphones or laptops [9–12].

In fig. 4 we show a distance prediction for this case. A conventional ITU Indoor radio propagation for model a LOS case was chosen for calculation of pathloss:

$$L = 20 \log_{10} f - N \log_{10} d - 28$$

Here N is a scenario-dependent constant.

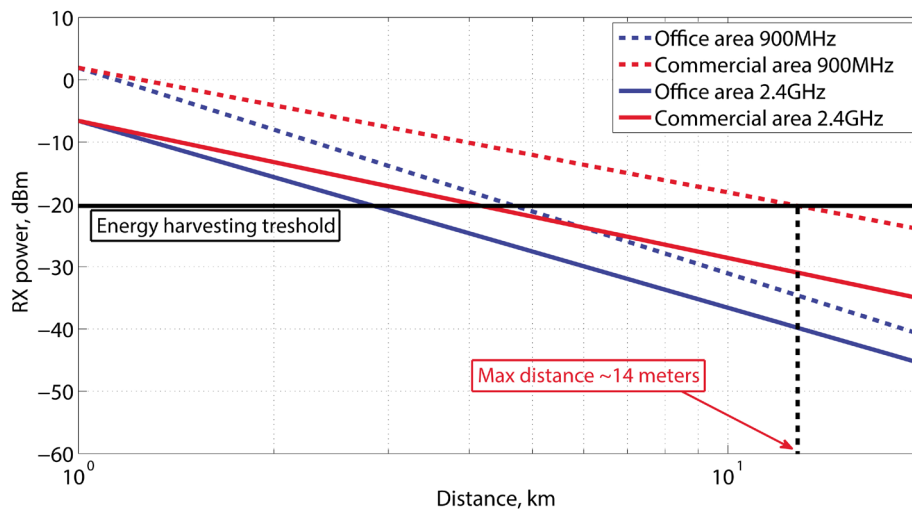


Fig. 4. Distance prediction for WiFi access points

V. CONCLUSIONS

Our estimations shows that:

- despite a huge transmission power, using of TV or GSM signals for remote power supply only within a limited distance from a station;
- in case of WiFi AP usage a few meters distance can be achieved;
- investigation of gains provided by beamforming on a WiFi AP is an interesting question for a further research.

VI. REFERENCES

- [1] X. Lu, P. Wang, D. Niyato, D. I. Kim, and Z. Han. Wireless Networks with RF Energy Harvesting. *arXiv:1406.6470v6*, 2014.
- [2] <http://www.powercastco.com/products/powercaster-transmitters/>.
- [3] <http://www.wirelesspowerconsortium.com>
- [4] DTV Reception Maps, Web: <http://transition.fcc.gov/mb/engineering/dtvmaps/>
- [5] List of North American broadcast station classes.
- [6] U. Batoool, A. Rehman, N. Khalil, M. Islam, M.U. Afzal and T. Tauqeer, "Energy Extraction from RF/ Microwave Signal", 15th International Multitopic Conference (INMIC), 2012.
- [7] Vronique Kuhn, Fabrice Seguin, Cyril Lahuec and Christian Person, "A multi-tone RF energy harvester in body sensor area network context", Loughborough Antennas & Propagation Conference, 2013.
- [8] M. Pinuela, P. D. Mitcheson, and S. Lucyszyn. Ambient rf energy harvesting in urban and semi-urban environments. *IEEE TRANSACTIONS ON MICROWAVE THEORY AND TECHNIQUES*, 61:2715–2726, 2013.
- [9] U. Olgun, C.-C. Chen and J. L. Volakis, "Design of an efficient ambient WiFi energy harvesting system", *IET Microwaves, Antennas & Propagation*, vol.6, 2012, pp. 1200-1206.
- [10] Fatima Alneyadi, Maitha Alkaabi, Salama Alketbi, Shamsa Hajraf and Rashad Ramzan, "2.4GHz WLAN RF Energy Harvester for Passive Indoor Sensor Nodes", *Proceedings of IEEE-ICSE*, 2014.
- [11] E. Abd Kadir, A.P. Hu, M. Biglari-Abhari and K.C. Aw, "Indoor WiFi energy harvester with multiple antenna for low-power wireless applications", *Proceedings of IEEE 23rd International Symposium on Industrial Electronics (ISIE)*, 2014.
- [12] Vamsi Talla, Bryce Kellogg, Benjamin Ransford, Saman Naderiparizi, Shyamnath Gollakota and Joshua R. Smith, "Powering the Next Billion Devices with Wi-Fi", *arXiv:1505.06815v1*, 2015.

CALCULATION OF DIFFRACTION LOSSES IN THE SYSTEM «OPTICAL FIBER – LENS»

Vasily Kazakov
postgraduate student

Saint-Petersburg State University of Aerospace Instrumentation
Saint-Petersburg, Russia

This work was supported by the Russian President's scholarship for young scientists and graduate students carrying out advanced research and development in priority areas of modernization of the Russian Economics (СП-536.2016.5)

vasilykazakov@mail.ru

II. METHOD OF DIFFRACTION LOSSES CALCULATION

Abstract

Method of calculation of diffraction losses in the system «fiber – lens» is proposed, which is based on the wave method of analysis of optical signals propagation. Main relations which are determines of diffraction losses level in this system is obtained. Graphical illustrations which are allow to estimate losses according to chosen parameters of optical system: wavelength, focal length and aperture of lens is showed.

I. INTRODUCTION

Analysis of the propagation of optical signals in a lens system is based mainly on the principles of geometric optics [1, 2]. This approach greatly simplifies the task of calculating the losses and distortions introduced by the system, but however, has several drawbacks. Firstly, the principles of geometrical optics ignore diffraction divergence of the optical beams, since the path of rays in the free space is rectilinear. Secondly, according to the principles of geometrical optics, an optical beam is focused by a lens into a point, which corresponds to an infinitely large energy density and inappropriate physical picture of the phenomenon. In some cases this description is not acceptable. The above-mentioned disadvantages of the principles of geometrical optics do not allow to describe transformation spatial optical signal by optical system. This gives rise to the need to apply the methods of wave propagation analysis of optical beams in optical systems. However, the analysis of wave beams in lens system insufficient attention is given. This is due primarily to the complexity of the calculations required to obtain the fields at the system output.

The basis of almost any optical information processing system includes a lens, an aperture limiting wave beams in space, as well as layers of free space between the lens and the aperture. Developed by this moment theoretical analysis assumes an infinite size of the lens, which plays a role only phase transparency, and does not limit the wave beam in space. In a real system, we have to operate with bounded apertures of lenses included in the optical information processing systems. Fig. 1 illustrates the appearance of the diffraction losses due to limitations of the lens aperture.

This paper discusses the diffraction losses caused by the propagation of part of the optical radiation outside the lens aperture, and provides an assessment of values of these losses, depending on various parameters: the optical radiation wavelength (λ), the distance from the fiber end to the lens (z), and lens aperture (D).

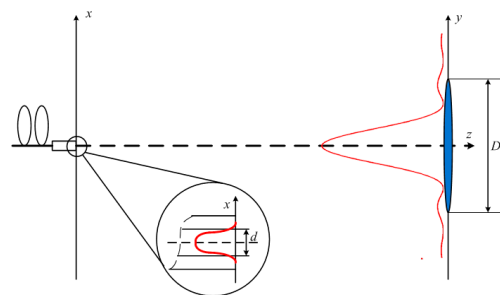


Fig. 1. The appearance diffraction losses in the optical system

Let us consider the process of transformation of the optical field $u(x)$ in the system from the end of the fiber, which is quite well approximated by a Gaussian distribution:

$$u(x) = K \cdot \exp\left(-\frac{x^2}{d^2}\right), \quad (1)$$

where K – coefficient, d – diameter of the fiber core.

Graphically the field distribution is shown in fig. 2.

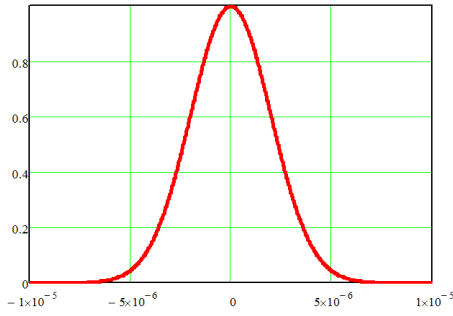


Fig. 2. Distribution of the field at the end of the fiber

The field distribution in the near zone is determined by the Fresnel diffraction [3]:

$$U(y) = \sqrt{\frac{e^{ikz}}{i\lambda z}} \int_{-\frac{d}{2}}^{\frac{d}{2}} u(x) \exp(i\frac{k}{2z}(x-y)^2) dx, \quad (2)$$

where $k = \frac{2\pi}{\lambda}$ – wavenumber, z – distance from the end of the fiber to lens, λ – optical radiation wavelength.

It is obvious that lens diameter D should be such that the main part of the diffracted field fit into the aperture of the lens, otherwise it will lead to the losses of the field, propagated beyond the lens aperture. However, the question of the relationship between the parameters d , D and z , in which the losses of fields are permissible, hitherto not been raised. Finite lens aperture causes errors of signal transmission by the optical system. In paper [4] proposes to use relative fraction of the energy which is not involved in the further transformation the optical signal, i.e. extends beyond the lens system as an evaluation of errors criterion.

The losses of optical radiation arising due to the limited aperture of the lens can be written as:

$$\Delta = 1 - \frac{\left(\int_{-\frac{D}{2}}^{\frac{D}{2}} I(y) dy \right)}{\left(\int_{-\frac{d}{2}}^{\frac{d}{2}} I_0(x) dx \right)}, \quad (3)$$

where $I_0(x) = |u(x)|^2$, $I(y) = |U(y)|^2$ – optical field intensity distribution on the x and y axis, respectively, D – lens aperture.

From expressions (2), (3) it follows that the optical losses of the diffracted field depend explicitly on the following parameters: wavelength, distance between the input aperture and the lens and aperture of the lens, which allows to estimate distortion of the transmitted signal depending on these parameters. With the help of Matlab system program has been created, which allows to calculate the losses of optical radiation in the system. The calculation results are shown in fig. 3 and fig. 4, respectively.

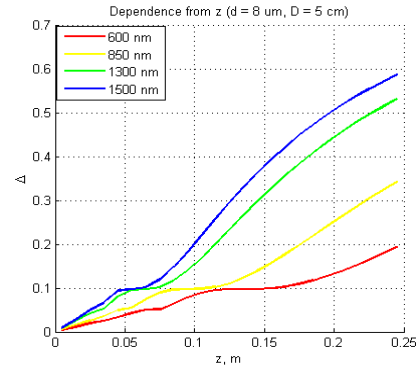


Fig. 3. Dependence of error from z

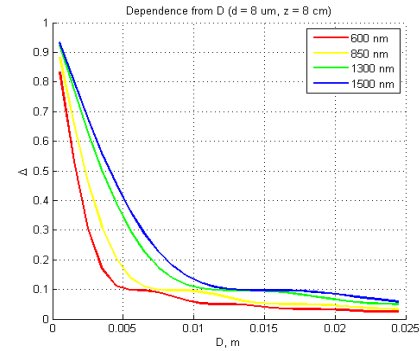


Fig. 4. Dependence of error from D

The obtained graphical dependences allow to define the optimal parameters of the lens (the diameter D and the focal length f) for a particular optical system at an acceptable level of energy losses in the system.

III. EXPERIMENTAL RESEARCH THE DIFFRACTION LOSSES IN THE LENS SYSTEM

To confirm the proposed methodology for calculating of diffraction losses the laboratory experiment using the set-up shown in fig. 5 was performed.

Laboratory setup includes a He-Ne laser, a collimator, a unit of inputting of radiation in optical fiber 1, a lens with a variable aperture, a unit focusing the radiation to the second optical fiber and the optical power meter. Methods of measuring diffraction losses were as follows. Since the measuring of optical power directly on the end of the optical fiber 1 was not possible due to the peculiarities of the laboratory setup, instead the level of power $P_{\max} = -31,5$ dBm at the maximum aperture (60 mm) was taken as an initial. The distance from the lens to the fiber end is equal to its focal length (94 mm). Operating laser wavelength is $\lambda = 630$ nm. Optical fiber type - single-mode with core diameter 8 μ m. Next, during the experiment the aperture size in steps of 5 mm was changed and the values the optical power was measured. The experimental results and further mathematical processing are shown in Table 1.



Fig. 5. Experimental setup

Table 1

Results of experiment

d , mm	5	10	15	20	25	30	35	40	45	50
P , dBm	-50	-36,9	-33,4	-33	-33	-32,8	-32,6	-32,6	-32,4	-31,9
P , nW	10	204	457	501	501	524	549	549	575	645
P/P_{max}	0,014	0,288	0,645	0,707	0,707	0,74	0,775	0,775	0,812	0,911
$\Delta = (1 - P/P_{max}) \cdot 100\%$	98,6	71,2	35,5	29,3	29,3	26	22,5	22,5	18,8	8,9

The results of theoretical calculation and experiment are shown in fig. 6.

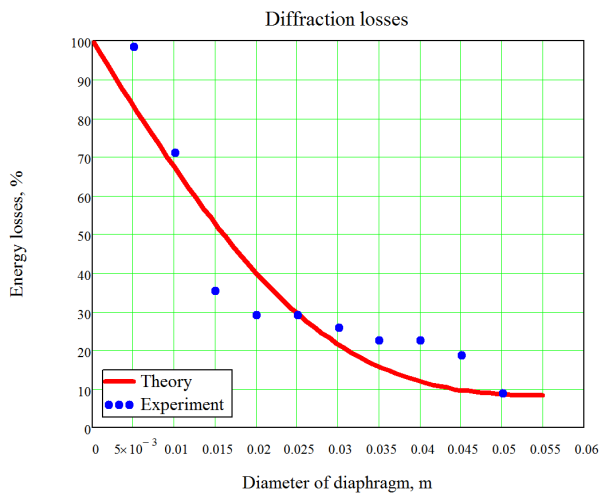


Fig. 6. Experimental and theoretical calculations of energy losses

It's possible to say that the proposed method of calculation of diffraction losses was confirmed in an experiment and can be applied to more complex optical systems.

IV. CONCLUSION

In this paper a method estimation of power losses caused by diffraction divergence wave beam from the end of the optical fiber was proposed. Convenient graphical representation of the obtained relationships allows for the choice the optical elements of the system with the most suitable parameters in terms of minimizing the energy losses in the system.

I express profound gratitude and appreciation to my supervisor PhD, Associate Professor Oleg D. Moskaletz for responsive guidance, valuable advices and comments.

V. REFERENCES

- [1] Тарасов, К. И. Спектральные приборы – Л.: Машиностроение. 1968. – 388 с.
- [2] Ю. М. Беляков, Н.К. Павлычева. Спектральные приборы // под ред. Н. К. Павлычевой. – Казань: КГУ, 2007. – 204 с.
- [3] Патулис, А. Теория систем и преобразований в оптике. – М.: Мир, 1971. – 495 с
- [4] V. I. Kazakov, S. N. Mosentsov, O. D. Moskaletz. Influence of aperture lens system on optical information processing. Proc. of SPIE Vol. 9598, pp. 959809-1-9. 2015.

PARAMETERS AND MODES OPTICAL SPECTRAL DEVICES BASE ON THE ACOUSTO-OPTIC TUNABLE FILTER

Georgy Korol
student

Saint-Petersburg State University of Aerospace Instrumentation
Saint-Petersburg, Russia

G-King7@yandex.ru

Abstract

Consider method of analysis of the spectra dynamic signals optical range techniques acousto-optics at light diffraction on a traveling acoustic wave excited by a periodic sequence of radio pulses with a rectangular envelope and linear variation of the instantaneous frequency. As part of the research acousto-optic interaction is thought of as a bilinear transformation of the spectral components, which are radio and optical radiation. Analysis of the spectrum in the optical range is seen as the result of the optical signal at the determined diffraction screen, that is, the acousto-optic modulator, which is driven deterministic acoustic wave. The results of the research are the relation describing the electrical oscillations at the output of the photodetector, which in turn are the result of the spectral measurements at different rates of change of the instantaneous frequency of oscillation of the control, as well as mathematical simulation results describing the process.

I. INTRODUCTION

The optical spectral instruments on the based of an acousto-optic tunable filter have the highest speed among systems with sequential reading spectrometric information. The restructuring of the acousto-optic tunable filter over a range of frequencies can be analyzed linear speed: how consistent and for a given program. Management acousto-optic tunable filter is easy to organize with the help of a computer.

The resolution of the optical spectral device based on acousto-optic tunable filter of the same order, and spectral lattice devices and can reach units angstrom.

A very important advantage of optical spectral devices based on the acousto-optic tunable filter is the possibility of correction of the frequency characteristic preliminary acoustooptic interaction, and therefore, only the optical path of the measuring sys-

tem by changing power supplied control signal. It should be added that such spectral instruments have a number of advantages, such as: reliability, small size and weight [2]. This is a decisive argument in favor of the use of equipment in the considered spectral optical spectral device based on an acousto-optic tunable filter.

II. COMPLEX HARDWARE FUNCTION

In this paper the analysis of the spectrum of optical radiation at its diffraction on elastic wave.

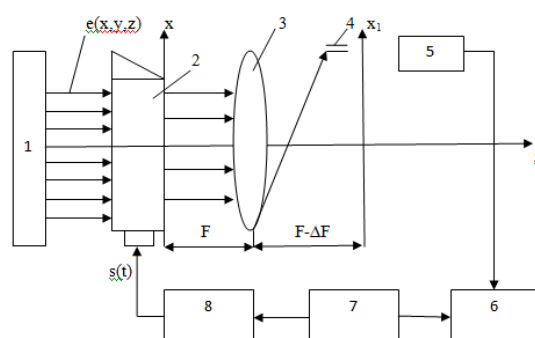


Fig. 1. Block diagram of the optical spectral device based on acousto-optic tunable filter

In fig. 1 the following notation: 1 – forming optics, 2 – solid state acousto-optic modulator, 3 – lens with a focal length F, 4 – slot, 5 – photodetector, 6 – display, 7 – synchronizer, 8 – generator.

Distribution light in a plane $z=F$:

– transparency function is a linear map of the electric oscillations $S(t)$, the exciting environment acousto-optical interaction acousto-optic modulator in a plane acoustic wave $U(x_1, t)$;

$$U(x,t)=Vs(t), \quad (1)$$

where t – current time; V – linear operator transition from fluctuations $s(t)$ to a uniform plane acoustic wave;

– plane light wave $e(Z, t)$, is normally incident on an acoustic wave $U(x_1,t)$;

– attenuation and dispersion of acoustic waves in the acousto-optic modulator acousto-optical interaction neglect;

– an optical Fourier transform processor comprising a cylindrical lens and two layers of space ideally performs either a spatial Fourier transform or spatial Fresnel transform [3];

– signals $S(t)$ and $e(t)$, determined by acoustic and light waves are adequately defined and Fourier-Stieltjes integrals

$$S(t) = \left(\frac{1}{2\pi}\right) \int_{-\infty}^{\infty} \exp i\omega'_s dt Z_s(\omega'_s), \quad (2)$$

$$e(t) = \left(\frac{1}{2\pi}\right) \int_{-\infty}^{\infty} \exp i\omega'_t dt Z_1(\omega'_t) \quad (3)$$

It is assumed that the fluctuations of $e(t)$ correspond to a uniform plane light wave. The function $A(\omega'_s, \omega'_t, x_2, t)$ is the kernel of the bilinear transform spectral

$$F(x_2, t) = \int_{-\infty}^{\infty} \int_{-\infty}^{\infty} A(\omega'_s, \omega'_t, x_2, t) dt \quad (4)$$

If $\omega'_1 = \omega'_0 \text{ const}_1$, $dZ_1(\omega'_1) = \delta(\omega'_1 - \omega'_0) d\omega'_1$ we get a comprehensive hardware function diffraction spectral instrument optical range in the fall of acousto-optic modulator homogeneous plane monochromatic light wave.

$$S(\omega_{1_0}, \omega'_s, x_2, t) = \alpha \exp i(\omega_{1_0} + \omega_s) t S_0(\omega_{1_0}, \omega'_s, x_2) = \dot{\alpha} \exp i(\omega_{1_0}, \omega'_s) t \int_{-0,5L}^{0,5L} \exp i \quad (5)$$

$$[\omega_{1_0} x_2 \frac{1}{F} \frac{1}{C} - k'_s(\omega'_s)] x_1 dx_1.$$

At $\omega_{1_0} = \omega_s = \text{const}_2$, dZ_s

$(\omega'_s - \omega_{s_0}) d\omega'_s, k(\omega_{s_0}) = \omega_{s_0} \frac{1}{v_0}$, we get a comprehensive hardware function diffraction spectral instrument optical range in the fall of acousto-optic modulator homogeneous plane monochromatic light wave.

hensive hardware function diffraction spectral instrument optical range in the fall of acousto-optic modulator homogeneous plane monochromatic light wave.

$$L(\omega_{s_0}, \omega'_t, x_2, t) = \alpha \exp i(\omega'_{s_0} + \omega'_t)$$

$$tL_0(\omega_{s_0}, \omega'_t, x_2) = \dot{\alpha} \exp i(\omega_{s_0}, \omega'_t) t \int_{-0,5L}^{0,5L} \exp i \quad (6)$$

$$[\omega_{s_0} \frac{1}{v_0} - \omega'_t x_2 \frac{1}{F} \frac{1}{C}] x_1 dx_1$$

Where in the acoustic wave acts as a diffraction grating, thereby forming a structure in the form latticed acousto-optic modulator [4].

Integrated hardware functions (5) and (6) define moving (instant) spectra and light electric oscillations, provided movement analyzed by fluctuations fixed window, and the ratio (4) makes sense superposition integral for the corresponding spectral instrument, that is the acousto-optic analyzer radio spectrum or diffraction spectral instrument optical range in the diffraction optical radiation latticed structure in the form of acousto-optic modulator.

Since the information signals are adequately described in the theory of stochastic processes, in

case the analysis of the spectrum of radio signals takes place deterministic diffraction light wave on a stochastic screen, and the analysis of the optical spectrum, diffraction occurs at a determinate wave stochastic screen.

For oscillations with finite spectrum frequency dependence can be approximated by entire functions on the basis of this and the Paley-Wiener $S(\omega_{s_0}, \omega'_t, x_2)$ и $L(\omega_{s_0}, \omega'_t, x_2)$ are entire functions of exponential type in both variables, their values at all points determined by two-dimensional sampling theorem in the spectral region.

Acousto-optic modulator in fig. 2 as a one-dimensional transparency, converts the complex amplitude of $E_1(x)$ is incident on a plane monochromatic wave uniform rule $E(x, t) = E_0 T(x, t)$, where in $E(x)$ the complex amplitude distribution at the output face (the right along the axis z) of the acousto-optic modulator; $T(x, t)$ – transparency function acousto-optic modulator as a banner.

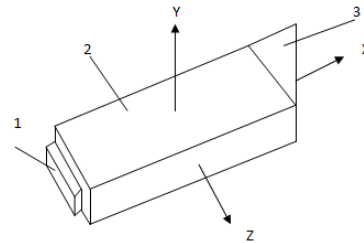


Fig. 2. Acousto-optic modulator

Fig. 2 shows a diagram of the acousto-optic modulator, which includes a piezoelectric transducer 1, media 2, acoustic absorber 3.

III. HARDWARE FUNCTIONS OF OPTICAL SPECTRAL INSTRUMENTS BASED ACOUSTO-OPTIC TUNABLE FILTER

In this paper the analysis of the optical spectrum at its diffraction by elastic waves excited by a periodic sequence of rectangular radio pulses with a duration τ with linear variation of the instantaneous frequency [1] and a repetition period $2T$. Next there is a view of an idealized model of observing the diffraction of light by elastic waves, assuming that the condition [5].

To determine the integrated hardware functions is sufficient to consider one cycle of operation, this corresponds to an electrical oscillation as a function of time t ,

$$s(t) = S_m \exp[-i(\Omega_0 t + 0,5M t^2)], \quad t \in \left[-\frac{\tau}{2}, \frac{\tau}{2}\right], \quad (7)$$

where

$$M = \frac{d\Omega(t)}{dt} = \text{const} \quad (8)$$

– the rate of change of the instantaneous frequency control electric fluctuations; Ω_0 – average frequency electric fluctuations.

Within the radio-optical analogies connection input-output optical processor under consideration is given by

$$g(x_1) = \int_{-\infty}^{\infty} \int_{-\infty}^{\infty} f(\xi) \exp[i\gamma_1(\eta - \xi)^2] \exp(i\gamma_1\eta^2) \exp[i\gamma_2(\eta - x_1)^2] d\xi d\eta \quad (9)$$

Integration over η leads to the expression

$$g(x_1) = \frac{\pi^{\frac{1}{2}}}{i} \exp(-i\gamma_1 \frac{1}{\gamma_0} x_1^2) \int_{-\infty}^{\infty} f(\xi) \exp[i\gamma_0(\xi - \gamma_1 \frac{1}{\gamma_0} x_1)^2] d\xi \quad (10)$$

where $\gamma_0 = \gamma_1(1 = \gamma_1 \frac{1}{\gamma_2}) = \omega' \frac{1}{2c_0 F_0} (1 - z_0 \frac{1}{F_0})$

we obtain from the original formula for the complex hardware function optical spectral device based on acousto-optic tunable filter

$$K(M, t, \Delta\omega) = A_0 \omega' \int_{-L_0}^{L_0} \exp\{i[Mt \frac{1}{v} + \Delta\omega' \frac{1}{\omega_0} \Omega_0 \frac{1}{v}] \xi\} \times \exp(\omega' \frac{1}{\omega_0} M 2 \frac{2}{v} \xi^2) d\xi \quad (11)$$

Mathematical modeling was carried out on the basis of the following parameters:

$$c := 3 \cdot 10^8 \quad v := 2000$$

$$L := 0,01 \quad t := -2, (-2 + 0,01)..2$$

$$\lambda := 565 \cdot 10^{-9} \quad M := 1 \cdot 10^6$$

$$\Delta\omega := 10^9 \quad M1 := 1,5 \cdot 10^6$$

$$\omega := \frac{2 \cdot \pi \cdot c}{\lambda} \quad M2 := 2 \cdot 10^6$$

$$A := 6,6721 \cdot 10^{13}$$

$$K(t) := \left| \frac{1}{A} \cdot (\omega + \Delta\omega) \int_{-L}^L e^{i\left[\left(\frac{Mt}{v} + \frac{\Delta\omega\Omega}{\omega v}\right) \cdot x + \left(\frac{(\omega + \Delta\omega)Mt}{2\omega v^2}\right) \right]} dx \right|$$

$$K1(t) := \left| \frac{1}{A} \cdot (\omega + \Delta\omega) \int_{-L}^L e^{i\left[\left(\frac{M1t}{v} + \frac{\Delta\omega\Omega}{\omega v}\right) \cdot x + \left(\frac{(\omega + \Delta\omega)M1t}{2\omega v^2}\right) \right]} dx \right|$$

$$K2(t) := \left| \frac{1}{A} \cdot (\omega + \Delta\omega) \int_{-L}^L e^{i\left[\left(\frac{M2t}{v} + \frac{\Delta\omega\Omega}{\omega v}\right) \cdot x + \left(\frac{(\omega + \Delta\omega)M2t}{2\omega v^2}\right) \right]} dx \right|$$

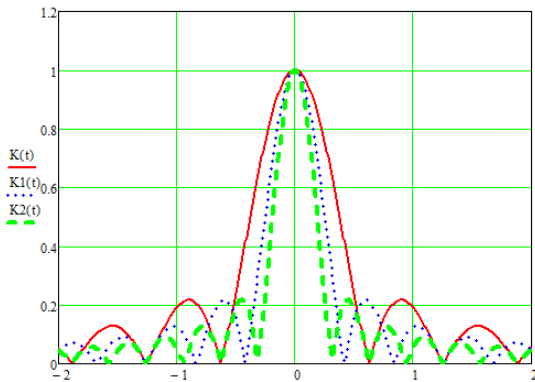


Fig. 3. Mathematical modeling of the hardware function

Fig. 3 shows the results of mathematical modeling of complex hardware functions of the optical spectral device based on an acousto-optic tunable filter.

IV. CONCLUSION

The present work shows the role of spectral measurements in the optical range and marked dignity optical spectral device based on acousto-optic tunable filter.

A general expression of complex hardware functions of optical spectral device based on acousto-optic tunable filter and parameters are specified on which it depends.

As a result of the research, it was found that the acousto-optic interaction can be considered as a bilinear transformation on the spectral components that are physically: radio spectrum and the spectrum of the optical radiation. In the general form of linear transformations defined by the expansions of the nonlinear operator in a Taylor series and the establishment of the linear approximation.

As a result of this work, a formula for calculating the square of the modulus of the instrumental function of the optical spectral device based on acousto-optic tunable filter. This formula takes into account all the parameters and modes of operation of the optical spectral device based on acousto-optic tunable filter.

V. REFERENCES

- [1] *О. В. Гусев, В. В. Кудзин.* Акустооптические измерения. Л.: Издательство ЛГУ, 1987.
- [2] *Калинин В. А.* Спектральные измерения в оптическом диапазоне с передачей анализируемых сигналов по оптическому волокну: дис. канд. тех. наук: Спец. 05.13.01: защищена 30.05.2006 / Калинин Владимир Анатольевич. СПб., 2006. 133с.
- [3] *Москалец О. Д.* Один из видов дифракции света на акустических волнах как билинейное преобразование. Материалы XII всесоюзной конференции по акустоэлектронике и квантовой акустике. Часть 1 Саратов 1983. С. 286-287.
- [4] *Москалец О. Д.* Динамические сигналы и спектральные измерения, 2013. С.152-158.
- [5] *Georgy Korol, Dmitry Moskaletz, Oleg Moskaletz* «Effect of rate of change of frequency characteristics of the optical spectral device based on acousto-optic tunable filter» Proc. of SPIE Vol. 9216 92161F.

SPECIAL FEATURES OF PRODUCTION TECHNOLOGIES OF MICROMECHANICAL SENSORS ON SURFACE ACOUSTIC WAVES

Alexander Kozhev
student

Saint-Petersburg State University of Aerospace Instrumentation
Saint-Petersburg, Russia

al.kozhev@gmail.com

Abstract

Specific features of production technologies of micromechanical sensors on surface acoustic waves, methods of production, structure of the sensor are examined here. As well are examined main problems in the production of sensors, and the actions that need to be taken to eliminate or minimize these problems.

Keywords: sensor, surface acoustic waves, micromechanics.

I. INTRODUCTION

One of the key technological challenges that must be solved in the production of micromechanical inertial sensors based on surface acoustic waves – gyroscopes and microaccelerometers – is the formation on a surface of the substrate additional inertial elements – localized mass, increases sensitivity to portable inertial forces, depending on the measured parameters of the object.

II. FORMATION OF LOCALIZED MASSES

Usually these masses are deposited and laminated layers from titanium (*Ti*) and gold (*Au*), sequentially formed on the surface of piezo crystal foundation (*LiNbO₃*, *TaNbO₃*).

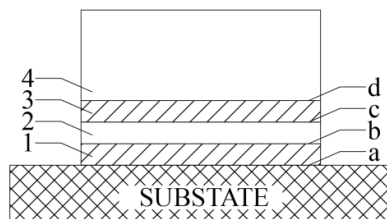


Fig. 1. Inertial element.

1 – *Ti*; 2 – *Au* (deposited); 3 – *Ti*; 4 – *Au* (Galvanic deposition); *a, b, c, d* – interphase boundaries of membranes

Durability of these structures is defined by adhesion between the deposited titanium (*Ti*) and galvanic deposited gold (*Au*), depending on a degree of hydrogenation in the area of interface *C* (fig. 1)

III. SPECIAL FEATURES OF SENSORS AND CALCULATION OF OPERATING FORCES

The distinctive feature of these sensors compared to other MEMS consists in that what functionally important structural components are synthesized on the crystal surface on which surface acoustic waves are propagated in the process. If adhesive force between the sprayed and galvanic deposited layers and the substrate is smaller than arising wave processes of inertia force applied to the center of mass of the inertial element, it becomes necessary to adopt measures to prevent the possible destruction of products due to the development of micro-cracks in the zones of adhesive contact, such as titanium membranes with a significant level of hydrogenation. One way of overcoming these difficulties is creating special conditions for occurrence apart adhesive and also chemical bonds as a result of forming in transition area between substrate and membranes of the transition layer with a common crystal lattice, the occurrence of which may be stimulated by the introduction into the process of additional implantations and subsequent diffusion of implanted atoms on both sides of the phase boundary. In this case, while properly determining the composition and the depth of the diffusion layer, may increase the adhesion strength by approximately one order as compared with the strength of Van der Waals forces responsible for the adhesion layers.

The inertial force exerted on structural element arises during vertical displacement of the inertial element contact areas with crystal while generating a surface acoustic wave.

On inertial element in this case effects force of inertia $F_u = m_u \cdot a$, here m_u – mass of inertial element, a – acceleration of mass center.

Inertial element has cylindrical shape with a height $h=20$ micron and diameter $2R=20$ micron, vertical cross section of which is shown on fig. 1.

Then

$$F_u = m_u \cdot a = \rho_{Au} \cdot V \cdot a = \rho_{Au} \cdot \pi R^2 \cdot h \cdot A_0 \cdot \omega^2;$$

ρ_{Au} – density of gold; $V = \pi R^2 \cdot h$ – amount of inertial element; A_0 – amplitude of the surface wave $\sim 1 \text{ nm} = 1 \cdot 10^{-9} \text{ m}$; $\omega = 2\pi\nu$ circular frequency of wave process, $\nu = 6 \cdot 10^7 \text{ Hz}$; $\omega = 2\pi \cdot 6 \cdot 10^7 = 3.7 \cdot 10^8 \text{ s}^{-1}$.

Wherein

$$F_u = \rho_{Au} \cdot \pi R^2 \cdot h \cdot A_0 \cdot \omega^2 = 1.83 \cdot 10^{-3} \text{ H.}$$

Considering the size of the inertial element and small surface of contact adhesive, should be recognized that the value is greatly large.

Generated inertia force in the structure strain:

$$\sigma_u = \frac{F_u}{\pi R^2} = \frac{1.83 \cdot 10^{-3}}{3.14 \cdot (10 \cdot 10^{-6})^2} = 5.8 \cdot 10^6 \text{ Pa.}$$

The counter-force of inertial force of adhesion is the force of intermolecular van der Waals, electrostatic nature and having manifested as the force of electrostatic interactions of dipoles operating at distances close to the parameters of the crystal lattice. Van der Waals force combined three types of interactions:

1. Orientation caused by polar molecules having a permanent electric dipole moment. The strength of the interaction in this case is called a force of Kizoma.

2. The induced interaction (Debye force). Occurs between the polar and non-polar molecules, resulting in an electric field of a polar molecule with a permanent dipole moment induced polarization initially unpolarized molecule.

3. The dispersion interaction (force of London). This interaction is universal and is more or less usual, since there are involved non-polar molecules and atoms. The non-polar atoms and molecules in accordance with the uncertainty principle have instantaneous dipole moments, which are different from zero and interact with each other.

Exactly this type of interaction is typical for adhesion of metallic and dielectric membranes, metal membranes and foundation metal.

All van der Waals force has different physical description, however, have a common dependency on r the distance between the interacting objects.

According [1, 2], f – force of van der Waals, which characterizes the dispersion interaction between nonpolar atoms and molecules in the vapor metal membrane–dielectric and metal membrane–

metal, has the form $f = \frac{6A_3}{r^7}$.

Here A_3 – Hamaker constant, hard-defined parameter characterizing a pair of interacting atoms and molecules. Hamaker constant is generally ex-

pressed in terms of two parameters of interacting substances as follows:

$$A_3 = \frac{3I_1 \cdot I_2}{2(I_1 + I_2)} \cdot \chi_1 \cdot \chi_2,$$

where I_1 and I_2 – ionization potentials of the reactants, χ_1 and χ_2 – polarizability of corresponding atoms and molecules.

Unfortunately, for most substances, in addition to chemical elements and simple chemical compounds, such as the value of polarizability of can be varied over a wide range (up to 50 times), and for the complex composition of compounds of this data is not always reliable. Given these circumstances use averaged polarizability and evaluation of the ionization potential for $LiNbO_3$ and Ti .

Considering $A_3 = 1 \cdot 10^{-78} \text{ J} \cdot \text{m}^6$, $r = 0.5 \cdot 10^{-9} \text{ n}$, we will obtain a pair of atoms involved in the dispersion interaction, force of London:

$$f = \frac{6A_3}{r^7} = \frac{6 \cdot 1 \cdot 10^{-78}}{(5 \cdot 10^{-1} \cdot 10^{-9})^7} = 0.78 \cdot 10^{-12} \text{ H.}$$

To evaluate adhesion force linking to substrate, despite the fact that in one cubic centimeter of solid is contained 1–1022 atoms. Then the number of atoms in the surface layer area 1 sm^2 amounts

$\xi = (1 \cdot 10^{22})^{2/3} \sim 1 \cdot 10^{15} \text{ am/cm}^2$. Adhesion force between inertial member and crystal $LiNbO_3$, calculated under these assumptions, will be equal to:

$$\begin{aligned} F_A &= f \cdot \xi \cdot \rho_0 = \\ &= 0.78 \cdot 10^{-12} \cdot 1 \cdot 10^{15} \cdot 3.14 \cdot (1 \cdot 10^{-3}) = \\ &= 2.45 \cdot 10^{-3} \text{ H} \end{aligned}$$

As can be seen from the comparison in this case, the adhesion force $F_A = 2.45 \cdot 10^{-3} \text{ H}$ is comparable in magnitude to the force of inertia $F_u = 1.83 \cdot 10^{-3} \text{ H}$.

IV. METHODS OF PRODUCTION

Essentially, at the disposal of technologies is only one way to increase the strength of the laminated structure element, namely the creation of a chemical bond in addition to the adhesion between the layers of the ion implantation methods.

Specified method enables to create within metastable alloy layers, with a total lattice, facilitating a significant increase in strength of the multi-layer structure. Two methods are used to create metastable alloys.

In the first of these methods on the treated surface of the matrix element is applied in a membrane of thickness of several tens nanometers alloying element and a beam of accelerated ions irradiate Ar, Kr, Xe, or ions of elements A and B with an energy of 300 keV.

In another method, the surface of the matrix is applied sequentially layered system of alternating layers of elements A and B. The thickness of individual layers, usually not exceeding 10–15 nm and conditions selected from the alloying with the re-

quired relative concentration of elements A and B. The total thickness of the system less than 100 nm. This multi-layered system is irradiated with accelerated ions causing agitation.

At ion irradiation alloy multilayer systems formed at the boundary between the membrane and the substrate, and in principle can be obtained with a uniform distribution of alloy elements on depth. It is necessary in this case that the depth of ion implantation was greater beam mixing of the multilayer membrane thickness and the alloying elements were mixed ion beam effectively.

Detailed development of this part of the process, providing a significant increase in strength of the structure creating a transitional alloy by ion implantation, based on the phase diagram (Ti–Au), which allows optimizing the ratio of the alloy components, providing the required mechanical properties of the structure.

Inertial element of sensor is a cylinder with a nearly equal height and diameter of foundation, which does not regardless of the size treat it as a membrane structure.

From theory and practice of electrochemical processes is known that structure best characteristics obtained by galvanic deposition, in their synthesis rotating disc electrode for high values of the current density j (about $1\text{A}/\text{cm}^2$). High purity, strength and ductility of deposited metal due to high deposition rate; high pressure crystallization, resulting in displacement of impurities.

At thicknesses up to 70 mm pellet has shiny surface (high j and Ω – angular velocity of rotation of the electrode) due to the characteristics of crystallization in the electric field on the mechanism of normal growth atomically rough surface is completely accessible to embed the deposited metal cations.

Dynamics of changes in the surface roughness of rainfall was studied on the cathodes with a model microprofile (grooves, projections in the form of triangles, perpendicular to the flow of electrolyte).

Analysis of the dynamics of growth projection shows a three-fold difference in the growth rates of sediment at various locations.

With an increase in sediment is the development of surface roughness due to the redistribution of power, attributable to the ridges and valleys as far as the preferential growth of sediment on the projections, the increase in deposition rate on the projections and depressions on its decrease (increase ratio $\Delta h_x/\Delta h_y$). This fact is of fundamental importance, because it considered inertial element has a height of 20 m, a height commensurate with irregularities Δh_x , reached by at a rather early stage of the deposition process.

An increase in roughness sludge thickening process at a constant current density increases the average dispersion cations flow toward the cathode surface. With an increase in precipitate growth rate increases at a certain thickness and roughness may become higher than acceptable.

Improved sludge structure and reduction roughness can be achieved by incorporating into the electrolyte organic additives. "Leveling" effect of additives on the adsorption-diffusion mechanism during cathodic deposition difficult in a turbulent fluid movement and high current densities.

Improving the process of influencing evolution of micro-relief sludge thickening is possible due to the transition to a cyclic mode electroplating sludge build-up. In cyclic mode impact on the process it is due to two factors – stress the shape and change the distance between electrodes.

V. CONCLUSION

As a result of research the main critical factors were identified that could lead to failure of the product in operation:

- inability to control the adhesion strength of structural elements and the inertial element to each other during the planar operations
- inevitable hydrogenation of surface of the titanium membrane and the galvanically deposited gold with galvanic growing inertial element and a sharp decrease in the mechanical strength of the structure due to hydrogen embrittlement;
- difficulties in providing predetermined shape of the inertial element in the galvanic deposition of non-uniformity of the deposition rate on anterior and posterior surfaces.

Listed factors can be eliminated or minimized by the following measures.

1. Proper research of surface states of the crystal in order to identify deposits formed during chemical cleaning operations. The purpose of this, including a determination of the effective area of interaction between the crystal surface and the first Ti layer is thermally sprayed.
2. Not using only Ti as a component of a multilayered structure of other chemical elements. Its disadvantages as the material – the basis for the galvanic deposition of gold apparent ability to hydrogen embrittlement is higher than that of most metals. High chemical durability of the oxide membrane on the surface effectively limits the deposition of gold plating and reduces adhesion to Au Ti.
3. In order to increase mechanical strength of the construction is necessary to provide transition regions by ion synthesis metallurgy alloy surface, facilitating connection of a purely adhesive layer to create a combined crystalline lattice. The efficiency of this technology is proven in many experimental studies; moreover, it is, in fact, has no alternative.
4. For successful cultivation of galvanic inertial element given the cylindrical shape is necessary to know process of galvanic deposition of the inertial element on the surface of titanium substrate. The current level of electrochemical technology is sufficient to competent management through the deposition process parameters to achieve maximal approximation of the inertial element to required form.

VI. REFERENCES

- [1]. *Bestugin A., Ovodenko A., Kirshina I., Filonov O.* Methods of increase of durability of designs of micromechanical sensors on surface acoustic waves with galvanic besieged sensitive elements. //Proceeding of the XII International Academic Congress "Science, Education and Technology in the Modern World" (United States, Cambridge, Massachusetts, 18-20 April 2015). ELSEVIER, "Harvard University Press", 2015. – P. 67 -74.
- [2]. *Filonov O. M., Kirshina I. A., Okin P. A.* Technology factors influencing operational reliability of micromechanical sensors on surface acoustic waves with additional internal elements//«Applied Science and technologies in the United States and Europe: common challenges and scientific findings»: Papers of the 7th International Scientific Conference (June 25, 2014). Cibunet Publishing. New York, USA. 2014. – P. 116-122.

THE TREATMENT OF THE SURFACE GAP FOR PHOTOMETRIC STEREO

Vitaliy Kuznetsov
postgraduate student

Saint-Petersburg State University of Aerospace Instrumentation,
Saint-Petersburg, Russia

k.avk-c@mail.ru

Abstract

This article discusses the method of extraction of the features of the surface gap and treatment of it in the process of integrating the gradient obtained by photometric method stereo. Light configuration consists of five fixed light sources. With this configuration, additional features of shadows, inter reflections and highlights during the image segmentation can be used. A local path algorithm is used for integrating the gradient.

Keywords: photometric stereo, shadows detection, gradient integration.

I. INTRODUCTION

The Photometric Stereo technique performs the calculation of the surface orientation in every visible point, illuminated at least from 3 different light sources, placed not in the same plane. Gradient field, calculated based on the surface reflection properties [1, 2] or reference object [3-5], corresponds to infinite number of surfaces. It occurs, cause of presence of the surface gap, and can be a reason for the high level of integration errors. Two approaches to solving the problem of surface gap were considered:

- exclusion of areas, which probably contains the gap, and subsequent gradient integration from the different point of view;
- preliminar processing of images to obtain the additional features, which can be useful in the integration process.

The choice of approach depends on the scanning conditions and purpose. The paper presents a method for the case when it is necessary to obtain the maximum number of points of the surface with only one view direction.

II. SURFACE INTEGRATION

There is a variety of gradient integration methods [6-13], which are often divided into two groups: local and global methods. First group [6,

13] uses fixed route or route generated in process of integration. Global methods [6-13] use criteria of matching with the original data.

Not all methods of integration can use additional features in the calculation of points cloud: the property of integrability [7], the weight or error estimation [13], constraints based on the shadows segmentation. For the surface integration we apply the method, using the route generated in the integration process, because it is more flexible to use additional criteria, and can be easily applied to build a part of visible surface. The method based on the curvilinear integral

$$z(x_1, y_1) = z(x_0, y_0) + \int_{x_0}^{x_1} p(x, y_0) dx + \int_{y_0}^{y_1} q(x_1, y) dy$$

where $z(x_0, y_0)$ – initial point of integration, $z(x_1, y_1)$ – any point, $p(x, y)$, $q(x, y)$ – surface gradient.

The disadvantage of this method is dependent on the choice of the initial point of integration. It is carried out by the manually point marking or searching of the well illuminated areas.

III. SURFACE GAP

Because of the set of points is discrete, the problem isn't only the presence of the gap or overlap of the surface, but the omission of the surface inclination. In the following, this situation is equivalent to the presence of the gap (fig. 1). Imaging process is not taken into account.

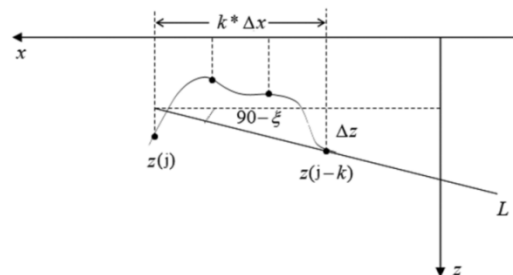


Fig. 1. Surface cut

Fig. 1 shows the several points of the surface, where ξ – the angle between the view direction and the light direction L , view direction is opposite to the

direction of the axis z , j , k – indexes of the discrete points. As shown on fig. 1, when $\Delta z > \Delta x * \text{Ctg}(\xi)$, the presence of the gap leads to casting shadow on the source images for which was chosen the light direction \mathbf{L} . According on the geometric calculations, we can obtain the inequality including shading and shaded surface point:

$$z(j) < z(j-k) - k * \Delta x * \text{Ctg}(\xi) \quad (1)$$

If the shadow index of the point was defined, then constraints of the $z(x,y)$ can be established (example for image I_2)

$$\begin{cases} z(x,y) < z_{cs}(x_0,y) - \Delta x \text{Ctg}\phi_s, & S(x,y) = 1 \\ z(x,y) > z_{cs}(x_0,y) - \Delta x \text{Ctg}\phi_s, & S(x,y) = 0 \end{cases}$$

where $S(x,y)=1$ is the case of shaded point, $S(x,y)=0$ otherwise. It's obvious that point $z_{cs}(x_0,y)$ casting shadow can't be shaded. For the shaded points z_{cs} the last not shaded point in right direction. Generally z_{cs} for the point (x,y) can be selected based on the equation:

$$\begin{aligned} z_{cs}(x_0,y) - (x-x_0)\text{Ctg}\phi_s = \\ = \max(z_{cs}(x_k,y) - (x-x_k)\text{Ctg}\phi_s) \end{aligned}$$

where $x_k < x$. If the previous point is illuminated, then $x_0 = x-1$. Constraints of the illuminated part are true even if the image does not present shading.

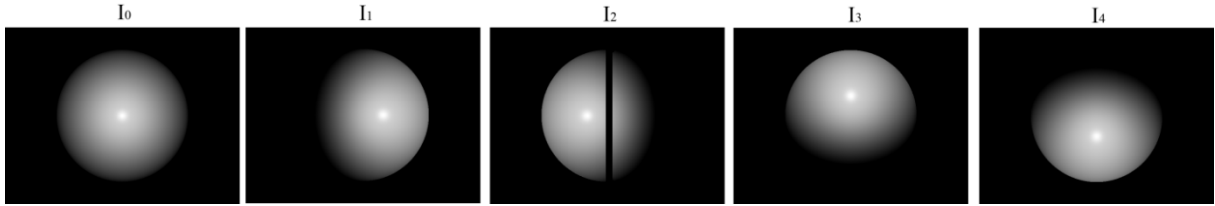


Fig.2. Test set of images

Method presented in [14] is used to obtain shadow indexes. It gives the map of shadows, highlights and interreflections as result of minimization

$$R(x,y) = \sum_{k=0}^{N-1} (s_k(x,y)\mathbf{L}_k \mathbf{n} - i_k(x,y))^2,$$

where number of images $N=5$. In order to distinguish cast shadows from shading it is necessary to calculate "clear" brightness of the point

$$i_k(x,y) = \mathbf{L}_k \mathbf{n},$$

where \mathbf{n} – the normal to the surface. If the brightness is greater than a certain positive threshold, this point will be assigned to a cast shadow, therefore, and gap will be found.

Fig. 3 shows grouped set s_1, s_2, s_3, s_4 . Interested area colored blue $(0,1,1,1)$, corresponding to the shadows on image I_2 , and some area colored brown $(0,1,0,1)(0,1,1,0)$, corresponding to the shadows on image I_2 at the same time with shadows on image I_3 or I_4 .

Search for determining $z_{cs}(x,y)$ carried out in four directions: in data rows in forward and reverse order, and in columns in forward and reverse order.

For each point it can be determined 8 inequalities for the value $z(x,y)$, two inequalities based on each image. From these inequalities, the interval of value $z(x,y)$ can be defined.

If there is the different casting shadow point z_{cs} in the shaded area then it will be impossible to establish the existence of this point.

IV. THE TREATMENT OF THE SURFACE GAP

Construction of a surface containing a gap has several stages:

- segmentation of shadows on the source images;
- the search in the direction of light to determine $z_{cs}(x,y)$ and length of cast shadows;
- construction of parts of the surface;
- determination the mutual position of the parts, if received parts more than 1.

Test set contains 5 images of sphere with generated gap (fig. 2). Light configuration consists of 5 light sources: 4 placed in pairs in the basis planes of coordinate system (axis z is coincide with view direction) and 1 additional light source on the z axis.

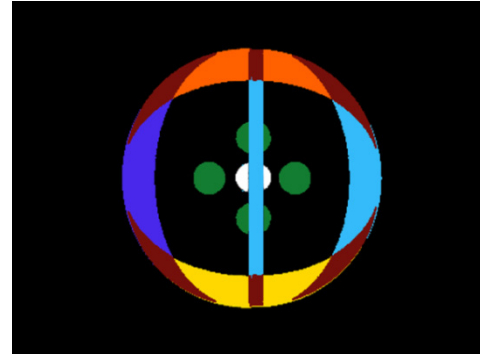


Fig. 3. Segmentation of source images

Input data for integration algorithm is: the gradient field (p,q) , set s_0, s_1, s_2, s_3, s_4 , set z_{cs} , the initial points $z(x_i, y_i)$, the angle of the light ξ .

In this case, the surface portion right from the gap is not available for integration from the initial point, selected in the left part. The second initial point is selected.

Selection of the starting point is carried out in several steps:

1. Current index is $fc = 1$, for all points initial index is $f = 0$

2. Select a random point in the visible area with $f = 0$, index value change to current $f = f_c$
3. Index value of all neighboring visible points, if they do not belong to the shaded area, is changed to f
4. Step 3 is repeated for all the points, which in the previous step has been assigned the index f
5. The process ends when in step 4, the index has not been changed
6. If there are points that are visible on the source images with $f = 0$, the f_c is increased by 1 and repeat step 2
7. For each area the initial point is chosen such that the total brightness in a given neighborhood of the additional image is the greatest. For all initial points coordinate $z(x_i, y_i)$ assigned to 0.

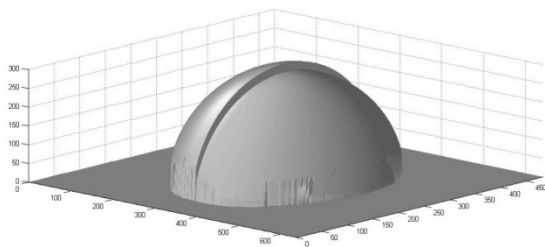


Fig. 4. The result of the integration of the gradient

To determine the mutual position of the equation 1 is represented as

$$z_{is}(j) = z_{cs}(j-k) - k * \Delta x * \text{Ctg}(\xi).$$

For each point on the boundary of the casted shadow the difference between $z_{is}(x, y)$ and the obtained value $z(x, y)$ is calculated. The average value will adjust the mutual position of parts of the object.

The resulting point cloud is shown in fig. 4. Relative error of calculation of z is 0.93%.

V. CONCLUSION

The results give an opportunity for automatization of the processing of data obtained during the 3D scanning and, in some cases, exclude the need for manual handling.

VI. REFERENCES

- [1] *Solomon F. and Ikeuchi K.* Extracting the Shape and Roughness of Specular Lobe Objects Using Four Light Photometric Stereo // IEEE Transactions on Pattern Analysis and Machine Intelligence, 18(4), April 1996 — P. 449-454.
- [2] *Barsky S., Petrou M.* The 4-source photometric stereo technique for three-dimensional surfaces in the presence of highlights and shadows // IEEE Transactions on Pattern Analysis and Machine Intelligence, 25(10), October 2003 — P. 1239-1252.
- [3] *Woodham R. J.* Photometric Method for Determining Surface Orientation from Multiple Images // Optical Engineering, vol. 19, no. 1, 1980. — P. 139-144.
- [4] *Woodham R. J.* Gradient and Curvature from the Photometric-Stereo Method, Including Local Confidence Estimation // Journal of Optical Society of America, vol. 11, no. 11, Nov. 1994. — P. 3050-3068.
- [5] *Hertzmann A. and Seitz S. M.* Example-Based Photometric Stereo: Shape Reconstruction with General Varying BDRFs // IEEE Transactions on Pattern Analysis and Machine Intelligence, 27 (8), August 2005 — P. 1254 – 1264.
- [6] *Klette, R., Schlüns, K.* Height data from gradient fields // Proc. Machine Vision Applications, Architectures, and Systems Integration V, SPIE 2908, Boston, Massachusetts, Nov. 18-19, 1996, 204-215
- [7] *Frankot R. T., Chellappa R.* A method for enforcing integrability in shape from shading algorithms // IEEE Trans. on Pattern Analysis and Machine Intelligence, 10, 1988. — P. 439-451
- [8] *Wang G., Yang J., Cheng Y.* Surface Reconstruction from Gradient Fields Using Box-Spline Kernel // International Journal of Multimedia and Ubiquitous Engineering, Vol.9, No.5, 2014, — P.155-168
- [9] *Agrawal A., Raskar R., Chellappa R.* What is the range of surface reconstructions from a gradient field? // In Proc. 9th European Conf. on Computer Vision (ECCV), volume 3951, 2006, — P. 578-591
- [10] *Agrawal A., Chellappa R., Raskar R.* An algebraic approach to surface reconstruction from gradient fields // In Proc. 2005 Intl. Conf. on Computer Vision (ICCV), 2005, — P. 174-181
- [11] *Qingxiang Yang, Narendra Ahuja.* Surface reflectance and normal estimation from photometric stereo // Computer Vision and Image Understanding 116, 2012, — P. 793-802
- [12] *Zhang R., Tsai P. S., Cryer J. E., Shah M.* Shape from Shading: A Survey // IEEE Transactions On Pattern Analysis And Machine Intelligence, Vol. 21, No. 8, August 1999, — P.690-706
- [13] *Saracchini R., Stolfi J., Leitão H., Atkinson G., Smith M.* Robust multi-scale integration method to obtain the depth from gradient maps // Computer Vision and Image Understanding, 116, 2012. —P. 882-895
- [14] *Кузнецов В. А.* Алгоритм сегментации исходных снимков для фотометрического метода трехмерного сканирования // Информационно-управляющие системы. 2015. № 3. С. 29-34.

**SYSTEM ANALYSIS AND PRACTICAL SOFTWARE REALIZATION
OF MAKING DECISION IN THE CONDITIONS OF UNCERTAINTY
AT TRANSPORTATION GOODS ON RAILWAY TRANSPORT**

Mariya Makarenko
postgraduate

Saint- Petersburg State University of Aerospace Instrumentation
Saint-Petersburg, Russia

makarka-m@mail.ru

Abstract

In this article is described the method of making decision in the conditions of uncertainty by means of the software package «CTM-office» at transportation goods on railway transport.

Keywords: system analysis; goods transportation; making decision in the conditions of uncertainty

In the sphere of goods transportation, as well as in any other, there are various situations which sometimes are rather difficult for ordinary person to predict without any help. Making decision in the situation is called «making decision in the conditions of uncertainty». We will consider adoption of such decisions in the sphere of goods transportation on railway transport.

Uncertainty on the railway transport consists of the following components:

– there are a lot of various freight forwarders (carriers) in the market which are engaged in goods delivery. To find the optimal solution, i.e. to learn the price for transportation of this or that good, it is required to address several carriers, learn their prices and choose that most of all approaches a specific objective;

– besides a large number of forwarding agents, there are also numerous routes of delivery of good, because the railroads is rather «branched» network with various features of departure, transit or destination stations, i.e. at these stations various capacity and goods turnover [2].

To help the consignor make the right decision in the conditions of uncertainty can the universal matrix of the income or losses, which is based on the following data:

– transfer all possible situations which aren't depending on person of the making decision (further the decision-maker) which influence on the

final choice of a freight forwarder (in our case all this carriers which we have addressed);

– make the analysis of all possible alternative decisions of transportation of goods, i.e. to describe all options of a route of transportation of goods;

– determine the cost of delivery of good by this or that route for each carrier, i.e. to learn the expected expenses of transportation [1].

After definition of above-mentioned data the decision-maker create a matrix and can determine by it what conditions more approach proceeding from a route and the cost of delivery.

But to facilitate and accelerate the choice of the decision-maker, because time of making decision is too very important factor, there is a software package «CTM-office» in which it is possible to use the «Rail-Tariff» program. It allows to calculate quickly and with little effort a tariff of transportation different types of goods proceeding from the entered data: stations of departure and destination, a type of sending, the description of good (a code, good weight in one car, a tariff class, and, if it is necessary, danger class), the description of the used rolling stock, additional conditions.

Finally the program shows on the screen detailed calculation of a tariff, the covered distance, the VAT, in what currency was made the calculation, and also a detailed route of transportation on which displays all stations and time of a delay on them. Therefore, at desire of the decision-maker can be changed a route, if time of delivery doesn't suit it [3].

Also the decision-maker can change a type of shipment, for example, transport good not in the combined car or the container, but in separate one. Moreover, it is possible to change and choose a necessary sort of a rolling stock, for example, instead of a 4-axis platform choose 6-axis or the covered car with the increased length and etc. If it is necessary, for good is possible to organize protection which cost will be included in a tariff of transportation [4].

The tariff of transportation of good depends on several factors (which aren't depending on the decision-maker):

- 1) exchange rate in a day of making calculation;
- 2) a political situation on the international scene;
- 3) rates on transportation of good;
- 4) accessory of a rolling stock to any state, etc.

All four points are considered in the «Rail-Tariff» program that is reflected in calculation settings (points 1 and 4), various messages and comments when calculating a tariff of transportation (it is highlighted in bold type and red color) (points 2 and 3). So the decision-maker can always monitor changes of these parameters, and, therefore, consid-

er them at making decision for optimization specific objective.

At making decision the decision-maker can liquidate uncertainty conditions by means of the «Rail-Tariff» program, since there is an opportunity to count necessary or enough options of transportation, which the best gets out on his opinion [3].

We will provide an example of creation of a real route of transportation of good in the «Rail-Tariff» program below. In fig. 1 are displayed parameters of transportation of good and calculation of a tariff [4].

On fig. 2 is presented the main route of transportation on a network of the railroads and with independent input of intermediate station [4].

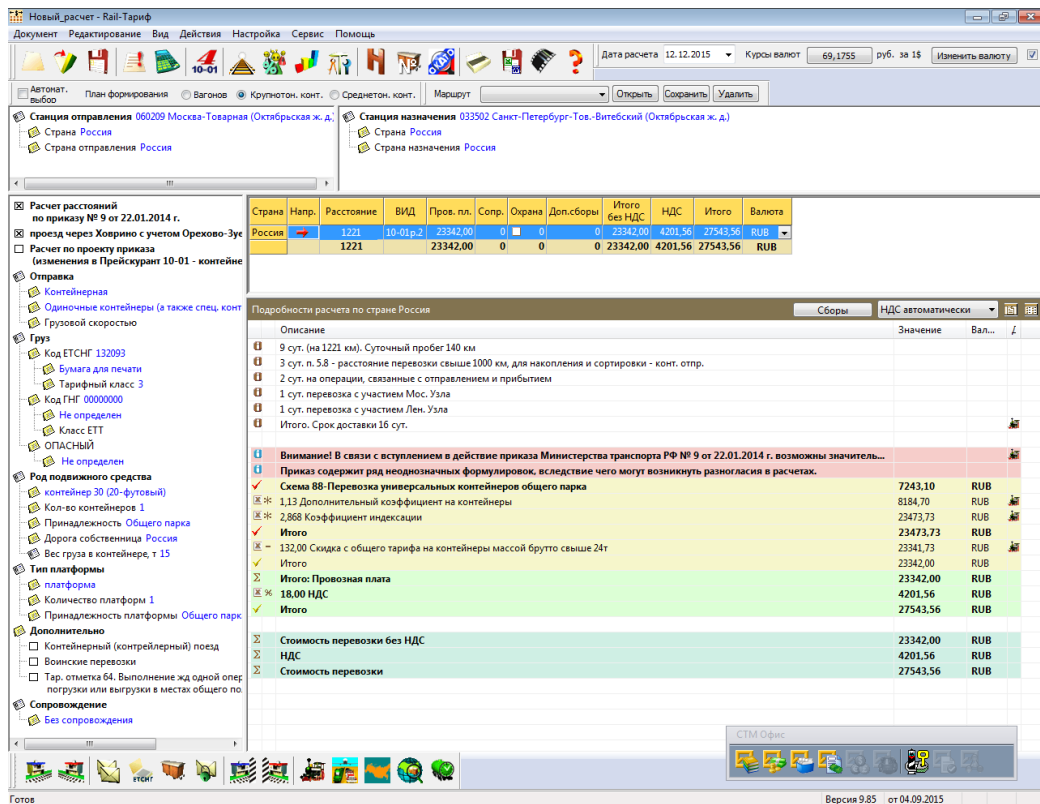


Fig. 1. Result of calculation in Rail-Tariff

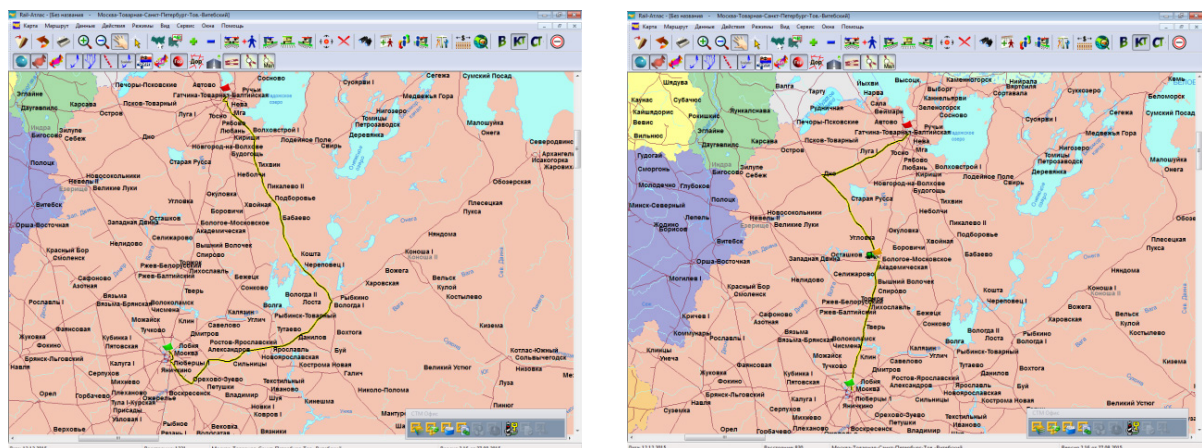


Fig. 2. The first constructed and changed transportation route

CONCLUSION

We have a constructed route for rail transportation, calculated cost of tariff and after it we can make decision which carrier offer best conditions. So, with the help software «СТМ» we could in practice liquidated uncertainty situations in decision making.

REFERENCES

- [1] *Бродецкий Г. Л.* Системный анализ в логистике. Выбор в условиях неопределенности / –М.: Academia,

2010. - 336 стр.
- [2] Грузоведение: учебное пособие / Н. А. Слободчиков, Д. В. Кочнев, О. А. Диняк ; ред. В. А. Фетисов ; С.-Петерб. гос. ун-т аэрокосм. приборостроения. - СПб. : Изд-во ГУАП, 2013. - 432 с.
- [3] *Майоров Н. Н.*, Практические задачи моделирования транспортных систем/ Н. Н. Майоров, В. А. Фетисов. - СПб.: ГУАП, 2012. - 185 с.
- [4] «СТМ-офис», электронный ресурс для программного обеспечения в России <https://www.ctm.ru/>

MODELS AND METHODS OF ESTIMATION OF INNOVATIVE POTENTIAL OF NOVELTY

Antonina Makeeva
student

Saint-Petersburg State University of Aerospace Instrumentation,
Department of innovation and integrated quality systems
Saint-Petersburg, Russia

tonechka.by@yandex.ru

Abstract

The article provides a rationale for the evaluation of the technical level and the innovation potential of the developed products. Method of estimation of innovative potential of novelty is also offered, allowing to identify the potential of high-tech products, as well as to monitor the activities of departments of development and planning of putting into production of new products.

Keywords: innovation, technological level, innovative potential, quality assessment.

I. INTRODUCTION

To improve the efficiency of research and production systems are developed organizational and technical solutions, such as: the methodology and the technical level of pricing models, methods

of analysis of innovative potential of both businesses and new products.

The technical level of production is a relative characteristic of the quality of products, based on a comparison of values of quality indicators that characterize the technical excellence of products evaluated, with the corresponding baseline values. Thus, determining the technical level of production, we can get an idea of the quality characteristics of the product [1].

Definition of the technical level of new products contributes to the identification of promising technologies that will ensure the future success of the company-developer on the market, including advanced development than its competitors.

To evaluate the technical level of production the following methods are used most frequently [2]:

- differential method;
- synthesis method;
- complex method.

Detailed description of the techniques is given in Table 1:

Table 1

Analysis of the technical level of valuation techniques

Designation method	Appointment	Formula	Description of formulas
Differential method	Differential method for evaluating the technical level (TU) products is to compare individual quality indicators evaluated products with the appropriate base sample rates.	$L_Q = \frac{P_i}{P_{ibas}}$ $i=1,2,\dots,n$	P_i – the value of the i-th indicator assesses the quality of products; P_{ibas} – the value of the i-th sample index of the quality of basic; n – the amount received for the evaluation of the technical level of quality indicators.
Synthesis method	The synthesis method is used when a large number of indicators evaluated products when their evaluation is difficult.	$Q = \frac{D}{n}$	D – relative quality, n – the amount of relative indicators
Complex method	Complex method of assessing the level of technical products used when necessary to consider a large number of individual indicators, making it difficult to decide on the level of quality of different products evaluated.	$Q = \sum_{i=1}^n m_i q_i$	q_i – single component products; m_i – weighting parameter.

II. FORMULATION OF THE PROBLEM

In order to implement the Russian Federation Innovative Development Strategy for the period up to 2020 "Innovative Russia – 2020" it is necessary to pay attention to the process of identifying and encouraging potential future products of domestic manufacturers.

By classified innovative potential future products is understood novation. Research essence of novation is to analyze its technical level. Carrying out technical level assessment procedure is to compare the characteristics of the test samples of the same innovations and products as well as a comparison between the innovation and the reference sample.

III. SOLUTION OF THE PROBLEM

To evaluate the technical level of the technique used to analyze the competitiveness of the object in terms of the technical level at any stage of the life cycle [3].

For example, Table 2 shows an analysis of the technical level of amphibious hovercraft "Le Corsaire" [4], as a counterpart selected lightweight boat amphibious hovercraft «Sagittarius» C-51 the RT [5]. The graph has been added for comparison table performance innovation with generally accepted benchmark in the sector in question.

Table 2

Analysis of the technical level

Characteristics	Novation	Competitor	Deviation from analog indicators, %	Reference object	Deviation from the standard indicators, %
	Amphibious hovercraft "LeCorsaire"	Easy boat amphibious hovercraft "Sagittarius" C-51 RT			
	<i>P_n</i> - indicator of the quality of innovation	<i>P_c</i> - indicator of the quality of competitor			
Destination indicators					
Dimensions, m:					
Length	5,0	5,2	-3,85	5	0
Width	2,2	2,3	-4,35	2,1	4,76
Height	2,4	1,8	33,33	2,2	9,09
Power, h.p.	240	50	380	150	60
Seating capacity, h	3	4	-25	5	-40
Capacity, kg	400	400	0	400	0
Dryweight, kg	850	320	165,63	300	183,33
Fuel consumption, l/h	21	20	5	20	5
Full speed, km/h:					
On water	90	90	0	90	0
On snow	90	70	28,57	90	0
The height of the obstacle, m	0,4	0,3	33,33	0,5	-20
Range of stroke, km	400	250	60	400	0
Reliability indicators					
Features of the case, point	Plastic housing having a low tendency to freeze, is not critical to low temperatures and has high strength –2	The core body structure with elastic connections –3	-33,33	3	-33,33
Repairability, point	Maintainability with the opportunity to replace any body parts in the shortest possible time –3	It does not require special conditions –3	0	3	0
Performance ergonomics					
Seat device, point	Possibility of independent modification of a design –2	Flip or removable seats –3	-33,33	3	-33,33

The technical level of analysis carried out in accordance with the assessment of indicators forming the inner essence of the object:

$$ILTI = \sum \frac{P_n}{P_c} \times m_i$$

where ILTI – an indicator of the level of technical innovation, i – another indicator, P_n – an indicator of the quality of innovation, P_c – an indicator of the quality of analog competitor, m_i – weighting factor.

Indicators evaluated products and analogues are normalized by dividing the indicators of innovation in the respective analog performance. Indicators are placed weighting in using peer review and are dimensionless quantities (Table 3)/

Deviation indicators of the object from a competitor performance in percentage terms gives an indication of the level of the enterprise-manufacturer development and adjust strategy to promote enterprise in technical and technological aspects in relation to competitors.

From Table 4 innovation (amphibious hovercraft "Corsair") has a normal technical level.

Then the total number of specifications have been chosen improved (compared to the analogue). Column "Improvement" contains a value that quantifies the changes made to the product. Consequently, the result of changes defined as achievement of qualitatively new characteristics and a significant excess of the level of social requirements (Table 5).

Table 3

Calculation ILTI

Characteristic	P_n . indicator of the quality of innovation	P_c . indicator of the quality of competitor	Relative value q_i	Weight parameter m_i	ILTI
Destination indicators					
Dimensions, m:					
Length	5,0	5,2	0,96	0,05	0,05
Width	2,2	2,3	0,96	0,05	0,05
Height	2,4	1,8	1,33	0,05	0,07
Power, h.p..	240	50	4,8	0,1	0,48
Seating capacity, h	3	4	0,75	0,08	0,06
Capacity, kg	400	400	1	0,1	0,1
Dryweight, kg	850	320	2,66	0,02	0,05
Fuel consumption, l/h	21	20	1,05	0,1	0,11
Full speed, km/h:					
On water	90	90	1	0,1	0,1
On snow	90	70	1,29	0,1	0,13
The height of the obstacle, m	0,4	0,3	1,33	0,04	0,05
Range of stroke, km	400	250	1,6	0,1	0,16
Reliability indicators					
Features of the case, point	Plastic housing having a low tendency to freeze, is not critical to low temperatures and has high strength –2	The core body structure with elastic connections –3	0,67	0,03	0,02
Repairability, point	Maintainability with the opportunity to replace any body parts in the shortest possible time –3	It does not require special conditions –3	1	0,05	0,05
Performance ergonomics					
Seat device, point	Possibility of independent modification of a design –2	Flip or removable seats –3	0,67	0,03	0,02
Average weighted rate					1,49

Table 4.

Interval estimation of the scale of the technical level

Interval	The quality of the technical level
0<ILTI<0,1	Extremelylow
0,1<ILTI<0,2	Verylow
0,2<ILTI<0,5	Low
0,5<ILTI<1	Moderate
1<ILTI<3	Normal
3<ILTI<6	Tall
6<ILTI<10	Verytall

Table 5

Analysis of the performance improvement

Characteristics	Novation	Competitor	Improvement, %
	Amphibioushovercraft "LeCorsaire"	Easy boat amphibious hovercraft "Sagittarius" C-51 RT	
Destinationindicators			
Height, m	2,4	1,8	33,33
Power, h.p.	240	50	380
Dryweight, kg	850	320	165,63
Fuelconsumption, l/h	21	20	5
Full speed, km/h:	90	70	28,57
The height of the obstacle, m	0,4	0,3	33,33
Rangeofstroke, km	400	250	60

Calculate the innovative level of novelty:

$$InnovLev = \sum I_{i_i} = I_{11} + I_{12} + I_{13} + I_{14},$$

where I_{11} – another characteristics of the changes, I_{11} – number of advanced specifications, I_{12} – number of improved consumer characteristics, I_{13} – the degree of progressivity of innovation, I_{14} – create a social effect.

Based on the tables 6, 7, have:

$$InnovLev = \sum I_{i_i} = 0,47 + 0,47 + 1 + 1 = 2,94$$

So, an innovative product level is 2.94.

This value is in the range $2 < InnLev < 5$ (table 8), from a technical point of view corresponds to improving innovation.

Table 6

Analysis of innovation of the product characteristics

Name the characteristics of the changes	Specifications	Formula	Result	Result, %
Number of advanced specifications (I_{11})	Height, m	$I_{11} = \frac{P_{imp.tech.ind.}}{P_{com.tech.ind.}}$ where $P_{imp.tech.ind.}$ – the amount of advanced technical specifications (7 indicators), $P_{com.tech.ind.}$ – the total number of specifications (15 indicators)	$I_{11} = \frac{7}{15} = 0,47$	47
	Power, h.p.			
	Dryweight, kg			
	Fuelconsumption, l/h			
	Full speed, km/h			
	The height of the obstacle, m			
	Rangeofstroke, km			
Number of improved consumer characteristics (I_{12})	Height, m	$I_{12} = \frac{P_{imp.consum.ind.}}{P_{com.tech.ind.}}$ where $P_{imp.consum.ind.}$ – the amount of advanced consumer specifications (7 indicators), $P_{com.tech.ind.}$ – the total number of specifications (15 indicators)	$I_{12} = \frac{7}{15} = 0,47$	47
	Power, h.p.			
	Dryweight, kg			
	Fuelconsumption, l/h			
	Full speed, km/h:			
	The height of the obstacle, m			
	Rangeofstroke, km			

Qualityfeatures

Characteristic measurements	Qualityfeatures (scale)					
	0,2	0,4	0,7	0,8	1	2
The degree of progressivity of innovation (I_{13})	Improving innovation of the secondary characteristics of the object	Improving the basic characteristics of innovation object	A significant increase in the basic characteristics of the object	A significant excess of the basic characteristics of innovation object	The achievement of qualitatively new features	Getting new products for the first time assimilated in the national economy
Create a social effect (I_{14})	Failure to social requirements (standards)	Providing certain social requirements	Ensuring social requirements (standards)	The improvement provided by the rules of certain social requirements	Improvement of the whole complex of norms	A significant excess of the level of social demands

Table 8

Scale evaluation of innovative products

Interval	Qualityinterval
$0 < \text{InnovLev} < 2$	Pseudo-innovation
$2 < \text{InnovLev} < 8$	Improving innovations
$8 < \text{InnovLev} < 10$	Basic innovation

III. CONCLUSION

Thus, innovation – amphibious hovercraft "Le Corsaire" – has sufficient technical level to be recognized as improving innovations.

The project was implemented within the framework of start-up companies, carried out by an autonomous institution of the Khanty-Mansiysk Autonomous Okrug Ugra "High Technologies Technopark". The analogue was chosen products are a major defense industry sector in the North-West region of Russia. The results of the analysis showed that the production of small innovative businesses has novelty improving innovation that has a positive effect on competitiveness.

IV. REFERENCES

- [1] ГОСТ 15467-79. Управление качеством продукции. Основные понятия. Термины и определения. М.: Изд-во стандартов, 1979. 30 с.
- [2] Пасько Т. В., Таров В. П. Оценка качества технических систем: учеб. пособие / Т.В. Пасько, В.П. Таров, Тамбов : Изд-во ФГБОУ ВПО «ТГТУ», 2014. 96 с.
- [3] Назаревич С. А. Методика оценки инновационности продукции / С.А. Назаревич // *Фундаментальные исследования*. 2015 г. №3. С. 119-123
- [4] Легкий катер-амфибия на воздушной подушке «Стрелец» С-51 RT: листок-каталог: разработчик и изготовитель Санкт-Петербург АО «НПП «РадарМмс», СПб, 2012. 10 с.
- [5] Амфибийное судно на воздушной подушке "Корсар": листок каталог: разработчик и изготовитель Новосибир. АО «Трансэкология». 2015. 2 с.

AN INNOVATIVE TECHNIQUE TO IMPROVE THE PHYSICAL PERFORMANCE OF A CYCLIST

Enrico Mancuso, Giuseppe Piazza, Abigail Mariotti, Eleonora Lao
students

“Kore” University of Enna
Enna, Italy

enrico.mancuso@unikorestudent.it giuseppe.piazza@unikorestudent.it
abigail.mariotti@unikorestudent.it eleonora.lao@unikorestudent.it

Abstract

This research is based on study and reworking from a graduation thesis “Analysis and development of Human-Machine Interaction’s techniques in virtual environment” [2015], by eng. Fausto Savarino. The target is to study which variables are able to stimulate a person to do a constant physical activity, through the use of an exercise bike and one oculus, so being able to train himself comfortably from home. It proposes, through a graphic interface, the purpose to analyze various factors, among which the motivational ones that play an important role.

We added reinforcements such as praise, applause and encouraging sentences in order to promote the user to use our prototype. Have been formulated and distributed several questionnaires to understand the user’s expectation. Have been realized many tests of the different version of the prototype until you get at the final one, with the intent to improve the final product.

I. INTRODUCTION

The task assigned to our group is based on the analysis of an interface in the virtual environment. The user has the opportunity to pedal on an exercise bike immersed in a virtual reality through the oculus rift (a system that expanding the user experience, allow him to see firsthand what happens in a graphical interface).

Our study start from a previous work realized by a university student, Fausto Savarino [1].

The main objective of our group is to encourage the user to do a most assiduous physical activity allowing him to train and have fun enjoying a beautiful landscape, using our product comfortably from home.

However in the prototype there were some problems regarding the effect of motion sickness “seasickness”, that is a set of autonomic nervous

system’s disorders that appear when the two vestibules, organs sensitive to body’s position in space and its changes, are solicited in an irregular and asymmetrical way. Vestibular signals “don’t get along” and this could cause nausea, sweating, vomit, dizziness or headache).

In order to reduce this problem, resorting to an expert advice, we thought to dispose the information to maintain the user’s look as much as possible at the centre of the screen (would be ideal keep at 45 ° above the horizon [2]). It’s also important to make the surrounding objects as close as possible to reality, maintaining the correct proportions. Usually the effect of motion sickness tends to decrease when the person gradually becomes familiar to virtual reality.

A possible solution is given by the implementation of a new laser technology [3] in the oculus rift that seems to significantly reduce the negative effects of motion sickness.

II. PROTOTYPE UPDATE

The use of our prototype require “resources” such as an exercise bike that detect the user’s heart-beat through the handlebars, an oculus, an ankle bracelet to detect the pedaling, and an app that you can download on your phone in order to monitor daily progress accomplished.

Compared to the previous version we have implemented the option to choose between different modes of use (free ride, lap time, championship and training) and a broader choice of tracks.

The user can also: choose the most suitable graphics quality in relation to its hardware, create an account, share its results on his favorite social networks and customize his bike and his sport clothes (through a token-economy program [4], based on coins collection usable at a later time on virtual purchases).

By the study of various motivation’s research, we concluded that people are much more motivated, persist and feel involved to a greater extent when what they are doing is the result of their choice. Therefore, we have decided to give at the user the opportunity, in free ride mode, to choose if

he want to see or not in the display the information of the covered kilometers.

In the remaining three modes, the user always has the possibility to choose which information to display and in addition he could share, if he want, its results online (because the fact "to be approved" increases self-confidence and so the motivation [5]).

In our prototype we placed mostly positive reinforcements because they have a direct acting effect on behaviors that preceded them immediately.

Their purpose is to reward the user's commitment [6] by praises (using sentences such as "excellent", "Very Good! You commit yourself" and meaningful sounds like applause) (fig. 1).



Fig. 1. A positive reinforcements message

The reinforcements follow a variable relationship pattern, that consist in the appearance of reinforcements in an unpredictable manner around a mean value that produces a stable and high percentage of responses.

However, in the training mode we considered that is more functional to use a fixed interval pattern reinforcement, so the reinforcement of a response that compares after a fixed period and follows the previous reinforcement. Then a new interval begin [7].

Very important is the return of biofeedback [8] to users, or rather some physiological parameters such as heart rate. Some studies show how the monitoring of these physiological parameters enables the user to learn to recognize them and consequently acquire a greater control.

For this reason, we have decided, versus the previous edition and with the hint of a cyclist and experienced coach, to include the displaying on our interface of the user's heart rate (in the training mode) (fig. 2).

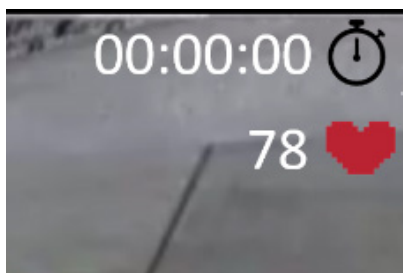


Fig. 2. Portion of HUD

III. INTERFACE'S DESIGN

For our prototype interface's design we followed as guidelines the ten Nielsen's heuristics [9]. We worked on the status system's visibility (by providing appropriate feedback in a reasonable time, through the use of sounds and textual messages), correspondence between system and the real world (using a kind of language shared by all), control and freedom (the user can control the information and move freely through the interface scenes), consistency and standards (consistency in details' arranging in the various stages of the interface), error prevention (the user has the possibility to go back avoiding ambiguous situations) (fig. 3). Therefore recognition rather than recall (simple layouts with easily recognizable information), flexibility of use (setting product based on the user's experience), minimalist design and aesthetic (using a very simple interface, avoiding distractions and unnecessary information), help the user (every major action ask to confirm), and documentation (the user always has the possibility to consult a guide).

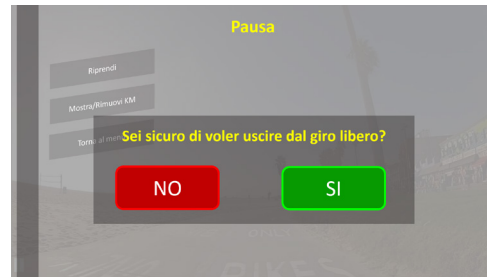


Fig. 3. Example of error prevention

Successively, by the reading of the book "The psychology of everyday things [10]" written by Donald Norman we realized that the sounds used as "signifiers" are essential as much as visual information, because detect invisible things, or things that might bypass us because our eyes are busy elsewhere.

For this reason we decided to implement sounds such as one beep per click that confirm to user he has pressed a button. Despite this, the data collection during user's test of the various version of the prototype revealed that sound alone is not always enough to provide appropriate feedback. For this reason, we decided to integrate, in some sections sound and visual stimulation.

When we did the test to users we have used the insight sheets (a lists of issues identified through user studies and insights about them that may affect design decisions), video and audiotape highlights (video or audio clips that illustrate significant observations about user and tasks) [11].

IV. TECHINCAL IMPLEMENTATION

As regard the technical aspect of prototype design we used knowledge already possessed in as-

sociation with a regular consultation of books which dealing this subject.

This helps us to do some implementation choices such as the creation of button key in the main menu (fig. 4), in the option menu and in other graphic aspects.



Fig. 4. The main menu

We used the parallax effect that avoids eye discomfort when you move from the main menu to the training mode and the information guide [12].

The information oriented us in the realization of launcher (fig. 5), counters and screens employed in the app and appearing overlapped in power point script [13].



Fig. 5. The Program Launcher written in Java

V. CONCLUSION

In conclusion, in our prototype we aimed to render the landscape as realistic as possible, maintaining proper proportion of surrounding objects

and placing the information in the central part of the screen with the intent to reduce the effect of motion sickness.

Moreover, we focused much more on the use of positive reinforcements to stimulate effectively the user to do physical activity making use our program. However, there would still be work out a program in which reinforcements gradually decrease with the intent to maintain a high rate of response from the user even in the absence of reinforcements.

VI. REFERENCES

- [1] Tesi di laurea "Analisi e sviluppo di tecniche di interazione uomo-macchina in ambiente virtuale" [2015] di Fausto Savarino, Università degli studi di Enna "kore".
- [2] <http://www.saninforma.it/malattie-dalla-a-alla-z/cinetosi-malattia-da-movimento>.
- [3] <http://www.videogiochi.com/news/2015/03/valve-con-vive-vr-abbiamo-eliminato-la-nausea-da-simulazione/>
- [4] Garry Martin, Joseph Pear [2000], "Strategie e Tecniche per il cambiamento", Milano, McGraw-Hill cap 23 pp. 331-341.
- [5] Rossana De Beni, Babara Carretti, Angelica Moè, Francesca Pazaglia [2008] "Psicologia della personalità e delle differenze individuali", Bologna, Il Mulino cap 2 pp. 59-66.
- [6] Mueller, C.M. & Dweck, C.S. [1998], Intelligence praise can undermine motivation and performance, in <<journal of personality and social psychology>>, n.75, pp.33-52.
- [7] Eysenk, M. W. [2006] "Psicologia Generale", pp. 111-112.
- [8] Olson, R. P., & Kroon, J. S. [1987], Biobehavioral treatments of essential hypertension in M.S. Schwartz (Ed.), biofeedback: a practitioner's guide. New York: Guilford.
- [9] <http://www.far.unito.it/usabilita/Cap5.htm>
- [10] Donald Norman [2014], "La caffettiera del Masochista. Il design degli oggetti quotidiani", Milano, Giunti Editore, pp. 163-164.
- [11] Joann T. Hackos, Janice Redish [1998], "User and Task Analysis for Interface Design" New York, John Wiley & Sons Inc.
- [12] Kelly S. Hale, Kay M. Stanney [2014], "Handbook of virtual environments: Design, Implementation, and applications", Florida, Taylor & Francis group.
- [13] Wu C. Thomas [2009], "Java fondamentali di programmazione", Milano, McGraw-Hill Education.

EFFECT OF INTERNAL ENERGY SOURCE AT NATURAL VIBRATION FREQUENCIES OF MEMS BASED RESONATORS

Aleksey Orlov, Arthur Paraskun
students

Saint-Petersburg State University of Aerospace Instrumentation,
Saint-Petersburg, Russia

zlakovoe@gmail.com, artur.paraskun@icloud.com

Abstract

The main functional elements of microelectromechanical systems (MEMS) are elastic elements, the operating mode of which are longitudinal and transversal forced oscillations. Operating frequency range, which is in the range from tens of kHz to several GHz.

These elastic elements are most often console or girder bridge, usually of rectangular cross section rigidly connected with the hulls.

I. MICRO-ELECTROMECHANICAL SYSTEM

In modern world we have found a wide application for MEMS in various fields of technology. As example – reference frequency resonators. Unlike quartz resonator, MEMS based resonator has better performance, impact resistance and smaller size. Fig. 1 shows a MEMS based resonator.

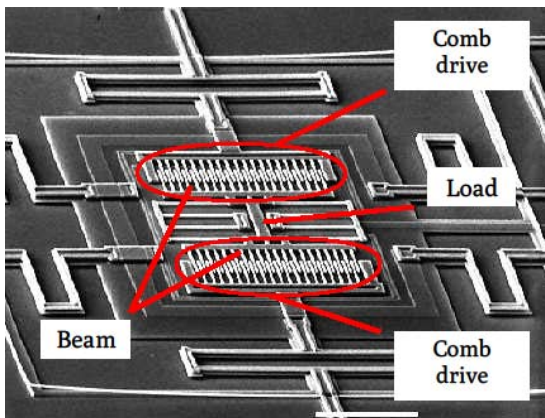


Fig. 1. MEMS based resonator

When forced vibrations through the different mechanisms of internal friction in single crystals of the thermal power generation is generated inside the elastic elements. Commission work of microstructure changes of materials consumes a Kinetic energy.

Generated heat changes temperature of the single-crystal elastic suspension until a stationary temperature distribution. This can affect the frequency of natural oscillations.

The calculated diagram of bridge beam is shown at fig. 2. All studied phenomena will be discussed based on this bridge beam.

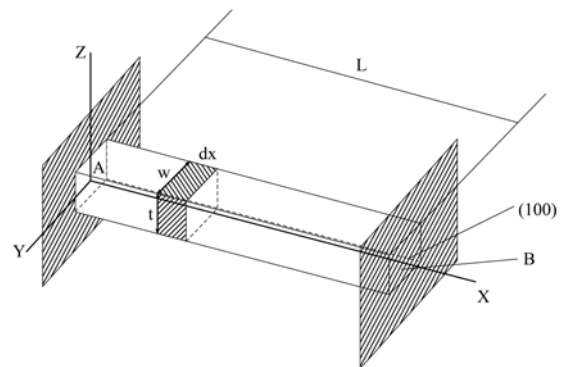


Fig. 2. Bridge beam with rigidly clamped sides

Here: $L = 100 \cdot 10^{-6} m$, $w = 20 \cdot 10^{-6} m$, $t = 5 \cdot 10^{-6} m$; w, t, L – bridge beam dimensions; (100) – crystallographic direction; A, B – bridge beam sides, rigidly connecting it with support.

The amount of generated energy in dv value at time unit is:

$$dp = \frac{\pi \sigma^2 \max v Q^{-1} \omega t dx}{E} \quad (1)$$

where $wt dt = dv$, σ – max normal pressure in dv unit while flexural vibrations of the bridge beam;

$Q_{TY}^{-1} = \frac{E \cdot \alpha^2 \cdot T}{C_p \cdot \rho} \cdot \frac{\omega \cdot \tau}{1 + (\omega \cdot \tau)^2}$ – thermoelastic internal

friction; $E(100) = 1,3 \cdot 10^{11} Pa$ – elastic modulus of monocrystalline silicon (crystallographic direction

(100)); $\omega = 6,67 \cdot \sqrt{\frac{E}{\rho}} \cdot \frac{t}{L^2}$ – reference frequency of

bridge beam oscillations; $\tau = \frac{C_p \cdot \rho \cdot h^2}{\lambda \cdot \pi}$ – relaxation

time of the heat flux in the bridge beam;

$\lambda = 150 \frac{W}{m \cdot K}$ – thermal conductivity coefficient of the Silicon;

T – absolute temperature;

$C_p = 800 \frac{J}{Kg \cdot K}$ – Mass specific heat capacity of Silicon;

$\rho = 2,33 \cdot 10^3 \frac{Kg}{m^3}$ – Silicon density;

$\alpha = 2,3 \cdot 10^{-6} K^{-1}$ – linear expansion coefficient of Silicon.

Thermoelastic internal friction Q^{-1} – is major part of internal friction processes in solid objects, which is transforms the Kinetic energy to heat.

Except Q_{TY}^{-1} the significant component in Kinetic energy scattering of oscillations is Q_M^{-1} , associated with structured changes in a monocrystal and with formation of defects. The value depends on the design and, follow [4], can be obtained with this equation:

$$Q_M^{-1} = A \cdot \frac{W}{L} \cdot \left(\frac{t}{L}\right)^4, \quad (2)$$

where w, t, L – bridge beam dimensions, A – factor, $2 \leq A \leq 4,5$.

Components have a additive losses, then at constant $Q^{-1} = Q_{MY}^{-1} + Q_M^{-1}$ components Q_{TY}^{-1} and Q_M^{-1} can be measured with widely limits, affect on heat spreading at elastic elements.

We have shown [5], that inner heat sources spreading in bridge beam depends on the ratio between main frequency and forced oscillations.

At major of MEMS devices working frequency is equal to main frequency of free oscillations or less, relaxation time $\tau \leq T_0 = \frac{2\pi}{\omega_0}$ – period of natural oscillations where ω_0 is frequency.

System thermal model, showed via COMSOL at fig. 3.

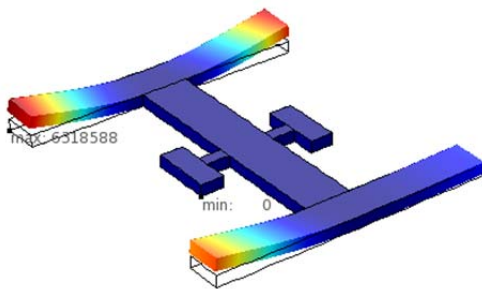


Fig. 3. System thermal model

Temperature gradient dissolves in the direction from the compressed to the stretched surface of bridge beam in these conditions, temperature becomes constant inside dv value, thermal process – isometric.

Thermal energy dispensed inside elastic element with these conditions can be obtained by (1) at V value.

$$\int_V dP_T = \int_0^L \frac{\pi \cdot \sigma^2(x) Q_{TY}^{-1} v \cdot w \cdot t}{E} dx = \frac{\pi \cdot Q_{TY}^{-1} v \cdot w \cdot t}{E} \int_0^L \sigma^2(x) dx \quad (3)$$

To determine the depending of $\sigma^2(x)$ we will create diagrams of shear force F и bending moment of bridge beam, shown at fig. 2.

Bridge beam sides jamming indeterminates it statically, method of moments to calculate the support reactions and reactive power [6].

Areas within the beam segments

$$\left(0 \leq x_1 \leq \frac{L}{2}\right), \left(\frac{L}{4} \leq x_2 \leq \frac{L}{2}\right), \left(\frac{L}{2} \leq x_3 \leq \frac{3L}{4}\right), \left(\frac{3L}{4} \leq x_4 \leq L\right)$$

The bending moment varies linearly, $\sigma_x = \frac{M_x}{W}$, where $W = \frac{w \cdot t^3}{6}$ – the moment resistance of the bridge beam cross-section,

$M_x = \frac{F}{2} \cdot \left(x - \frac{L}{4}\right)$, depending $\sigma^2(x)$ in case $\left(0 \leq x \leq \frac{L}{2}\right)$ shown at fig. 4.

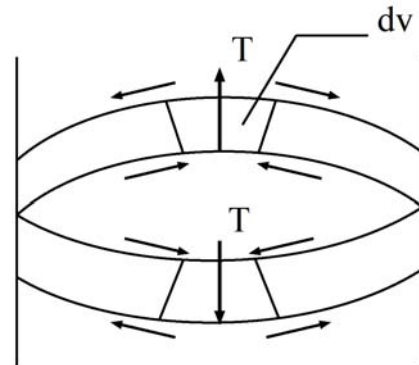


Fig. 4. The heat flow directions inside bridge beam with bending vibrations

Analysis of this distribution shows, that $\sigma^2(x)$ varies in $0 \leq x \leq \frac{L}{2}$ as square rule.

This relation is the same at $\frac{L}{2} \leq x \leq L$. Temperature spreading same at all, so temperature inside bridge beam aligns from $x=0$ and $x=\frac{L}{2}$ to $x=\frac{L}{4}$, from $x=\frac{L}{2}$ and $x=L$ to $x=\frac{3}{4}L$ until it reaches an isothermal condition.

Bridge beam heating via inner heat sources, with max $\sigma^2(x)$ until inner generated heat energy starts to radiate to the environment through bridge beam's surface.

Temperature value can be obtained:

$$\int_V P_T dt = \int_S S \cdot \chi \cdot \varepsilon \cdot (T^4 - T_0^4) ds \quad (4)$$

Here: $\int_S S \cdot \chi \cdot \varepsilon \cdot (T^4 - T_0^4) ds$ – Energy, emitted

from the surface of bridge beam at time;
 $S = 2 \cdot (w + t) \cdot e$ – square of membrane's side.

With previously viewed equations for P_T included quantities of heat balance beam equation, it corresponds to the isothermal state:

$$\frac{F}{2} \cdot \frac{E \cdot \alpha^2}{C_p \cdot \rho} \cdot \frac{\omega \cdot \tau}{1 + (\omega \cdot \tau)^2} \cdot \frac{\pi \cdot \nu \cdot \omega \cdot t \cdot L^2 \cdot T}{192 \omega^2 \cdot t^4} = \quad (5)$$

$$= 2 \cdot (\omega + t) \cdot L \cdot k \cdot \varepsilon \cdot (T^4 - T_0^4)$$

The amplitude of the external force F can be obtained with: $F_{\max} = \frac{192 \cdot E \cdot Y}{S_{\max} \cdot L^3} = 5,2 \cdot 10^{-2} N$, when

$$f_{\max} = 2 \cdot 10^{-6} m, Y = \frac{\omega \cdot t^3}{12} m^4.$$

Coefficient ε can be obtained practically, value ε depends on the technology blank–capsule processing – in limit of (0.15–0.6). Consider that $\varepsilon = 0.5$, we give (5) taking all contained parameters to: $2 \cdot 10^{-8} T = 1 \cdot 10^{-16} (T^4 - T_0^4) \rightarrow T^4 - 2 \cdot 10^8 T = T_0^4$, where T – the absolute temperature of the bridge beam in thermodynamic equal with environment. With this values $T_0 = 300 K$, $T = 600 K$.

This T value is max, all generated bridge beam inner energy reradiates from its side.

With inside support losses, heat removal to MEMS support elements because of thermal conductivity, approximate bridge beam temperature sets lower. Designing of MEMS with close to obtained distortions and fixing scheme, temperature of elastic element is 450–500 K, that require clarification design parameters of the oscillating system. With inner heating of rigidly fixed bridge beam it becomes to compressed condition because of action of axial bearings reactions.

Here is estimation of changes in the fundamental frequency of the bridge beam oscillations, which is shown in [7].

The value of normal stress under axial compression does not depends of bridge beam geometry and:

$$\sigma = \alpha \cdot E \cdot (T - T_0) = 2,3 \cdot 10^{-6} \cdot 1,3 \cdot 10^{11} \cdot 300 =$$

$$= 6 \cdot 10^7 Pa$$

$$V = w \cdot t \cdot \sigma = 1 \cdot 10^{-10} \cdot 6 \cdot 10^7 = 6 \cdot 10^{-3} N$$

Main frequency of bridge beam oscillations without axial compression ratio:

$$\omega_0 = \frac{\beta}{L^2} \sqrt{\frac{E \cdot I}{\rho \cdot F}} = 2,2 \cdot 10^7 s,$$

with axial compression ratio:

$$\omega_{0,N} = \frac{\beta}{L^2} \sqrt{\frac{E \cdot I}{\rho \cdot F}} \sqrt{1 - \frac{N \cdot L^2}{E \cdot I \cdot \pi}} = 1,84 \cdot 10^7 s,$$

where $I = 2,08 \cdot 10^{-22} m^4$.

It can be assumed that, given the kinetic energy loss in the bearings oscillation frequency change will be in the range of 15–20% of ω . This Takeo deviation is unacceptable and it is necessary to use the device with temperature compensation, which is realized in modern MEMS generators. This deviation is unacceptable and, therefore, it is advisable to use temperature compensation device, which is done in today's MEMS oscillators.

II. CONCLUSION

Having more precise data will allow for more accurate temperature compensation device design, in order to achieve higher accuracy MEMS. Therefore, this method of calculating the kinetic energy dissipation is sufficient.

III. REFERENCES

- [1] *Работнов Ю. Н.* Механика деформируемого твердого тела / Ю.Н. Работнов. – М.: Наука, 1988.
- [2] *Постников В. С.* Внутренне трение в металлах / В.С. Постников. – М.: Metallurgiya, 1974.
- [3] *Балалаев Ю. Ф., Постников В. С.* Об ультразвуковом нагреве металлов / Ю.Ф. Балалаев. – Физика и химия обработки металлов №9, 1968
- [4] *Митрофанов В. П.* Колебательные системы с малой диссипацией / В. П. Митрофанов – М.: МГУ, 2010.
- [5] *Candler R.* Impact of slot location on thermoplastic resonators / R. Candler – Solid-State sensor, Actuators and Microsystems, 2005, transducers'05. The 13th international Conference. p. 597–600 Vol. 1.
- [6] *Феодосьев В. И.* Сопротивление материалов / В.И. Феодосьев – М.: Наука, 1974.

**PHOTOVOLTAIC EFFECTS AS THE PHYSICAL BASIS
OF A NEW GENERATION OF MICROELECTROMECHANICAL SENSORS AND SYSTEMS**

Boris Oskolkov
student

Saint-Petersburg State University of Aerospace Instrumentation,
Saint-Petersburg, Russia

biontys@gmail.com

Abstract

The paper analyzes the prospects for the creation of a fundamentally new class of MEMS, which are based on the use of the photovoltaic effects of Dember, Kikoin–Noskov, photopiezoelectric effect in semiconductors for measuring various physical quantities.

Keywords: microelectromechanical sensors, photovoltaic effects, photo-emf, the sensing element.

I. INTRODUCTION

At present the basic requirements for the electronic components – is minimization, ease and efficiency. The ever-rising demands on these parameters can satisfy the sensors that are based on the photovoltaic effect.

Different variants of designs of sensors, which are allowing their technical implementation without making fundamental changes in the existing technology have been reviewed. It is shown that the sensors based on photovoltaic effects are high-tech products, which is provided including extreme simplicity of the construction and technological route of their manufacture.

The main problems that will require considerable effort on the part of developers and constructors of these products are likely to be associated with the processing of the output signal and increasing the sensitivity of the sensor to the measured physical quantities.

II. DEMBER EFFECT

If the semiconductor is illuminated by light with a wavelength corresponding to the intrinsic absorption: $\hbar\omega = E_n$ (E_n – width of the energy gap of the semiconductor), near the sample surface, where light absorption takes place, occur electron-hole pairs. These charge carriers diffuse (fig. 1) from the illuminated region deeper into the semiconductor. As electrons have higher mobility than

holes, the electrons will move deeper into the crystal than the holes. This difference in the diffusion of the charge carriers leads to the fact that the semiconductor surface will be positively charged relative to its volume. The emerging electrical field is directed so that it accelerates holes having lower mobility and slows mobile electrons, therefore the total current is zero. Bulk EMF arising in illuminated semiconductor due to the difference in the diffusion coefficients of electrons and holes, called Dember’s EMF.

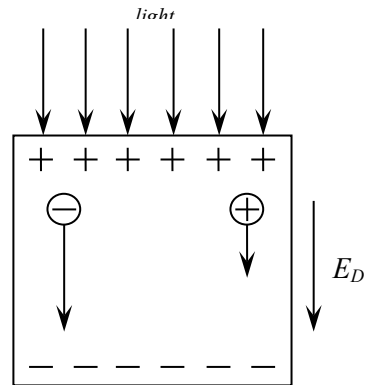


Fig. 1. The appearance of Dember’s EMF

The size of EMF Dember in the absence of traps and excluding surface recombination is determined by the formula:

$$U = - \frac{D_n - D_p}{\mu_n + \mu_p} \int_0^l \frac{d\sigma}{\sigma}, \quad (1)$$

where D_n – the electron diffusion coefficient, D_p – hole diffusion coefficient, μ_n – electron mobility, μ_p – hole mobility, l – distance from the illuminated surface to a place where there is no non-equilibrium carriers, σ – conductivity of the system.

Denoting $b = \frac{\mu_n}{\mu_p}$, considering the Einstein relation $eD_{n,p} = \mu_{n,p} k_B T$ and taking the integral,

$$U = \frac{kT}{e} \frac{b-1}{b+1} \ln \frac{\sigma(0)}{\sigma(l)} \quad (2)$$

From (2) it follows that the greater the EMF Dember, the stronger different electron and hole mobilities. Dember's EMF is usually very small, it is a little more kT/e (~ 26 mV) [1].

III. KIKOIN–NOSKOV EFFECT

The appearance of an electric field (EMF) in a semiconductor placed in a magnetic field, while covering his strongly absorbed light, has been called photo-magnetolectric effect.

If the semiconductor is illuminated by light with a wavelength corresponding to the intrinsic absorption: $\hbar\omega = E_n$ (E_n – width of the energy gap of the semiconductor), near the sample surface, where light absorption takes place, occur electron-hole pairs. This occurs when their concentration gradient leads to diffusion of carriers in the flow direction of the incident radiation. If the magnetic field H is applied along the oz axis (fig. 2), the light beam and the diffusion flux – along the y -axis, the magnetic field deflects the electrons and holes in different directions, causing direction oh spatial separation of charges. If the ends of the sample shorted, current j_x flows in the circuit, otherwise – emf (fig. 3).

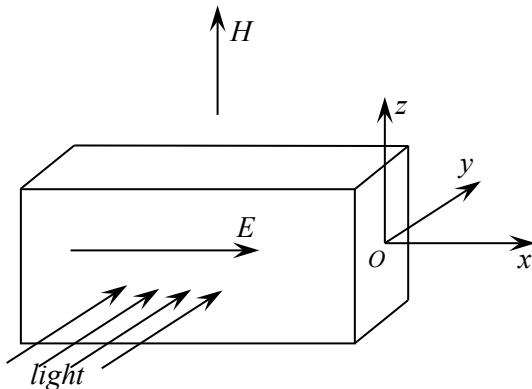


Fig. 2. The sample for measurement of photo-magnetolectric effect

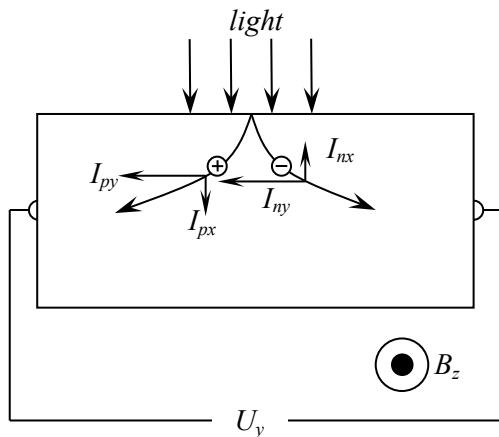


Fig. 3. The appearance of voltage U_y at the photo-magnetolectric effect.

In weak magnetic fields EMF Kikoin–Noskov effect is proportional to the magnetic field H and changes its sign when the direction H on the opposite (odd photoelectric effect).

In weak magnetic fields ($uH/c \ll 1$, u – charge carrier mobility) current density

$$j_x = -eD \frac{H}{c} (u_n + u_p) \frac{dn}{dy}, \quad (3)$$

where D – the coefficient of ambipolar diffusion of the charge carriers, n – concentration of nonequilibrium charge carriers. View the distribution n is generally difficult because it depends on the diffusion-recombination parameters of semiconductor from the light absorption coefficient and quantum yield photogeneration carriers.

The single-crystal semiconductors effect Kikoin–Noskov is an isotropic – the value and sign of the EMF depends on the relative orientation of the crystallographic axes and H . As anisotropy is associated with anisotropy of the diffusion coefficient D of carriers in the presence of a magnetic field, its research allows to determine effective masses of electrons and holes along different crystallographic axes sample.

On the basis of photo magnetolectric effect simple and reliable methods for the determination of parameters of semiconductors, as the lifetime of nonequilibrium charge carriers, diffusion length, surface recombination velocity, as well as radiation detectors and magnetometers are created.

The voltage level of this effect [2] is 10 mV.

IV. PHOTOPIEZOELECTRIC EFFECT

The essence of the photo piezoelectric effect appearance EMF is due to the difference in the energy gap of the semiconductor illuminated screen, which changes under the influence of deformation.

If the energy gap E_G is different along the entire length of the semiconductor and the beginning of the illuminated area, this value will be equal of E_{Gb} , and in the end – E_{Gc} , EMF value will be determined by the following equation:

$$U = -\frac{1}{e} \Delta t_1 (E_{Gc} - E_{Gb}), \quad (4)$$

where e is the absolute value of the electron charge,

$$\Delta t_1 = t_1 - t_{10}, t_1 = \frac{\sigma_1}{\sigma}, t_{10} = \frac{\sigma_{10}}{\sigma_0}, \sigma$$

is the total electric conductivity during illumination, σ_0 is the total conductivity in the dark, σ_1 and σ_{10} are the conductivities corresponding to electrons in the conductivity band.

The research [3] on samples of germanium, silicon and gallium arsenide, shows that the optical pulse irradiation is variable photo-EMF in the volume of the crystal and through the inverse piezoelectric effect generates the elastic vibrations in the longitudinal mechanical resonance frequency. The variable compression plate stretching deformation leads to the appearance of EMF pulses on its opposite surfaces by transverse piezoelectric effect.

The described effect can be used to selectively receive the optical signals using both bulk and surface acoustic waves.

V. CONCLUSION

The above described effects are united by one condition: the presence of the illuminated area of the semiconductor. The sensors that are based on these effects have extraordinary high manufacturability because the work piece of a semiconductor material processing require a minimum for using photovoltaic effects. The only problem – a small voltage level obtained on the plates of such sensors. This problem can be solved by extensive research

of photovoltaic effects and a completely new design solutions.

VI. REFERENCES

- [1]. *К. В. Шалимова*. Физика полупроводников. М.: Энергоатомиздат. 1985. С. 366-368
- [2]. *И. К. Кикоин, С. Д. Лазарев*. Фотоэлектромагнитный эффект. Успехи физических наук, том 124, выпуск 4. М.: Наука. 1979. С. 588-616.
- [3]. *JanTauc, MilenaZavetova*. Photo-piezoelectric effect in semiconductors. Czechoslovak Journal of Physics, 9, 1959.P. 572-577

THE RESEARCH OF THE COMPONENT OF THE COMBINED PRODUCTION TECHNOLOGY OF AIRCRAFT PARTS

Evgeniia Petrashkevich
student

Saint-Petersburg State University of Aerospace Instrumentation
Saint-Petersburg, Russia

Dgonya.94@mail.ru

Abstract

The article presents the results of the research of the combined production technology of aircraft parts, the essence of which is the use of additive technology. As a result, based on the analysis of 3D-printing powder technologies conclusions were made about the feasibility of using one of them.

Keywords: aerospace products, the production of planes, import substitution, additive technology.

I. INTRODUCTION

At the end of the 20th century in Russia degradation of one of the most important sectors - the aviation industry was observed. Because of this, the program of the Russian Federation "Development of the aviation industry for 2013–2025", which is directed on the elimination of aircraft production at a new technological level was created [1].

Russian plans are to increase import substitution and the position on the world market of aircraft construction, get a share of supply at the domestic market of the country to 60%. To achieve this goal it is necessary to create highly competitive aviation industry [2].

Based on the research of basic tasks of the aviation industry, a series of studies based on the study of the production cycle of aircraft parts of one of the plants of PJSC "United Aircraft Corporation" has been carried out, with the result that the conclusions about the necessity of technology development and study its applicability in practice were made.

As a problem decision there is offered the combined production technology in the aviation industry, which aims to create a modern production, secured with mobility and adaptability of enterprises to innovation and new products with fast scaling possibility, as well as secured with the possibility of observance of specified parameters of quality and production efficiency.

As a result, it will be possible to increase the functionality of production, improve the quality characteristics of the products, reduce time and material costs [3].

II. RESEARCH PART

At the present stage of industrial competition, the main direction of the production improvement is the modernization of existing and creation of new technological processes.

The leading role is played by the additive technology (layered synthesis technology) – this is a process of creating a computer model of the future detail and obtaining of the product through a phased application of building material on the generated object on special equipment using different methods.

Usually, when people talk about mass production they mean an amount, measured in thousands or hundreds of thousands of units. However, in the case of the aviation industry for mass production means production, measured in tens or hundreds of products.

The main interest of the aviation industry to the additive technologies, with the help of which it is possible to grow products with complex geometry of special materials, instead of traditional manufacturing methods, is economic feasibility (fig. 1). In some cases, with objective calculations of the real cost it turns out, that additive technologies are less expensive than traditional.



Fig. 1. Parts of aircraft engines

For now there are such 3D-printing technology as the curing liquids technology, the technology of extrusion of the molten material, the powder technologies and other. Due to the significant expansion of the range of the metal-powder materials the choice fell on powder technologies.

Most plants have laser as a source of energy for the compound particles of metal-powder composition.

A common feature of the technologies using radiation heat source is the need for special supports – specific «anchors» that hold under construction part from the thermal deformations. When parts build from polymer powders it is not necessary.

The power of the laser is more therefore the metal melts faster and details are build faster. On the other hand, at this melting point is brought a large amount of energy, the process goes very intensively, the metal boils, it is splashed and the part of a construction material is thrown out of a melt spot. This can cause increase of porosity, considerably deterioration of the surface quality. In such conditions, the construction of difficult thin-walled component of parts problem is solved by applying an additional laser of lower power, but in this case with reduced performance [4]. This is the main technological difference between technology of selective laser melting of the metal powder (SLM technology) and the conventional technology of selective sintering of powdered materials by laser beam (SLS) system.

SLM technology has a higher density of material on the output and accuracy of construction (fig. 2). SLS installations are more productive and therefore they are intended for the manufacturing of larger consignments.

During the research comparative characteristics of quality indicators were obtained and were

deemed deviation indicators D (1) of installation using SLS technology from installation with SLM technology (fig. 3), by which it was provided an assessment differences, which allowed to highlight the benefits of both technologies [5].

$$D = \frac{P_2}{P_1} * 100 - 100, \quad (1)$$

where D – deviation of the indicators of installation with the use of SLM technology from the installation of the SLS technology (%), P₁ – quality indicators of installation of SLM technology, P₂ – quality indicators of installation of SLS technology.

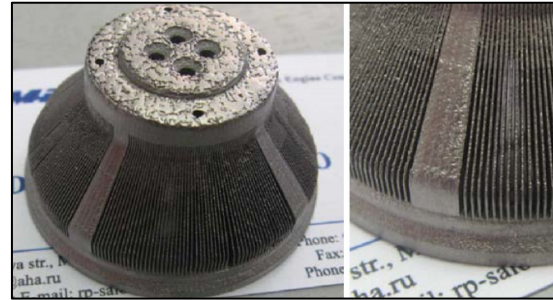


Fig. 2. Detail of the electrical device with a thickness of edges 0.35 mm, built on SLM Installation

For further comparison of technologies there is a table where the technology of the metal powder selective laser melting (SLM technology) and technology of selective sintering of powder materials by laser beam (SLS – Selective Laser Sintering) system are considered.

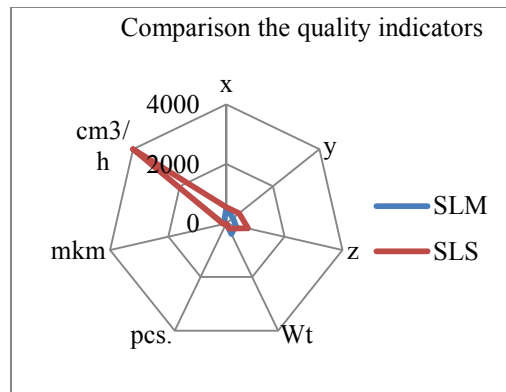
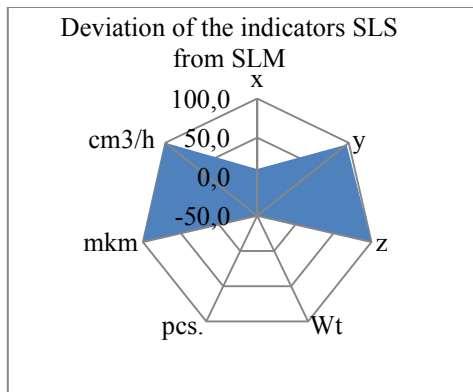


Fig. 3. Deviation of the indicators (D, %) and comparison the quality indicators of installation using SLM technology from the installation with SLS technology

Table

Quality analysis on the most important indicators

Parameter		SLM, P ₁	SLS, P ₂	Weight, m	k ₁	k ₂	Q ₁	Q ₂
The size of the working area, mm	x	500	550	0,1	0,909	1	0,091	0,100
	y	280	550	0,1	0,509	1	0,051	0,100
	z	330	750	0,1	0,440	1	0,044	0,100
The power of the laser	Wt	400	200	0,1	1,000	0,5	0,100	0,050
The number of lasers	pcs.	2	1	0,1	0,500	1	0,100	0,050
Thickness of layer	mkm	47,5	100	0,3	1,000	0,5	0,300	0,143
Construction speed	cm ³ /h	105	4000	0,2	0,026	1	0,005	0,200

Quality evaluation on the most important indicators (2) will help to compare technologies on a quantitative level.

$$Q_i = \sum k_i \cdot m_j, \quad (2)$$

Where Q_i – quality evaluation on the most important indicators, k_i – attitude of indicator of the installation to the biggest indicator of parameter, m_j – weight parameter based on expert evaluations.

As a result, it should be noted that significant difference was not observed, but studies have shown that $Q_1 < Q_2$, and therefore the installation using selective laser beam sintering of the powder materials technology has more advantages and is best suited in the production of aircraft components.

III. CONCLUSION

According to preliminary research, it is possible to speak about prospects of application of additive technologies in the aviation industry. It is also able to identify the additive technology, which

is more appropriate to use in the basis of the combined production technology of aircraft parts. This will allow to lower time and material costs, reduce waste from the production and improve the accuracy of the manufacturing of complex products.

IV. REFERENCES

- [1] Россия и мир: 2015. Экономика и внешняя политика. Ежегодный прогноз / Рук. проекта - А.А. Дынкин, В.Г. Барановский. ИМЭМО РАН. М., 2014. 166 с.
- [2] Спецвыпуск «Промышленное производство России в 2014 году: курс на импортозамещение»/ Белгород. ОАО "Корпорация "Развитие", 2014. 154 с.
- [3] Чабаненко, А. В. Стандартизация наукоемкой продукции/ А. В. Чабаненко // Стандарты и качество. 2015. № 1. С. 42-49.
- [4] Довбыш, В. М. Аддитивные технологии и изделия из металла / В. М. Довбыш, Забеднов П. В., Зленко М. А. // Библиотечка литейщика. 2015. № 1. С. 37-43.
- [5] Назаревич, С. А. Методика оценки инновационности продукции/ С. А. Назаревич // Фундаментальные исследования. 2015. № 3. С. 119-123.

**“VIRTUAL ACT DEFUSION”:
A JAVA-BASED SOFTWARE TO JOIN ACT PSYCHOTHERAPY WITH THE VIRTUAL REALITY**

Salvatore Platania, Adriano Gandolfo, Laura L’Episcopo, Marta Merlino
Students

“Kore” University of Enna
Enna, Italy

salvatore.platania@unikorestudent.it, adriano.gandolfo@unikorestudent.it,
laura.lepiscopo@unikorestudent.it, marta.merlino@unikorestudent.it

Abstract

The object of our work has been the creation of the “Virtual Act Defusion” software (fig. 1), with the purpose to give to ACT psychotherapist, handy means for the management of his patients’ sessions using virtual reality.

The main benefit is to decrease the paper-based documents from one’s own studio, because the report of the sessions, together with patient’s personal data, will be stored by the program itself.

To enjoy these benefits will not only be the psychotherapist but also the patient, because he will have the ability to directly manage his sessions from his own device.



Fig. 1. “Virtual ACT Defusion” logo

I. INTRODUCTION

Virtual reality (VR) is a rapidly growing field that has the inherent potential to manipulate people's minds with a superlative 3D experience. With the improvements made so far in VR, now it seems more feasible to provide user experiences that were previously thought to be only a dream or a nightmare [1].

Besides the videogame or military field, virtual reality is also used in the therapeutic field to fight, for example, specific phobias and this is done through the exposure of the patient through the virtual reality to specific phobia [2].

The object of this software is to provide handy means to interface the ACT psychotherapist with a virtual reality device (such as the Oculus Rift), to consider the sessions made by their patients and to acquire the actual data.

The patient, through his own device, can execute a new session using the virtual reality and he can display the already carried out session through a diary.

ACT is a psychological intervention based on experimental evidences that uses, to increase the "psychological flexibility" of an individual, strategies based on acceptance, mindfulness and behavior modification.

With the psychological flexibility expression, we refer to the ability of an individual to be fully in touch with the present moment, as conscious human being and, based on what the situation allows, to change or persist in behaviors that pursue the values that were chosen as important elements of their lives.

Goal of ACT is to help the patient to choose to act effectively, with actual behaviors, in line with its values, in the presence of difficult or private events that interfere with daily life. ACT is somewhat counterintuitive: instead groped to eliminate or reduce the appearance of emotions and thoughts that cause suffering, teaches patients and therapists to make room for these [3].

This paper is so organized: in Section II we talk about the way in which data have been collected and the purpose that have had, Section III describes the program destined to the psychotherapist while Section IV is dedicated to the program developed for the patient; finally, Section V summarized the paper by discussing of the several future works in order to improve the app.

II. DATA COLLECTION

For the development of the application, it has been used a “cascade” design model, that considers, besides the design and the implementation, a requirements’ analysis.

For this analysis have been used two techniques, that are focus group and interviews.

Focus Group

We have collected different point of views by potential users and have analyzed the different needs, trying to implement their suggestions.

Interviews

The questionnaire administered to ACT therapists has been the aim to verify if they would use ACT defusion exercises with the help of VR.

From the data obtained has emerged that:

- 72% of ACT therapists uses technology;
- 30% has had a direct experience with virtual reality;
- 97.7% knows what is virtual reality, but only 11.40% already uses it in the therapies;
- 86.10% would use the defusion exercise in virtual reality;
- 74.30% would use the tablets to analyze patients' sessions.

The purpose of the questionnaire administered to the general public, has been to verify if people external of the informatics and psychological sphere, would be willing to use our software.

We have divided population into three age groups in according to Erickson's stadial development model [4, 5]:

- 17/19 years: represents the fifth stage, characterized by the development of identity opposite to a dispersion identity's process (adolescence), characterized by bodily modifications, together with psychological changes;
- 20/39 years: represents the "young adult", that constructs a stable identity, thanks to the creation of bonds of friendship, trying intimacy and affiliation but, if attempts should fail, the person retreats into isolation;
- 40/60 years: represents the "mature adult", that shows generativity represented by the interest in creating and leading the next generation but, on the other hand, the lack of individual's generativity is expressed by the absence of psychological growth, stagnation, self-absorption, boredom.

From the first segment, has emerged that 65% would be willing to try a psychological therapy in virtual reality, the second sector that would be willing to try it about 81.7% and the last 85%.

Through the data collected, it has been verified that there are effectively the exigency and the will to try this new technology in this sector and it has been the reason that incited us to move forward.

III. THE SOFTWARE FOR THE PSYCHOTERAPIST

The Java-based software exploits a relational model database, written in SQL language, to save sessions' and patients' data. It also has been made as simple and intuitive as possible with a graphical interface that can be used for different platforms, fixed or mobile.

In fact, home page (fig. 2) consists of four buttons that allow an immediate access to the four main program areas:

- the registration of a new session;
- the report of all sessions made by the patients;

- the registration of a new patient;
- patients' register.

Choosing to use this kind of layout for the homepage, arises from the fact that our brain has the capability to assimilate up to seven information at one time [6].

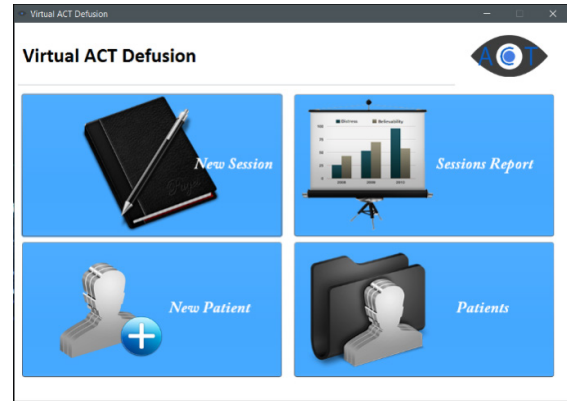


Fig. 2. Program's home page that will be used by the psychotherapist

The "New Session" button allows the therapist to evaluate the session performed by the selected patient.

Diagnosis and assessment's type is centered on the psychological flexibility that derives from processes' "sum", that are represented by the so-called *hexaflex* model, that in ACT leads the assessment process and the psychotherapeutic session [7].

The psychological flexibility is represented as a six sided diamond; each one indicates a process.

In ACT, it's usually to talk about two hexaflex: the psychological one to aim for and the pathological one to avert for regarded as two sides of the same coin [8].

This kind of evaluation has been digitalized (fig. 3), because once chosen the values for each scale, using the appropriate buttons, the program will calculate the patient's psychological flexibility dynamically.

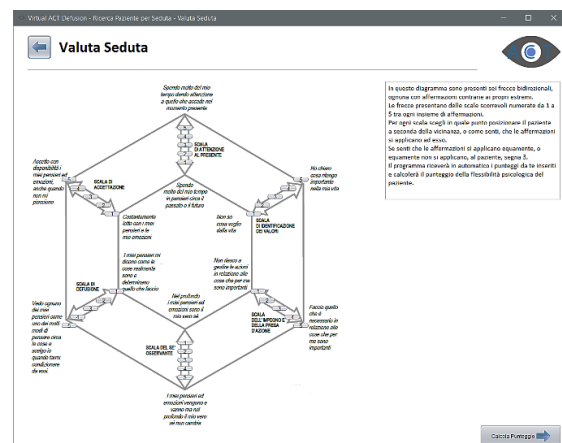


Fig. 3. Evaluation centered on hexaflex

According to his score, the user will display a radar diagram that will match the hexagonal pattern of the hexaflex model. If he wanted to, the therapist will see in detail the diagrams for each scale concerning the session made.

In fact, each image corresponds to a button that allows to visualize in detail the relative diagram (fig 4).



Fig. 4. Details of the six scales

From a psychological viewpoint, the program has several *positive reinforcers* namely the processes whereby are increased the possibility of an instrumental response associating it with a positive result [9].

An example is the automatic calculation of patient's psychological flexibility which, otherwise, would require using of calculators or similar.

The "Sessions Report" section allows to display the data obtained through the VR device; the therapist, in fact, can visualize the sessions which have been made.

The "New Patient" section allows to register a new patient and, particularly, his personal and billing data.

In case personal data such as name, address, city and state should coincide with the billing information, in this section is included a button which copies those identical values in the appropriate fields, acting as a positive reinforce.

Has been introduced possibility to insert patient's photo (which can be modified or deleted at any time), in order to make the recognitions easier and permit the therapist to have a human contact.

Finally, in "Patients" section (fig. 5), it is possible to choose a specific patient and then display the data.

Besides personal data and billing information sections (that are possible to edit), there will be a tab for all the sessions carried out by the patient, displayed as mentioned above and a diary of the sessions.

The latter is compiled by the patient, if he wants to, at the end of a session and at the beginning of another (but always concerning the results of the previous one), as a questionnaire, in order to let him acquire knowledge about work he has done.

To be able to display the diary page about a certain date, the therapist can just click the chosen

date on an appropriate calendar located at the left of the interface.

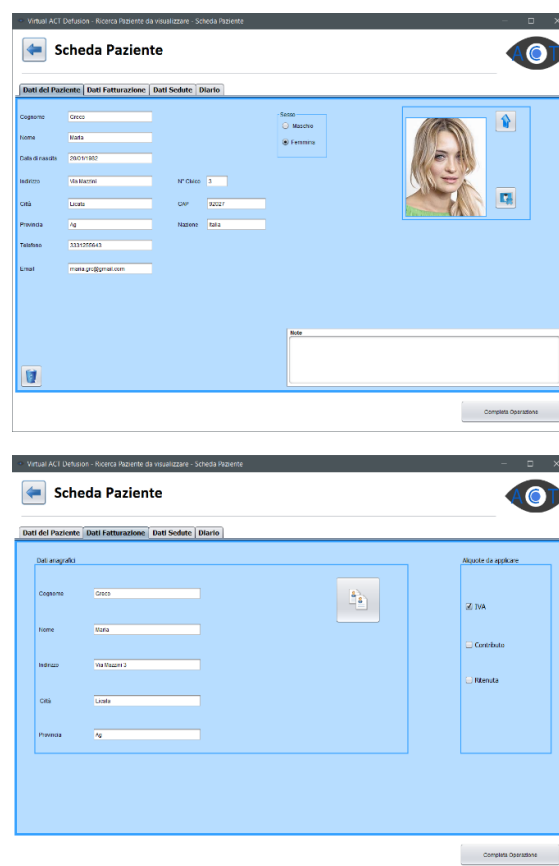


Fig. 5. The "Patients" section

IV. THE SOFTWARE FOR THE PATIENT

The software, which is also Java-based, will match the features seen for the therapist program.

Software's home page (fig. 6) in fact, will be divided into four sections which will allow:

- the launch of a new session;
- the visualization of sessions' diary;
- the management of patient's account;
- a modification of general settings of virtual reality device.



Fig. 6. Program's home page that will be used by the patient

The "New session" button enables patient to interface with the Oculus Rift to launch a new session of the defusion exercise in virtual reality.

At the end of it, as it has already been said, the patient will be able to record a new page of his diary.

The "Sessions Diary" (fig. 7), will enable the user to view his diary's pages selecting a date from the calendar next to it.

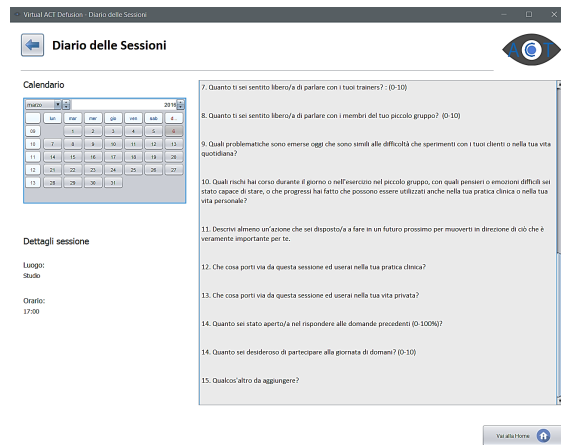


Fig. 7. Patient's sessions diary

Finally, the "Account" and "Quick Settings" sections allow the user, the first to view or to change his personal and billing data, and the second to change Oculus Rift's options such as brightness and contrast.

V. DEVELOPMENT CHOICE

To promote the usability of our programs, we rely to special studies in the branch of psychology. Relying on Nielsen's valuation, in fact, our choice has been to notify the user about the events which occur during the use of the program, involving appropriate images and sounds based on the type of event.

We have associated red color to error, because several researches show its correlation with danger, while green is associated with positive outcomes [10].

The sound is also associated to the visual stimulus in order to increase the association between a stimulus (positive and negative) and event. We show that the activity in the visual cortex retinotopic increased by the presence of concurrent auditory stimulus, regardless of any illusory perception [11].

VI. CONCLUSIONS AND FUTURE WORKS

In this paper it was shown how the two Java-based software are closely linked to each other, not only for graphics but also from an implementation point of view, because there is a constant data exchange.

Our project's object, in fact, is precisely to provide users (patient and therapist), this software package which is capable to perfectly interface with Oculus Rift, to exploit this new and powerful technology for a purpose that goes outside the entertainment industry.

In fact, the results obtained from questionnaires show a strong interest by the people for this technology; showing the program to specialists in the field, but also to possible patients, we have received very positive feedbacks and tips that we have already applied or will implement in future releases.

In this regard, in the next updates, patients' billing data management will be enhanced, with the possibility to directly print the invoice from our program and will be implemented new functionalities that may improve work of ACT psychotherapists.

VII. REFERENCES

- [1] International Journal of Engineering Trends and Technology (IJETT) – Volume 13 Number 4 – Jul 2014 ISSN: 2231-5381 <http://www.ijettjournal.org> Page 175, A Review Paper on Oculus Rift-A Virtual Reality Headset. Parth Rajesh Desai, Pooja Nikhil Desai, Komal Deepak Ajmera, Khushbu Mehta.
- [2] Moving from virtual reality exposure-based therapy to augmented reality exposure-based therapy: a review Oliver Baus and Stéphane Bouchard.
- [3] ACT e RFT: il linguaggio per fare una differenza nella pratica clinica. Giovambattista Presti, Giovanni Miselli, Facoltà di Scienze dell'Uomo e della Società, Università Kore, Enna AUSL, Reggio Emilia.
- [4] Erickson, 1959,1968.
- [5] Identità in transizione e compiti di sviluppo, Monica Pellerone, pag 18,19.
- [6] EL.LE ISSN 2280-6792 Vol. 2 – Num. 1 – Marzo 2013 Memoria e glottodidattica Compendio delle implicazioni essenziali Maria Chiara Naldini.
- [7] Miselli, Rabitti, Presti, & Moderato, 2009.
- [8] ACT e RFT: il linguaggio per fare una differenza nella pratica clinica, Giovambattista Presti, Giovanni Miselli, Facoltà di Scienze dell'Uomo e della Società, Università Kore, Enna AUSL, Reggio Emilia.
- [9] Psicologia Generale, M. W. Eysenck, G. Belelli, S. Di Nuovo, O. Matarazzo, pag 110.
- [10] Seeing Life through Positive-Tinted Glasses: Color-Meaning Associations Sandrine Gil, Ludovic Le Bigot University of Poitiers and CNRS (CeRCA, UMR 7295), Poitiers, France.
- [11] Neuroimage. 2006 Jul, Sound alters activity in human V1 in association with illusory visual perception. Watkins S, Shams L, Tanaka S, Haynes JD, Rees G.

IDENTIFICATION OF ORTHOGONAL FREQUENCY CODED SAW RFID TAGS IN COLLISION CASE

Alexander Sorokin
postgraduate student

Saint-Petersburg State University of Aerospace Instrumentation
Saint-Petersburg, Russia

Ultramagnus88@gmail.com

Abstract

Recently interest in RFID systems grows. Increasing of traffic leads to necessity of reliable identification of items and vehicles. These systems should have high-noise immunity, high operation speed, resistance to climate impacts. [1] The modern development level of SAW technology and ultra-high frequency of SAW RFID devices with low power allow to create devices which can solve the above issues. In the base of RF instruments was an integrated principle of work which based on piezoelectric properties of materials that provides high operational speed, the high level of environmental friendliness and safety in comparison with the existing systems of identification. However, the passive SAW RFID tags collision can be very problematic. When several tags are placed at the same time in the read field, response signals cover each other in time domain. It causes problems in identification each tag and encoding. This article discusses using of orthogonal frequency coded (OFC) SAW tags. Also this article considers identification method for two OFC passive SAW tags in collision case.

Keywords: SAW, RFID, collision, OFC

I. INTRODUCTION

Generally SAW RFID tags readers define identification code which depends on time delay. Time delay depends on tag topology and the reflector placement on it. Variety of reflector placement in slots determines quantity of unique identification codes. However, in the case when the reader interrogates simultaneously several passive tags, it increases the probability of coincidence of the code groups, resulting in misidentification. This case can occur for example with freight cars and goods. We suggest using of OFC SAW RFID tags and identification method for them in collision case.

II. OFC PASSIVE SAW RFID TAGS

Typically, the passive SAW tag uses a tag, shown schematically on fig. 1.

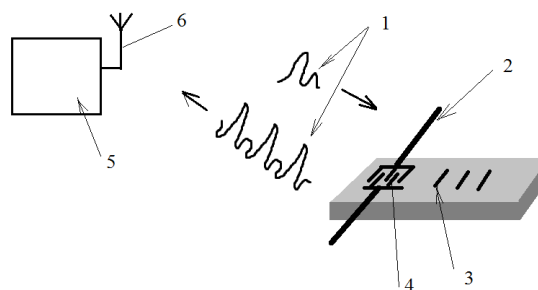


Fig. 1. Passive SAW RFID tag using time position encoding

The reader 5 sends the interrogation signal 1 through the antenna 6. Coming to the antenna 2 passive tags SAW IDT generates surface acoustic wave, which propagates along the tag substrate surface. Part of the SAW is reflected by the reflector 3, and returns to the IDT, generates a response signal comprising pulses delayed in time. The delay time between pulses is proportional to the distance between the reflectors. [2]. As a result, the response is delayed a number of correlation peaks in time, an example of which is shown on fig. 2.

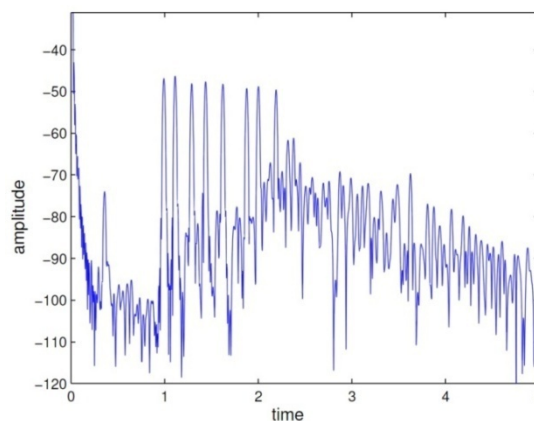


Fig. 2. SAW RFID tag response in time domain

In the case of imposition the time-domain response signal peaks from the tag, obtaining reliable identification code is much more difficult.

Therefore, it seems appropriate to use orthogonal frequency-coded (OFC) passive SAW tag, which is schematically shown in fig. 3 [3].

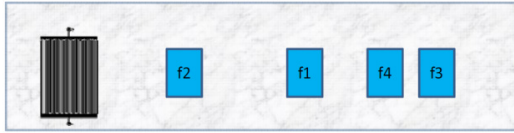


Fig. 3. OFC RFID SAW tag

The suggested tag consists of a unidirectional inter digital transducer (IDT) and a reflective structure, which reflectivity is determined by the interrogation impulses frequency. Each reflective structure sequentially arranged along the surface of the substrate of piezoelectric material. The number of reflective structure in the entire label is N . All reflective structure matched with a specific frequency and may be placed in any of the possible variants.

One of the interrogation pulse shaving the same frequency with the reflective structure is reflected to IDT. Other pulses propagate to the next reflective structure. Frequency of each structure is defined by given order from interrogation signal spectrum from f_1 to f_N . The value of the next reflective structure is selected by frequency shift concerning a pre-selected frequency of reference reflective structure. Response impulses are delayed each other on time relative to distance between reflective structures.

Topology of OFC SAW tag provides information about time and frequency for further encoding and identification each tag in collision case.

III. THE MATHEMATICAL MODEL OF TAG RESPONSE

A reader interrogates tags using the signal:

$$S(t) = [h(t - T_1') - h(t - T_2')] \cdot A \times \sum_{i=1}^N \sin(2 \cdot \pi \cdot f_i \cdot t - \varphi_i)$$

where: T_1' and T_2' – initial and finite time of interrogation pulse; A – pulse amplitude; f_i – frequency of the pulse; φ_i – phase of the pulse; N – the number of pulses for at one period of the interrogation signal.

The tag's response is formed in the interdigital transducer in the form of successive pulses:

$$S(t) = \sum_{i=1}^N [h(t - T_{1i}') - h(t - T_{2i}')] \times A_i \cdot \sin(2 \cdot \pi \cdot f_i \cdot t - \varphi_i)$$

where T_{1i}' и T_{2i}' – initial and finite time of response pulse.

IV. RESULTS

In this article is shown simply model with 4 slot sand one reference reflective structure which schematically shown in fig. 4. This model uses time slots $T_1 - T_{12}$, shown in fig. 5.

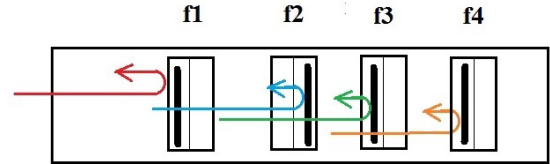


Fig. 4. Passive tag with reflective structures in the slots

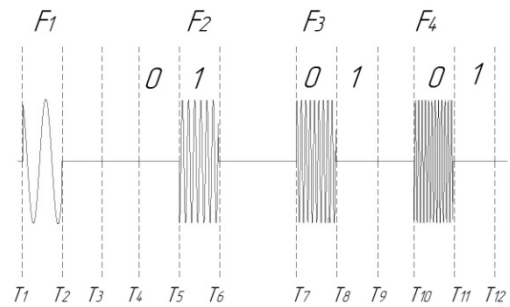


Fig. 5. Time slots of OFC SAW tag

In the model the position of the reflective structure in the time slot is matched with certain frequency, it determines the binary code. The first slot has a duration of T_1 to T_3 , second from to T_6 , third from T_7 to T_9 , fourth from T_{10} to T_{12} . Time slots $T_{11} = T_4 - T_3$, $T_{12} = T_7 - T_6$, $T_{13} = T_{10} - T_9$ are set between slots containing reflective structure.

Availability of time-frequency attributes allows create time-frequency matrix for the tag A, shown in fig. 6.

	$T_2 - T_1$	$T_3 - T_2$	$T_4 - T_3$	$T_5 - T_4$	$T_6 - T_5$	$T_7 - T_6$	$T_8 - T_7$	$T_9 - T_8$	$T_{10} - T_9$	$T_{11} - T_{10}$	$T_{12} - T_{11}$
F_1	0	1	0	0	0	0	0	0	0	0	0
F_2	0	0	0	0	1	0	0	0	0	0	0
F_3	0	0	0	0	0	0	1	0	0	0	0
F_4	0	0	0	0	0	0	0	0	0	1	0

Fig. 6 Time-frequency matrix for the tag A

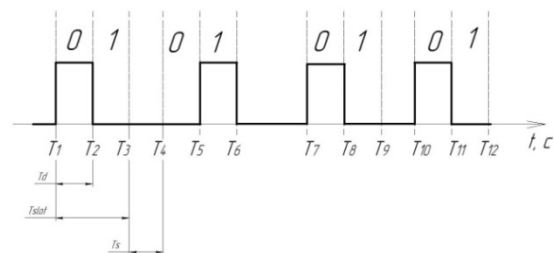


Fig. 7. Reflected signal of tag A

Thus, using information about time and frequency of first tag was formed binary code $A_2 = 0100100000$. Spacing between slots is filled

by zeros. Placement of the reflective structure in a certain position denotes either "0" or "1". The reflected signal from the label "A" in the time domain is shown in fig. 7.

Here the pulse length is T_d , time slots boundaries = T_{slot} , shift time of reflective structure T_s . Using time interval and frequencies of pulses at the collision situation moment allows to build time-frequency matrix. Then shifting both matrix in time domain with given step allows to separate them.

Similarly, we obtained the code of tag $B_2 = 01001001001$. Forming two time-frequency arrays A and B allows us to have a model of tags collision.

Shift of matrix A with each other on the pitch T_{slot} , creates the A and B tag codes. The resulting matrix C which was shifted by one step is shown in fig. 8.

	T_2-T_1	T_3-T_2	T_4-T_3	T_5-T_4	T_6-T_5	T_7-T_6	T_8-T_7	T_9-T_8	$T_{10}-T_9$	$T_{11}-T_{10}$	$T_{12}-T_{11}$	$T_{13}-T_{12}$
F_1	0	1	1	0	0	0	0	0	0	0	0	0
F_2	0	0	0	0	1	1	0	0	0	0	0	0
F_3	0	0	0	0	0	0	0	0	1	0	0	0
F_4	0	0	0	0	0	0	0	0	0	1	1	0

Fig. 8. Time-frequency matrix of tags A and B

The code bits which trapped to separation intervals $T_{11} = T_4 - T_3$, $T_{12} = T_7 - T_6$, $T_{13} = T_{10} - T_9$, $T_{14} = T_{12} - T_{13}$, determinite place of reflective structure of B tag. The presence of reference pulse makes it possible to separate tags in the given frequency range from F_1 to F_2 .

Response signal after FFT is shown in fig. 9.

According to a predetermined array of frequencies for each tag, in the first case is: $f=[10\ 25\ 50\ 76\ 90\ 125]*3$, we can divide the multiple tags in the frequency domain.

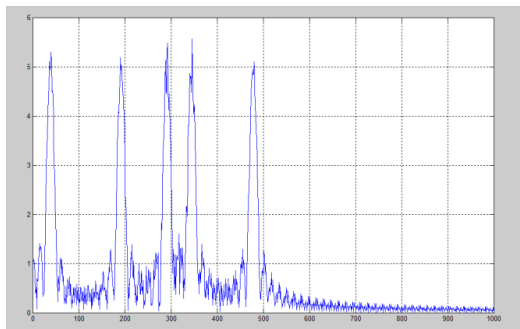


Fig. 9. Response of tag A after FFT

V. CONCLUSION

In this article we propose model of passive OFC SAW tags which allows to separate them each other in the time and frequency domains. The model of RFID OFC SAW tag contains reflective structures which are placed on the surface of the piezoelectric substrate. Their reflectivity is related by the certain frequency. Structures placement allows to separate tags in time domain. In this model reflective structure can be build as SAW bandpass filter which bandwidth is limited by given values for each slot. Modelling showed possibility of using OFC passive tags with time-frequency processing in the RFID systems in collision case.

Reference pulse allows to simplify tags separation in the frequency domain. Quantity of all separated tags is determined by the variety of placement reflective structures and technology possibilities.

VI. REFERENCES

- [1] Global RFID Market - Readers, Tags, Software and Services April 2015 Industry Experts 481 pages <http://www.reportlinker.com/p02841920-summary/Global-RFID-Market-Readers-Tags-Software-and-Services.html>
- [2] Surface Acoustic Wave RFID Tags S. Härmä and VP Plessky, Helsinki University of Technology, GVR Trade SA, Finland Switzerland, InTechOpen, Published on: 2009-01-01
- [3] Alfred Binder, Gudrun Bruckner and René Fachberger (2011). SAW Transponder – RFID for Extreme Conditions, Deploying RFID - Challenges, Solutions, and Open Issues, Dr. Cristina Turcu (Ed.), ISBN: 978-953-307-380-4, InTech, DOI: 10.5772/17526. Available from: <http://www.intechopen.com/books/deploying-rfid-challenges-solutions-and-open-issues/saw-transponder-rfid-for-extreme-conditions>

**TOWARD THE FERROELECTRIC DOMAIN AND DOMAIN WALLS ELECTRONICS:
INVESTIGATION OF DOMAIN WALL MOTION IN THIN PZT FILM
IN A TEMPERATURE RANGE FROM 4.2 TO 295 K**

Alexander F. Vakulenko
Student

Peter the Great Saint-Petersburg Polytechnic University,
Saint-Petersburg, Russia

vakulenko705@gmail.com

Abstract

This paper studies the influence of temperature on the rate of growth 180 degree domains in thin (60nm) film of ferroelectric $\text{PbZr}_{0.3}\text{Ti}_{0.7}\text{O}_3$. Cryogenic atomic force microscope attocube AFM I was used for growth and visualization of the domains. The series of experiments was done in wide range of temperature (4K – 280K), further studies are needed to explain rather weak temperature dependence of the domain lateral expansion.

Key words: ferroelectric, thin film, piezoresponse force microscopy, atomic force microscopy, domain wall.

I. INTRODUCTION

Ferroelectrics are materials possessing reversible spontaneous electric polarization and hysteresis loop in a temperature range, below the Curie temperature. Spontaneous polarization of this kind of materials appears below the Curie temperature, at which all the electric dipoles in a given material prefer to be pointed in one direction. Due to the fact, that in this case an electrostatic energy of the system should be extremely large, ferroelectric domains are formed to minimize system's potential energy. These domains contain a large number of dipoles aligned in a one direction. Domains are separated by domain walls, or edges between two domains with different directions of polarization. This work is an attempt to understand physical mechanisms driving the domain walls motion in thin ferroelectric films in the broad temperature range starting from 4.2 K and up to 295 K.

Since early 1960s bulk ferroelectrics became an essential components for many electronic devices due to their physical properties. Starting with early 1990s ferroelectric thin film components for electronic devices started to be actually developed. In 1987 the first ferroelectric memory integrated with silicon complementary metal-oxide semiconductors (CMOS) was demonstrated [1]. On the ex-

ample of portable telephones, appeared in the late 1990s, a contribution of using polar thin films, in the device miniaturization and improving its performance, could be demonstrated. Starting from 2000s ferroelectrics thin films are widely applied and developed for memories, microwave electronic components and microdevices with pyroelectric and piezoelectric microsensors/actuators. In the area of micro electro mechanical systems (MEMS) piezoelectric based thin films microdevices include ultrasonic micromotors [2], micropumps and microvalves [3], accelerometers and gyroscopes [4], acoustic sensors [5], sensing and actuating elements in atomic-force microscope [6], RF and optical switches [7] and ultrasonic transducers for medical [8] and sonar [9] applications. In the area of tunable microwave electronics, thin polar films are applied as a base for varactors, phase shifters, delay lines, tunable filters and antennas. Thin ferroelectric films are the prospective materials for mass storage application where a bit size is determined by the size of the domain. The principle of the domain writing and reading, in this case, is based on the next scheme: a prospective conductive sharp needle (with a radius of curvature smaller than 10 nm) is placed on the FE thin film, a short voltage pulse is applied between a needle and a bottom electrode of the film, this causes the domain formation and could be attributed to the writing process. The reading process implies the determination of the polarization distribution over the film surface with the same needle and special regime of scanning. The most important technological aspects of using thin polar films in electronics are the possibility of miniaturization and their integration onto one substrate, what determines cost and size reduction of the devices based on these materials.

All these facts gave an impetus to intense research directed to deeper understanding physical properties laid in functioning of ferroelectric materials. It was found that the domain walls have their own properties, moreover, they are mobile. This fact could give rise to a new type of technology where mobile domain walls will be the "active ingredient" of the device [10].

II. EXPERIMENT

In this work we use a scanning piezoresponse force microscopy to investigate the process of nucleation and domain growth in thin ferroelectric film in a broad temperature range. This method allows imaging of ferroelectric domains. This is achieved by bringing a sharp conductive probe into contact with a ferroelectric surface and applying an alternating voltage bias to the tip in order to excite deformation of the sample through the converse piezoelectric effect. The resulting deflection of the cantilever is demodulated by use of a lock-in amplifier.

The domain-wall motion in thin FE films at the room temperature (RT) is now well studied [11–13]. In homogeneous defect-free single crystals, domain-wall motion is determined by the interaction of the domain wall with the crystal lattice. The motion of domain walls in ferroelectric thin films and disordered ferroelectrics acquires the form of a thermally activated creep process governed by their interactions with a disor-

dered pinning potential created by structural defects [15]. At zero absolute temperature, domain boundaries should remain pinned while driving electric fields E smaller than the critical field E_c .

We employ the piezoresponse force microscopy (PFM) to study the growth of ferroelectric domains in $\text{PbZ}_{0.3}\text{Ti}_{0.7}\text{O}_3$ epitaxial films in a temperature range from 4.2 to 295 K. The experiment was carried out using a cryogenic atomic force microscope AttoAFM I (Attocube Systems, Germany) equipped with an external lock-in amplifier SR844 (Stanford Research Systems, CA) and a functional generator FC120 (Yokogawa Electric Corporation, Japan). We employed the n-type silicon cantilevers with the tip radius of curvature $r_{\text{tip}} \approx 10$ nm at the apex.

Object of study is high-quality epitaxial $\text{PbZ}_{0.3}\text{Ti}_{0.7}\text{O}_3/\text{LaSr}_{0.7}\text{Mn}_{0.3}\text{O}_3$ bilayers, grew on (100)-oriented single-crystalline SrTiO_3 substrates by pulsed laser deposition. The PZT film has a nominal thickness of about 20 nm (Fig. 1.C). Specimen has been prepared in the Christian-Albrechts-Universität zu Kiel.

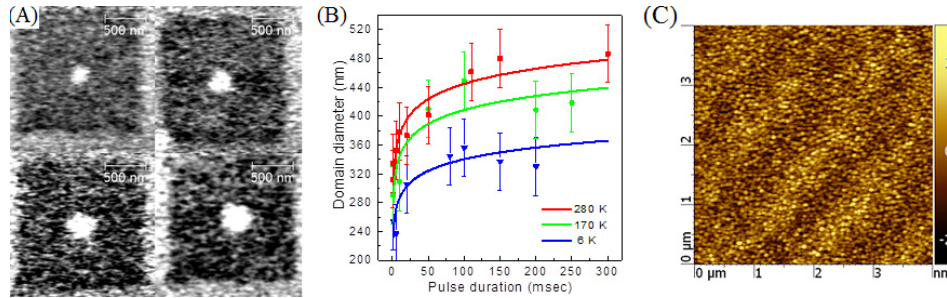


Fig. 1. Experimental data:

- A – four PFM images of written domains;
- B – domain diameter as function of the writing time and temperature, fitted with Eq. (3).;
- C – AFM topography of PZT film

Nanoscaledomains writing was done by applying dc voltage pulses to the bottom electrode while keeping the grounded AFM tip in contact with the film surface at a fixed point. In order to minimize the influence of native polarization distribution on the domain formation, the film was initially poled in the upward direction by scanning the surface at a positive DC voltage $V = 5\text{--}10$ V applied between the AFM tip and the bottom electrode. Then we used negative writing voltages to create domains with a downward polarization. The effective domain diameter D has been calculated from the reversed domain area.

III. RESULTS AND DISCUSSIONS

Nucleation and growth process is divided into two parts [13]: the formed embryonic domain (semi-ellipsoidal region of reversed polarization) grows rapidly along the film's depth until it crosses the whole film and transforms into a cylindrical 180° domain; its slower expansion in the film plane. Wall velocity v exponentially depends on the field intensity E according to the relation [13, 14]:

$$v(r) = v_\infty \exp \left[-\frac{U_a}{k_B \cdot T} \cdot \left(\frac{V_c}{V} \cdot \frac{r}{h} \right)^\mu \right], \quad (1)$$

where U_a – typical activation energy; k_B – Boltzmann's constant; T – temperature; V – applied voltage; V_c represents some characteristic voltage; $\mu = 0.5$ (when the random-bond disorder hinders the domain growth); $t_\infty = h/v_\infty$; h – film thickness. Using the (1) we can obtain the domain radii-time relation:

$$\begin{aligned} \frac{D}{2 \cdot h} &= \frac{V}{V_c} \cdot \left(\frac{k_B \cdot T}{U_a} \right)^2 \times \\ &\times \left\{ \ln \left[\frac{V_c}{V} \cdot \left(\frac{U_a}{k_B \cdot T} \right)^2 \cdot \frac{t}{t_\infty} \right] \right\} \\ &- \ln \left[\ln \left[\sqrt{\frac{V_c}{V}} \cdot \frac{U_a}{k_B \cdot T} \cdot \frac{t}{t_\infty} \right] \right]^2. \end{aligned} \quad (2)$$

Figure 1 shows images of written domains (A) and experimental radii-time dependence (B). The measured dependences $D(t)$ were fitted by the relation $D(t) = C_1 \cdot [\ln(t) + C_2]$ corre-

sponding to (2). With adjustable parameters $C_1=f(V,T)$ and $C_2=const$.

IV. CONCLUSIONS

We demonstrated that nanoscale ferroelectric domains can be created by short voltage pulses applied between the AFM tip and extended bottom electrode even at temperatures as low as 4.2 K. The observed low-temperature domain dynamic is consistent with the creep of domain boundaries occurring in the presence of structural defects, further studies are needed to explain rather weak temperature dependence of the domain lateral expansion. Our experimental findings and their theoretical analysis represent an important step towards the understanding of domain dynamics in ferroelectric materials.

V. ACKNOWLEDGMENT

The study was supported by the Ministry of Education and Science of the Russian Federation in the context of the implementation of a state plan.

VI. REFERENCES

- [1] *Eaton, S. S.* A Ferroelectric Nonvolatile Memory / S.S. Eaton [et al.] // IEEE Int. Solid-State Circuits Conference. – 1988. – P. 130.
- [2] *Dubois M. A.* PZT thin film actuated elastic fin micromotor / M. A. Dubois, P. Muralt // Ferroelectrics and Frequency Control. – 1998. – Vol. 45, N 5. – P. 1169-1177.
- [3] *Luginbuhl, P.* Microfabricated Lamb wave device based on PZT sol-gel thin film for mechanical transport of solid particles and liquids / P. Luginbuhl [et al.] // Microelectromechanical Systems. - 1997. Vol. 6, N 4. – P. 337-346.
- [4] *Nemirovsky, Y.* Design of novel thin-film piezoelectric accelerometer / Y. Nemirovsky, A. Nemirovsky, P. Muralt, N. Setter // Sensors and Actuators A: Physical. – 1996. – Vol. 56 N 3. – P. 239-249.
- [5] *Ledermann, N.* Piezoelectric Cantilever Microphone for Photoacoustic GAS Detector / N. Ledermann [et al.] // Integrated Ferroelectrics. – 2001. – Vol. 35. – P. 177-184.
- [6] *Fujii, T.* Feedback positioning cantilever using lead zirconatetitanate thin film for force microscopy observation of micropattern / T. Fujii, S. Watanabe // Applied Physics Letters. – 1996. – Vol. 68. – P. 467-468.
- [7] *Park, J. Y.* Micromachined RF MEMS tunable capacitors using piezoelectric actuators / J. Y. Park, Y. J. Yee, H. J. Nam, J. U. Bu // IEEE Microwave Symposium Digest – 2001. – Vol. 3. – P. 2111-2114.
- [8] *Baborowski, J.* Simulation and characterization of piezoelectric micromachined ultrasonic transducers (pMUTs) based on PZT/SOI membranes / J. Baborowski, N. Ledermann, P. Muralt, D. Schmitt // International Journal of Computational Engineering Science – 2003. – Vol. 4 N 3. – P. 471-475.
- [9] *Bernstein, J. J.* Micromachined High Frequency Ferroelectric Sonar Transducers / J. J. Bernstein [et al.] // Ferroelectrics and Frequency Control – 1997. Vol. 44 N 5. – P. 960-969.
- [10] *Salje, E. K. H.* Multiferroic Domain Boundaries as Active Memory Devices: Trajectories Towards Domain Boundary Engineering / E.K.H Salje // ChemPhysChem – 2010. – Vol. 11 N 5. – P. 940-950.
- [11] *Ganpule, C. S.* Polarization relaxation kinetics and 180° domain wall dynamics in ferroelectric thin films / C. S. Ganpule [et al.] // Phys. Rev. B. – 2001. – Vol. 65. – P. 014101.
- [12] *Tybell, T.* Domain Wall Creep in Epitaxial Ferroelectric Pb(Zr_{0.2}Ti_{0.8})O₃ Thin Films / T. Tybell [et al.] // Phys. Rev. Lett. – 2002. – Vol. 89 – P. 097601.
- [13] *Pertsev, N. A.* Dynamics of ferroelectric nanodomains in BaTiO₃ epitaxial thin films via piezoresponse force microscopy / N. A. Pertsev [et al.] // Nanotechnology. - 2008 - vol. 19. – P. 375703.
- [14] *Miller, R. C.* Mechanism for the Sidewise Motion of 180° Domain Walls in Barium Titanate / R. C. Miller, G. Weinreich // Phys. Rev. – 1960. – Vol. 117. – P. 1460.
- [15] *Chauve, P.* Creep and depinning in disordered media / P. Chauve, T. Giamarchi, P. Le Doussal // Phys. Rev. B. – 2000. – Vol. 62. – P. 624.

**SIMULATION AND RESEARCH THE IMPACT OF INDUSTRIAL NOISE
ON THE CHARACTERISTICS OF COMPRESSION PM AND LFM SIGNALS
IN SOLVING PROBLEMS OF NOISE IMMUNITY IN COMMUNICATION SYSTEMS**

Gysberth Maurits Wattimena
postgraduate student

Polytechnic of Ambon State
Ambon, Indonesia

mauritswattimena@gmail.com

Abstract

In solving the problem of noise immunity in communication systems are widely used compression characteristics PM and LFM signals. Under the influence noise, such as industrial or specially organized, compression characteristics of complex PM and LFM signals become worse faster. In the simulation method are researching the influence of such interference on the characteristics of signal compression using compression in the time range (matched filtering) and in the frequency range (Fourier Fast Conversion). The comparative analysis of these complex signals Interference and Interference methods of compression. The comparative analysis of noise protective this complex signals and noise protective methods their compression is held.

I. INTRODUCTION

Signals are used for transmission channels. The biggest problem with the transmission of information is possible interferences (intentional or accidental) on the outside of the transmission signal. In the capacity of such impact of electromagnetic interference may make other links, the impact of industrial and domestic equipment, malicious acts of third parties, etc. To get rid of the external action the various methods of protection are used: encryption, encoding, special modulation methods, shading lines, etc. However, to get rid of the disturbing influence completely is usually not possible, therefore, talking about a variety of transmission quality indicators: the number of errors per second, the maximum number of consecutive errors, etc. It is chosen various in quality communication channels and ways of protection for different purposes.

Currently, in order to improve the noise immunity of radio communication channels are widely

used methods of spectrum spreading. One of such methods should be attributed information transmission on the basis of using intra-Linear Frequency modulation (LFM) and Phase Modulation (PM). There are foreign radio standards [12] and technical solutions to build a radio transceiver device using LFM and PM signals.

Application of LFM and PM signals for transmission of information allows improving noise immunity of communication systems and telemetry, resisting selective fading and multipath signals. For transmission of digital information can be used LFM chirp radio pulses with positive and negative frequency modulation speed (FM) with different speeds, with different durations, as well as PM signals modulated Barker code, M-sequence or random even distribution law.

As noted above, the modulated signals are used to provide noise immunity. However, in the course of the signal it is exposed to various noises, which can lead to failure in the channel of information transmission.

Therefore, the aim is to research the impact of industrial impulse noise on the characteristics of compression PM and LFM signals in the transmission of information by radio link. To research the influence of industrial noise on algorithm compression of modulated impulse, is based on pulse compression algorithm with linear frequency modulation and PM. It simulates the effect of interference parameters, when the industrial pulse noise mixed with impulse on the background noise.

II. MODULATED PULSE MODELS AND COMPRESSION ALGORITHM

The modulated impulse signal is converted into a narrow pulse through a compression algorithm. For pulse modulation, the product of the pulse duration its bandwidth is significantly greater than one. Signals which possible increase pulse duration and bandwidth can be compressed, in frequency, this signal with a linear frequency modula-

tion, nonlinear frequency modulation and phase coding. In this paper, we have a limit to analysis, simulation pulse compression with linear frequency modulation, and phase encoding. Analysis, simulation represented in mathematical models.

The mathematical signal model with linear frequency modulation

Frequency-modulated (FM) signals are one of variety type complex signals. The great number of signals, FM can be written using this formula:

$$u(t) = \cos \left[2\pi \left(f_0 + \sum_{k=0}^{n-1} b_k \left(\frac{t}{T} \right)^{2k+2} \right) \right], \quad (1)$$

where T – duration pulse, c ; t – time, function argument, change in range $\left[-\frac{T}{2}; \frac{T}{2} \right]$ c ; b_k – coefficients expansion in the number of phase signal; f_0 – carrier frequency signal, GHz.

In $n=1$ get linear frequency modulated (LFM) signals, which coefficient b_0 – base signals – can be found as:

$$b_0 = \frac{T \Delta f}{2}, \quad (2)$$

where Δf – deviation frequency LFM signals, GHz.

If $n=1$ and deviation frequency $\Delta f=0$ GHz, The result is MONO signals or pulse signal with rectangular envelope. Thereby, model signal with linear frequency modulation can be represented by the formula

$$s(t) = A \cdot \cos(2\pi f_c t + \pi \cdot B / \tau \cdot t^2 + \varphi_0) \quad (3)$$

where A – amplitude, B – width pulse bandwidth, τ – duration pulse and φ_0 – initial phase.

Model signal and type spectrum pulse with linear frequency modulation (LFM) define as duration pulse is 1 microsecond, width pulse bandwidth is 50 MHz and frequency carrier is 3.7 GHz. Fig. 1 shows LFM pulse with linearly increasing frequency and fig. 2 showed the spectrum of LFM.

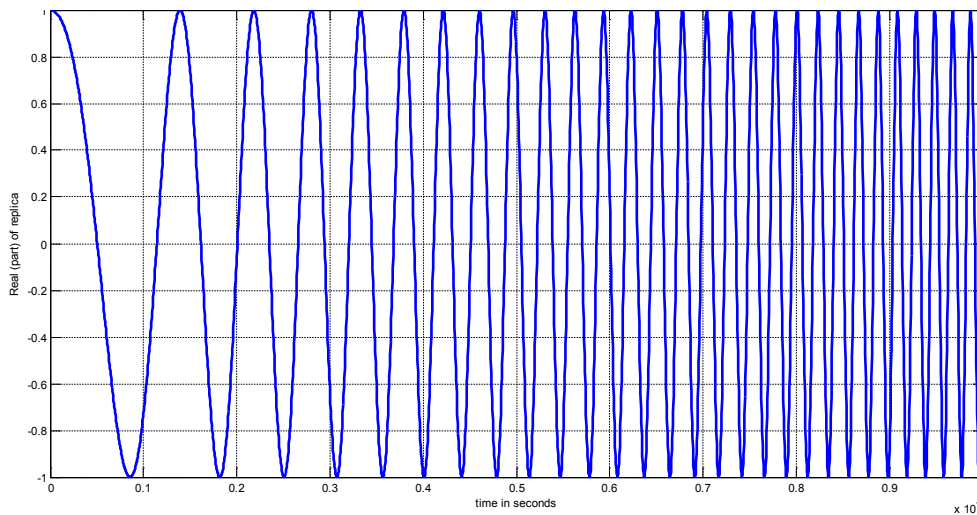


Fig. 1. LFM pulse

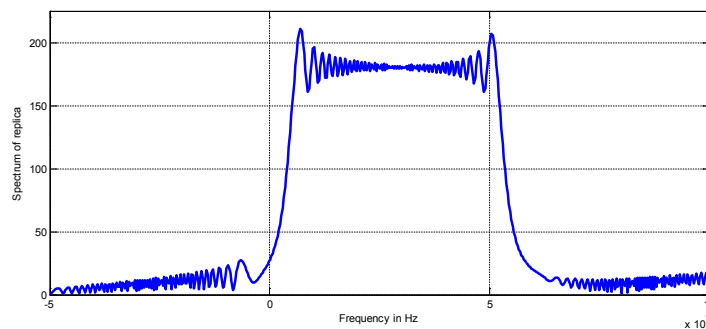


Fig. 2. LFM spectrum

Mathematical model of Phase Modulation signal

PM-signal represents a sequence of abutting one to another of simple impulses identical shape with duration t_{ii} the initial phase of the high-frequency which may take the given on discrete values. Let us assume that the number of possible

values $p=2$, that is considered a binary phase modulation. At duration of PM-signal, equal to T_s , the number of signals (discrete) $N=T_s/t_{ii}$. It is usually the discrete PM-signal has a shape closed to rectangular, and equal amplitudes, and the values of the initial phase 0 and π . In this case, sequence value of the initial phase high-frequency discrete

$\{\varphi_i, i = \overline{1, N}\}$ can be defined by a sequence of numbers $\{d_i, i = \overline{1, N}\}$, assuming values 0 and 1: if $\varphi_i=0$, for $d_i=0$; if $\varphi_i= \pi$, for $d_i= 1$.

For simplicity, we assume the amplitude of the discrete $A_i=1$. Then the complex envelope PM – signal may be represented as :

$$\dot{S}(t) = \sum_{i=1}^N U_0 [t - (i-1)t_u] \exp\{j\pi d_i\} \quad (4)$$

where the envelope of specific impulse

$$U_0(t) = \begin{cases} 1, & 0 \ll t \ll t_u \\ 0, & \text{in the other cases} \end{cases}$$

Considering, that $\exp\{j\pi d_i\} = \begin{cases} 1, & d_i = 0, \\ -1, & d_i = 1, \end{cases}$

expression (4) can be written:

$$\begin{aligned} \dot{S}(t) &= \sum_{i=1}^N (-1)^{d_i} U_0 [t - (i-1)t_u] = \\ &= \sum_{i=1}^N \theta_i U_0 [t - (i-1)t_u], \lim_{x \rightarrow \infty} \end{aligned} \quad (5)$$

where $\theta_i = (-1)^{d_i}$.

From (5) follows that properties PM-signal determined by properties sequences $\{\theta_i, i = \overline{1, N}\}$. Therefore the synthesis PM-signal generally consists in selecting a sequence $\{\theta_i\}$, which is called coding, having specified properties. Since the envelope of the signal on the output of the matched filter is determined by the correlation function signal, for which it is configured, so that the determinant in selecting a coding sequence is its correlation function, which must possess the necessary properties, in particular, specified by level of side tabs and a width of the main tab of the correlation function.

As the coding sequence (or just codex), Barker codes or M – sequence (binary sequences of the maximum period or length) can be used. In the radio system Barker codes are most widespread, which represent a binary sequence of finite length.

The given codes only exist for whose length $N=3, 5, 7, 11, 13$. Thirteen element code Barker is shown in fig. 3(a), and its corresponding envelope and PM-signal in fig. 3(b) and 3(c).

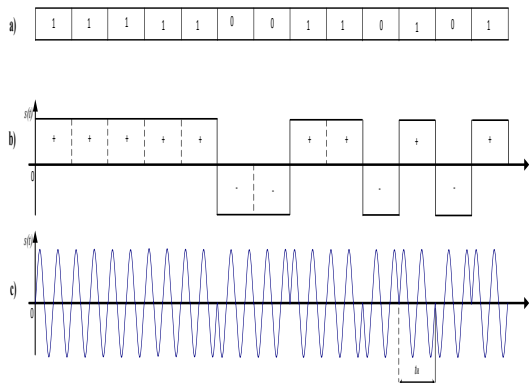


Fig. 3. (a) Element Code Barker 13; (b) Relationship with impulse; (c) PM-signal.

For hardware implementation of the processing devices LFM and PM-signals, the elements digital technology is the most commonly used. The given devices are formed simply or just used the software implementation of the compression filter in the processor on the receiving side.

Algorithm compression of modulated pulse is possible in the time and frequency domain. Procedure pulse compression in time domain is a linear convolution operation between receiver modulated pulse and its duplicate. Linear convolution in the time domain is equivalent to multiplication in the frequency domain. Here with appropriate to use a Fast Fourier Transform (FFT) to increase performance the process calculation.

Pulse compression algorithm in the frequency domain consists of the following steps:

- step 1. Spectrum of transmitting the modulated signal in the channel and its duplication is calculated by applying to FFT;
- step 2. Execute multiplication operation (multiplication, complex) between calculated spectrums on the first step;
- step 3. Pulse compression occurs by means of applying an FFT to the result of the multiplying spectrum in step 2.

The resulting compression of modulated pulse shown in fig. 4 and 5, which clearly can be identified from the noise narrow pulse, obtained after compression algorithm. Hence, using a modulated pulse compression algorithm can be separated transmitted information between the transmitter and receiver from high noise.

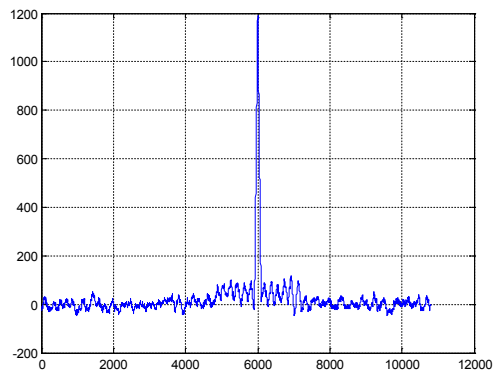


Fig. 4. Compression PM pulse

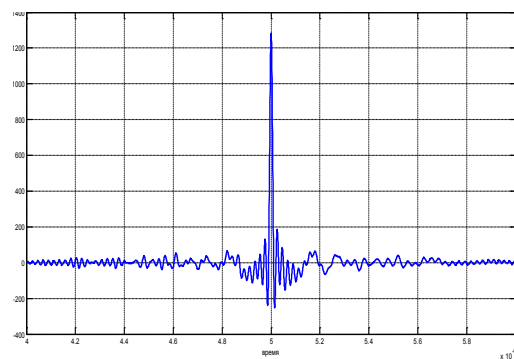


Fig. 5. Compression LFM pulse

However, it remains a question, how affect the industrial impulse noise on the algorithm of compression. For this we consider a model of industrial noise and prove their impact by using computer modeling.

III. MODEL INDUSTRIAL NOISE

In the work confine ourselves to the effect of active noise are beaten out at random:

- 1) One of the basic pulse, PM and LFM echo signal (fig. 6, 9);
- 2) Part of two pulses standing together (fig. 7, 10);
- 3) Combination of type 1 and 2 (fig. 8, 11).

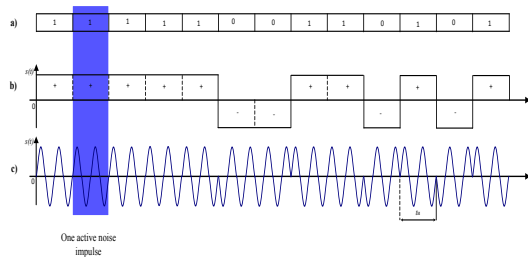


Fig. 6. The impact of industrial noise one of element pulses PM signal simulation with Barker code 13

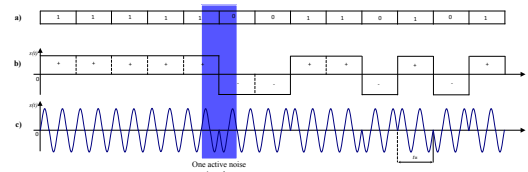


Fig. 7. The impact of industrial noise on two of element pulses PM signal simulation with Barker code 13

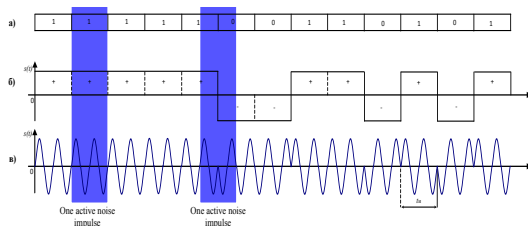


Fig. 8. The impact of industrial noise with one of element and two elements pulses FM signal modulated adjacent Barker code 13

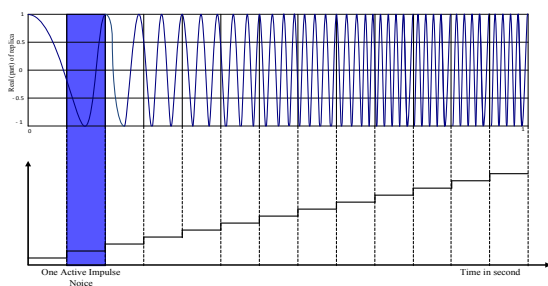


Fig. 9. The impact of industrial noise in one element impulses of LFM signal

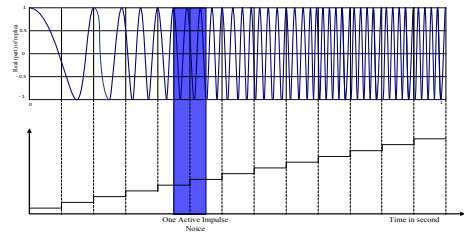


Fig. 10. The impact of industrial noise in two element impulses of LFM signal

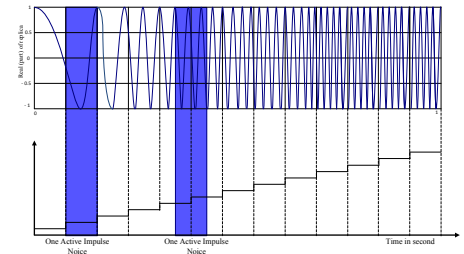


Fig. 11. The impact of industrial noise in two element impulse and two element impulses of LFM signal

IV. MODELING INFLUENCE INDUSTRIAL NOISE IMPULSE IN COMPRESSION ALGORITHM ECHOES SIGNAL

1) Result computer simulation, compression algorithm envelope PM-signal (Barker code length of 13) with noise, when influence impulse:

- a) noise type 1 (fig. 12, fig. 13);
- b) noise type 2 (fig. 14, fig. 15);
- c) noise type 3 (fig. 16, fig. 17).

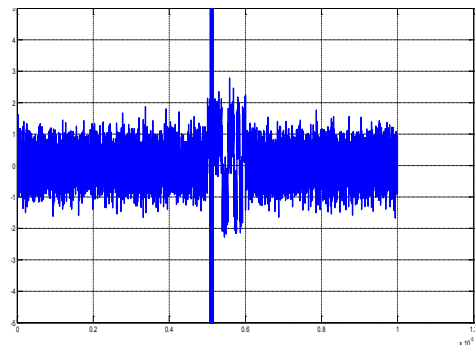


Fig. 12. PM modulated signal Barker code 13 with noise and interference type 1

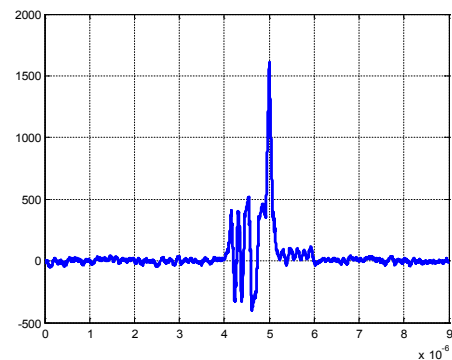


Fig. 13. The result of the compression algorithm

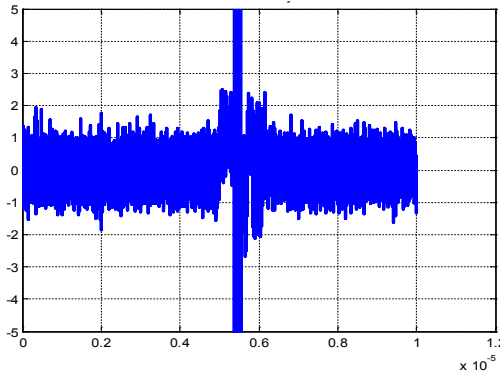


Fig. 14. PM modulated signal Barker code 13 with noise and interference type 2

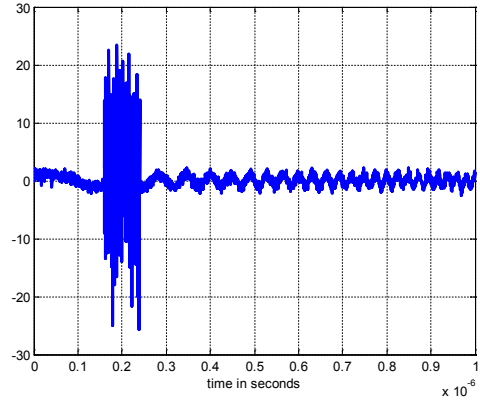


Fig. 18. LFM modulated signal with noise and interference type 1

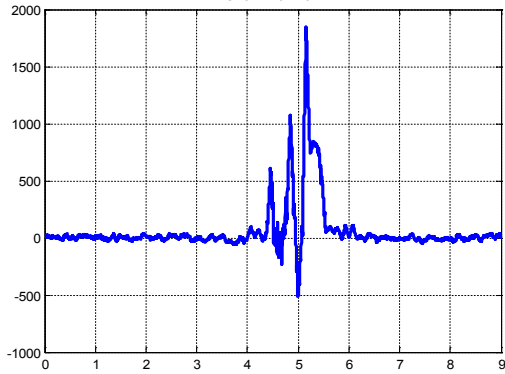


Fig. 15. The result of the compression algorithm

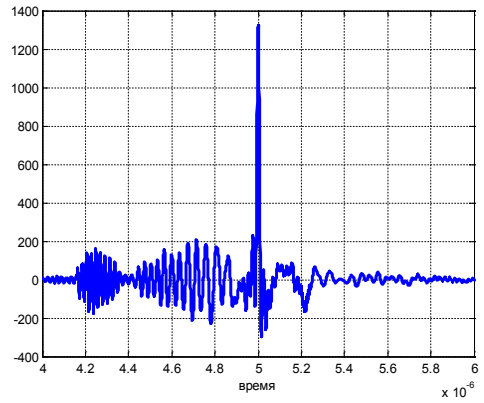


Fig. 19. The result of the compression algorithm

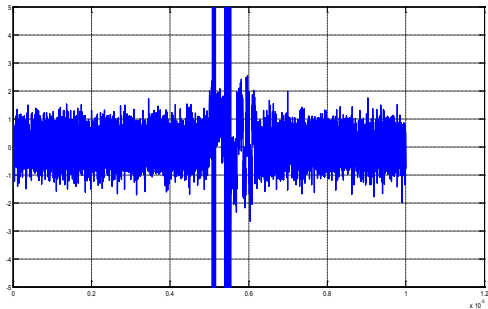


Fig. 16. PM modulated signal Barker code 13 with noise and interference type 3

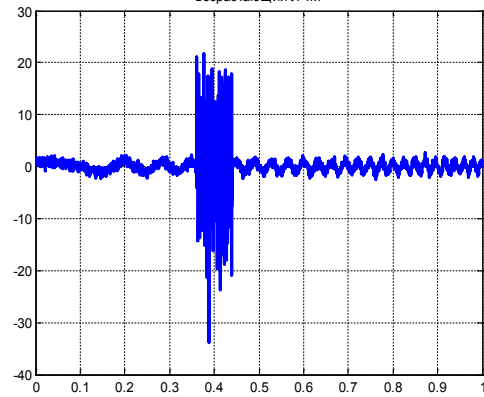


Fig. 20. LFM modulated signal with noise and interference type 2

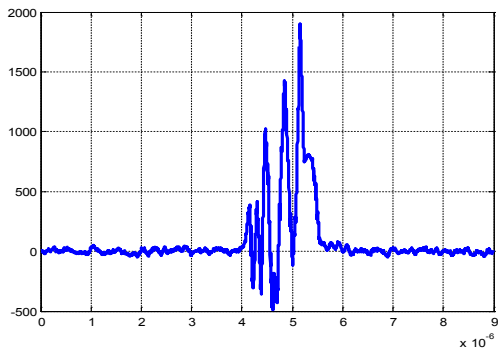


Fig. 17. The result of the compression algorithm

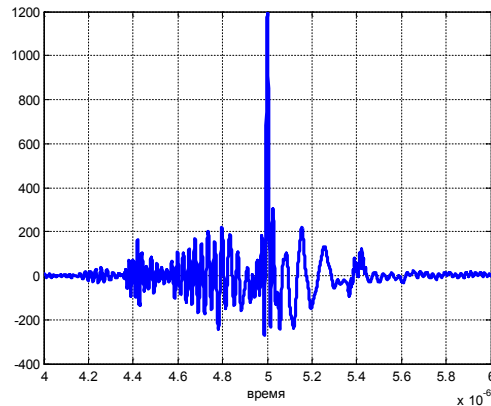


Fig. 21. The result of the compression algorithm

2) Result computer simulation, compression algorithm envelope LFM-signal with noise when LFM influence impulse:

- a) noise type 1 (fig. 18, fig. 19);
- b) noise type 2 (fig. 20, fig. 21);
- c) noise type 3 (fig. 22, fig. 23).

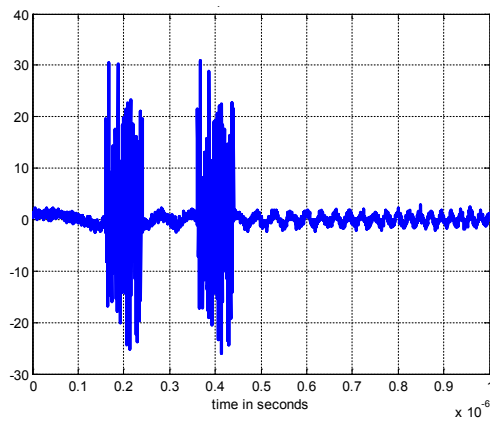


Fig. 22. LFM modulated signal with noise and interference type 3

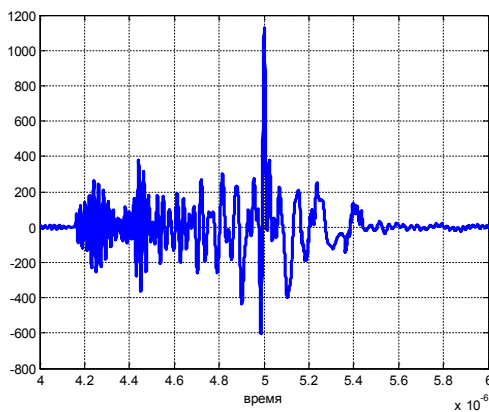


Fig. 23. The result of the compression algorithm

V. CONCLUSIONS

The article describes the basic model of modulated signals are used in telecommunication systems. Simulated a compression algorithm modulated pulse, based on the use of the matched filter in the time and frequency domain. The models of industrial impulse noise and show some of the impacts on the modulated pulse. Is shown modeling, compression LFM and PM signal when exposed to in-

dustrial noise. The results of impact industrial noise on the pulse compression algorithm.

The simulation results, obtained in this paper are important in research related to transmitted information in communication channels, noise prediction and selecting of characteristics communication systems in conditions interfering effects

VI. REFERENCES

1. *Baskakov, S.* Radio circuits and signals. Third editions - M.: «High school», 2000. – 462p.
2. *Gonorovskij I.S.* Radio circuits and signals. - 5th editions. - M.: Drofa, 2006. - 719p.
3. *Mahafza, B. R.* Radar Systems Analysis and Design Using MATLAB / Bassem R. Mahafza. - CHAPMAN & HALL/CRC, 2000. – 532p.
4. *Prokis, Jh.* - Digital Communications / Klovski D.D. - M.: Radio Communications, 2000 - 800p.
5. *Sklar, Bernard.* Digital Communications. Digital Communications: Fundamentals and Applications. - 2nd editions. — M.: «Williams», 2007. 1104p.
6. *Feer K.* Digital Communications: Modulation and Spread Spectrum Applications. - M.: Radio Communications, 2000. - 552 c
7. *Yakovov V. P.* Computer Mathematics. Theory and Practice. - SPb: «Piter», 1999, 2001. - C. 1296
8. *Aleksey E.R., Checnokova O.V.* MATLAB 7. Self Study - Press, 2005. – 464p.
9. *Olenev N.N., Pecenkin R.V., Chernechov A.M.* Parallel Programs in MATLAB and its application. M: VCRAN. 2007. 120p.
10. *Abilov A.V.* Communication network and telecommunication systems. M.: Radio Communications, 2004. – C.288
11. *Mahafza B. R.* MATLAB simulation for the design of the radar system, publishing house of electronics industry, 2009.
12. *Skolnik M. I.* Radar Handbook (3th edition), Publishing-House of electronics industry, 2010.
13. *Borisov V. I.* Radio communication and Jamming systems with spread spectrum signal pseudorandom adjustment method for working frequency. - M.: Radio Communications, 2000. - 384p.
14. IEEE Standard for Information technology Telecommunications and information exchange between systems Local and metropolitan area networks Specific requirements. Part 15.4: Wireless Medium Access Control (MAC) and Physical Layer (PHY) Specifications for Low-Rate Wireless Personal Area Networks (WPANs). IEEE Std 802.15.4a™-2007.

THE USE OF VIRTUAL 3D MODELS IN PROBLEMS OF SYNTHESIS OF THE REGULATOR

Alexander Zelenin
student

Saint-Petersburg State University of Aerospace Instrumentation
Saint-Petersburg, Russia

setius2@mail.ru

Abstract

In this paper discusses symbiosis computer aided design SolidWorks (CAD system) and MatLab. This symbiosis allows to accelerate and reduce the cost of design of new products.

Keywords: simulation, modeling, MatLab, SolidWorks, description of the mechatronic systems.

I. INTRODUCTION

Nowadays, the main tools for product design, have become different packages. Some packages computer-aided design (CAD) allows engineers to create visual representations of products in 3D space, while others allow you to simulate the behavior of components and products in general. Despite the great features of the CAD package SolidWorks to design and modeling of the influence of the environment on the object of development, the possibility of modeling it is limited. This situation is repeated in MatLab, but in the opposite direction. MatLab allows to simulate the behavior of complex systems and to design of controllers designed to maintain the flow of the developer necessary processes in these systems, but to describe the great system in MatLab will be difficult.

To create the product in the shortest possible time and to ensure the proper level of elaboration of the product, it is necessary to combine these two tools. In this paper we will use for building the geometric model package SolidWorks, and for the synthesis of controller using MatLab. Combine these tools will help us SimMechanics Link [1].

CAD-translator the SimMechanics Link works as follows [3]. After will be built in SolidWorks 3D assembly, SimMechanics Link will export a visual representation of a virtual physical model in MatLab, and create and bind the blocks Simulink (MatLab) in accordance with the 3D Assembly and imports the physical properties of the parts of 3D assemblies.

On the basis of the imported properties of the parts of a 3D assembly based virtual augmented physi-

cal model, which consists of: mass, inertia and constraints for each object represented in the 3D assembly.

Consider the controller synthesis on the example of 3D model of the manipulator.

II. THE ALGORITHM OF DESIGN OF CONTROLLERS

Preparing the environment

At this stage, must be installed on a computer:

- SolidWorks;
- MatLab;
- Library SimScape for MatLab;
- Library SimMechanics for MatLab;
- Addition SimMechanics Link to the SimMechanics library for MatLab.

Export 3D models
from SolidWorks to MatLab

Program for creating 3D models SolidWorks was chosen, as this program has the ability to assign a lot of 3D models.

In the process of creating 3D models of parts of the manipulator the weight was calculated by applying the mass density of the material chosen. As a material virtual 3D model was chosen ABS plastic. Properties of ABS plastic are shown in table 1.

Table 1
Properties of ABS plastic from SolidWorks

Properties	Value	Units
elastic modulus	$2 \cdot 10^9$	N/m ²
poisson's ratio	0.394	Not applicable
shear modulus	$3.19 \cdot 10^8$	N/m ²
mass density	$1.02 \cdot 10^3$	kg/m ³
tensile strength	$3 \cdot 10^7$	N/m ²
crushing stress	-	N/m ²
yield strength	-	N/m ²
thermal expansion coefficient	-	K ⁻¹
thermal conductivity	0.2256	W/(m·K)
specific heat	1386	J/(kg·K)
material damping factor	-	Not applicable

Created 3D models of individual parts of the manipulator will collect, in a 3D assembly. In the process of creating the 3D assembly of the manipulator will assign it to the parts of the constraints of the actual mechanical system of the manipulator (fig. 1).

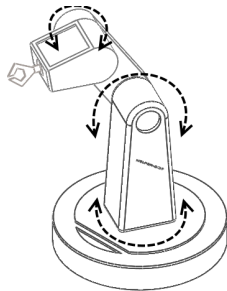


Fig. 1. The degrees of freedom of the manipulator

To enable the add SimMechanics Link to SolidWorks in MatLab you need to type the command `smlink_linksw`. After entering the commands `mmlink_linksw` in the SolidWorks interface appears SimMechanics Link. To export a model from SolidWorks to MatLab necessary in the SolidWorks interface select Tools > SimMechanics Link > Export > SimMechanics First Generation. If the export succeeds, you will see a dialog for saving the model in MatLab format filename.xml. To generate the model from MatLab filename.xml in MatLab you need to type the command `mehc_import('filename.xml')`. After entering `mehc_import('filename.xml')` in Simulink (MatLab) open model (fig. 2).

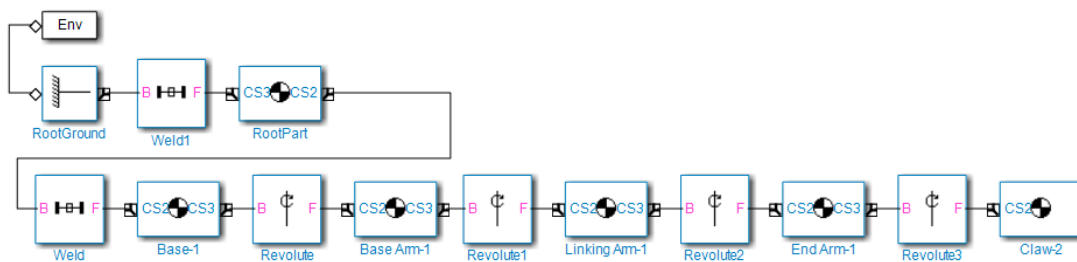


Fig. 2. The model of the manipulator in Simulink (MatLab)

Control synthesis in MatLab

Also available in MatLab 3D visualization of the exported model can be viewed in Simulink, you must click Simulation > Update Diagram. As a result of the Update Diagram window opens (fig. 3).

Uniting Body and mutually Revolute blocks in the subsystem for better representation of the manipulator model (fig.4).

The MatLab blocks according to the parts of the manipulator (fig. 5).

In subsystems “Shoulder 2–3” and “Grip” will assemble scheme (fig. 6).

In the setting of Revolve block in the column Number of sensor/actuator port will put value of 1. In the settings block Joint Actuator, in the Actuator with select Motion. These settings will allow us to lock the rotation of the “Shoulder 2–3” and “Grip” in their joints.

In the subsystem “Shoulder 1” will assemble scheme (fig. 7).

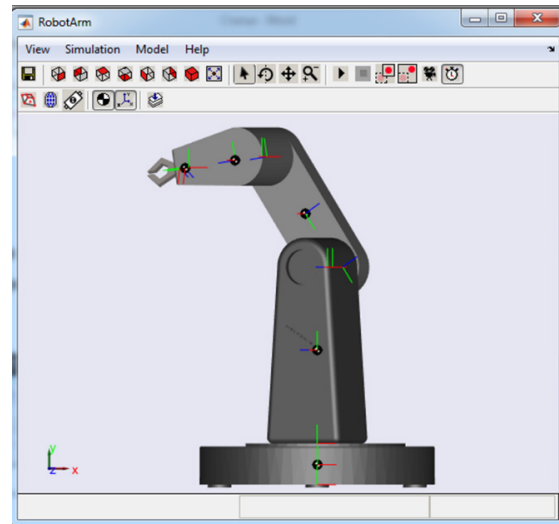


Fig. 3. The visualization model in MatLab

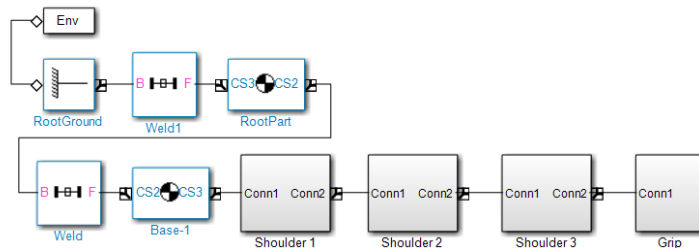


Fig. 4. Model of the manipulator after the merger

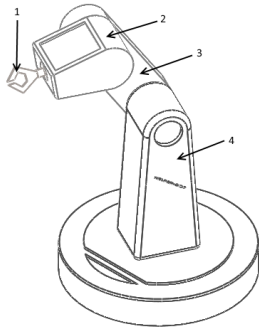


Fig. 5. The scheme of the block matching MatLab of the manipulator model
1 – Grip; 2 – Shoulder 3; 3 – Shoulder 2; 4 – Shoulder 1

In the setting of Revolve block in the column Number of sensor/actuator port will put value 2. In the settings block Joint Actuator, in the Actuator with choose the Generalized Forces, in the Applied torque units select mN/m.

We now turn to the synthesis of the PID controller. Go into the PID Controller block press the Tune button, in the opened window, move the sliders Response Time and Transient Behavior to achieve the required quality of the transition process. During configuration was obtained, the response of the system (fig. 8). The coefficients of the PID controller are presented in table 2.

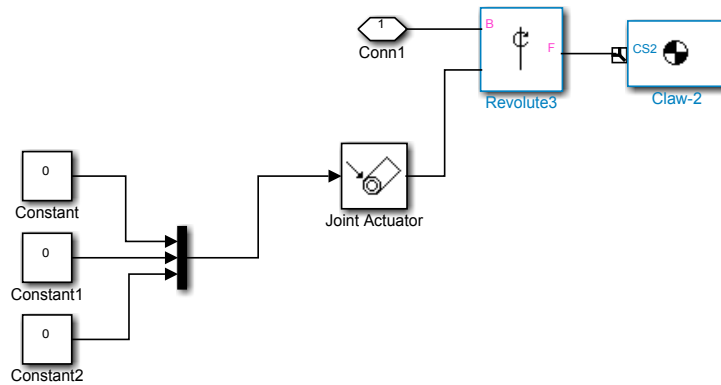


Fig. 6. Subsystem "Grip"

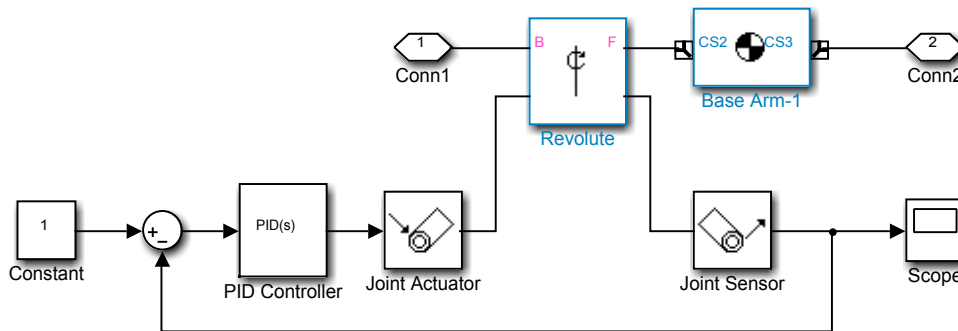


Fig. 7. Subsystem "Shoulder1"

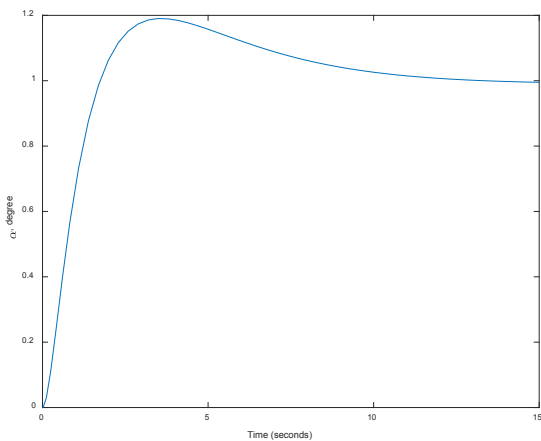


Fig. 8. Response of the system

Table 2
Coefficients of the PID controller

Coefficient	Value
Proportional (P)	0.35
Integral (I)	0.02
Derivative (D)	1.25
Filter coefficient (N)	5.45

After running the simulation model of the manipulator with the tuned controller in the subsystem "Shoulder 1", in block Scope, you can observe the behavior of the system with different inputs (block Const). Also with the simulation system runs the animation of the manipulator, which visually shows the behavior of the system.

III. CONCLUSION

This work showed the possibility of using 3D models in problems of synthesis of the regulator.

The combination of MatLab (SimMechanicsLink) and SolidWorks greatly increases the speed of designing through the use of 3D models as the basis for identification of the control object. Using SimMechanics Link commits to develop a 3D model, meet several requirements:

- the model must contain information about the mechanical properties of the material;
- moving parts in the assembly should be determined by conjugation.

IV. REFERENCES

- [1] <http://www.mathworks.com/help/physmod/smlink/ug/product-overview.html> - Description SimMechanics Link;
- [2] *О. В. Блинов, В. Б. Кузнецов, Е. Н. Калинин.* Исследование механических систем в среде SimMechanics (MatLab) с использованием возможностей программ трехмерного моделирования. Методические указания. Иваново 2012;
- [3] *К. М. Тихонов, В. В. Тишков.* SimMechanicsMatlab как средство моделирования динамики сложных авиационных робототехнических систем. Электронный журнал «Труды МАИ». Выпуск № 4.

CONTENTS

GREETINGS	3
<i>James W. Keaveney</i> ISA President 2016	3
<i>Gerald W. Cockrell</i> , ISA Former President (2009)	7
PROFESSIONALS SPEAKING	9
<i>Kryachko A. F., Kryachko M. A., Antonov K. V., Levin Y. Y., Losev V. K.</i> The Especially Scattering of Ultra-Wideband Pulse Wedge-Shaped Field	9
<i>Maiorov N. N., Fetisov V. A., Taratun V. E.</i> Analysis of the Technical State of the System Based on the Expert Evaluations	12
THE TWELFTH ISA EUROPEAN STUDENTS PAPER COMPETITION (ESPC-2014) WINNERS	15
<i>Aiello A., Alesci A., Manconi G., Mantellina A., Tinervia M., Villari L., Zapparrata W.</i> An Innovative Design in Order to Reduce the Workload of a Pilot During the Flight	15
<i>Alé M., Dimino A., Serra G.</i> Psicoterapy Act on Smartphone	18
<i>Baranow Y.</i> Web service IronBrain for improve remembering as an alternative to Anki	22
<i>Chabanenko A.</i> Analysis and Synthesis of Organizational and Technical Solutions in the Organization of the High-Tech Production.....	24
<i>Golovin E.</i> About Version Control Systems.....	29
<i>Gravagno M., Ferracane G., Roncade S., Burgio G., Salamone B.</i> “Dislhelp”: a Valuable Aid for Conducting Exercises to Dyslexic	31
<i>Grigoriev E., Zhuravlev A., Yudin I.</i> Method of Determining the Size of the Search Area a Moving Object on a Priori Information to Meet the Challenges of Modern Search Ministry for Emergency Situations Disaster Zones Structure.....	35
<i>Ivanov I., Shelest M.</i> Remote Energy Supply Efficiency Estimation for Far-Field E/M	37
<i>Kazakov V.</i> Calculation of Diffraction Losses in the System “Optical Fiber – Lens”	40
<i>Korol G.</i> Parameters and Modes Optical Spectral Devices Base on the Acousto-Optic Tunable Filter	43
<i>Kozhevín A.</i> Special Features of Production Technologies of Micromechanical Sensors on Surface Acoustic Waves	46
<i>Kuznetcov V.</i> The Treatment of the Surface Gap for Photometric Stereo	50
<i>Makarenko M.</i> System Analysis and Practical Software Realization of Making Decision in the Conditions of Uncertainty at Transportation Goods on Railway Transport	53
<i>Makeeva A.</i> Models and Methods of Estimation of Innovative Potential of Novelty.....	56
<i>Mancuso E., Piazza G., Mariotti A., Lao E.</i> An Innovative Technique to Improve the Physical Performance of a Cyclist.....	61
<i>Orlov A., Paraskun A.</i> Effect of Internal Energy Source at Natural Vibration Frequencies of MEMS Based Resonators	64
<i>Oskolkov B.</i> Photovoltaic Effects as the Physical Basis of a New Generation of Microelectromechanical Sensors and Systems	67
<i>Petrashkevich E.</i> The Research of the Component of the Combined Production Technology of Aircraft Parts	70
<i>Platania S., Gandolfo A., L’Episcopo L., Merlino M.</i> “Virtual Act Defusion”: a Java-Based Software to Join ACT Psychotherapy with the Virtual Reality	73
<i>Sorokin A.</i> Identification of Orthogonal Frequency Coded SAW RFID Tags in Collision Case	77
<i>Vakulenko A.</i> Toward the Ferroelectric Domain and Domain Walls Electronics: Investigation of Domain Wall Motion in Thin PZT Film in a Temperature Range from 4.2 to 295 K	80
<i>Wattimena G.</i> Simulation and Research the Impact of Industrial Noise on the Characteristics of Compression PM and LFM Signals in Solving Problems of Noise Immunity in Communication Systems	83
<i>Zelenin A.</i> The Use of Virtual 3D Models in Problems of Synthesis of the Regulator	89

The scientific edition

**BULLETIN OF THE UNESCO DEPARTMENT
“DISTANCE EDUCATION IN ENGINEERING” OF THE SUAI**

Collection of the papers
Issue 1

Computer imposition *V. N. Sokolova, V. N. Kostina*
Papers are published in author's edition

Сдано в набор 21.04.16. Подписано к печати 28.04.16. Формат 60×84 1/8.
Бумага офсетная. Усл. печ. л. 10,9. Тираж 150 экз. Заказ № 213.

Редакционно-издательский центр ГУАП
190000, Санкт-Петербург, Б. Морская ул., 67

Department of operative polygraphy
SUAI
190000, St. Petersburg, st. B. Morskaya, 67